REPORT DOCUMENTATION PAGE

AFRL-SR-AR-TR-04-

0273

1. AGENCY USE ONLY *(Leave blank)*	2. REPORT DATE	3. REPORT
	April 2004	Final Technical Report (01 May 02 - 30 Apr 03)

4. TITLE AND SUBTITLE
A Laboratory for System Identification of Mistuning in Integrally Bladed Disks

5. FUNDING NUMBERS
F49620-02-1-0223
3484/US
61103D

6. AUTHOR(S)
J. H. Griffin

7. PERFORMING ORGANIZATION NAME(S) AND ADDRESS(ES)
Carnegie Mellon University
Dept of Mechanical Engineering
Pittsburgh, PA 15213

8. PERFORMING ORGANIZATION REPORT NUMBER

9. SPONSORING/MONITORING AGENCY NAME(S) AND ADDRESS(ES)
AFOSR/NA
4015 Wilson Blvd., Room 713
Arlington, VA 22230-1954
Program Manager: Capt. Clark Allred

10. SPONSORING/MONITORING AGENCY REPORT NUMBER

11. SUPPLEMENTARY NOTES

12a. DISTRIBUTION AVAILABILITY STATEMENT
APPROVED FOR PULBIC RELEASE, DISTRIBUTION IS UNLIMITED

12b. DISTRIBUTION CODE

13. ABSTRACT *(Maximum 200 words)*

The funds received from the DURIP proposal were to be used to purchase a Polytech scanning vibrometer. The vibrometer is being used to make precise measurements of the mistuned modes and natural frequencies of integrally bladed disks (IBRs) in the Mistuning System Identification Laboratory. The resulting data is then used as input to system identification software that is being developed at CMU under a separate Air Force contract. The system identification software then determines the mistuning in each blade. This report documents the development of the vibration laboratory, the types of measurements that are being done, and the research that has been made possible through its use.

14. SUBJECT TERMS			15. NUMBER OF PAGES 57
			16. PRICE CODE
17. SECURITY CLASSIFICATION OF REPORT	18. SECURITY CLASSIFICATION OF THIS PAGE	19. SECURITY CLASSIFICATION OF ABSTRACT	20. LIMITATION OF ABSTRACT
U	U	U	

A LABORATORY FOR SYSTEM IDENTIFICATION OF MISTUNING IN INTEGRALLY BLADED DISKS

FINAL PERFORMANCE REPORT

AWARD NO. F49620-02-1-0223
AWARD DATE: 1 MAY 2002

PROJECT ENGINEER: D. MOOK
AFOSR

BY

J. H. GRIFFIN
DEPARTMENT OF MECHANICAL ENGINEERING
CARNEGIE MELLON UNIVERSITY
PITTSBURGH, PA 15213
[PHONE NO. (412) 268-3860]

APRIL 2004

1. INTRODUCTION

The funds received from the DURIP proposal were to be used to purchase a Polytec scanning vibrometer. The vibrometer is being used to make precise measurements of the mistuned modes and natural frequencies of integrally bladed disks (IBRs) in the Mistuning System Identification Laboratory. The resulting data is then used as input to system identification software that is being developed at CMU under a separate Air Force contract. The system identification software then determines the mistuning in each blade. This report documents the development of the vibration laboratory, the types of measurements that are being done, and the research that has been made possible through its use.

2. EQUIPMENT PURCHASED AND LABORATORY ESTABLISHED

2.1 The Polytec Vibrometer

The Polytec scanning vibrometer was purchased in 2002. The equipment is shown in Figure 1.

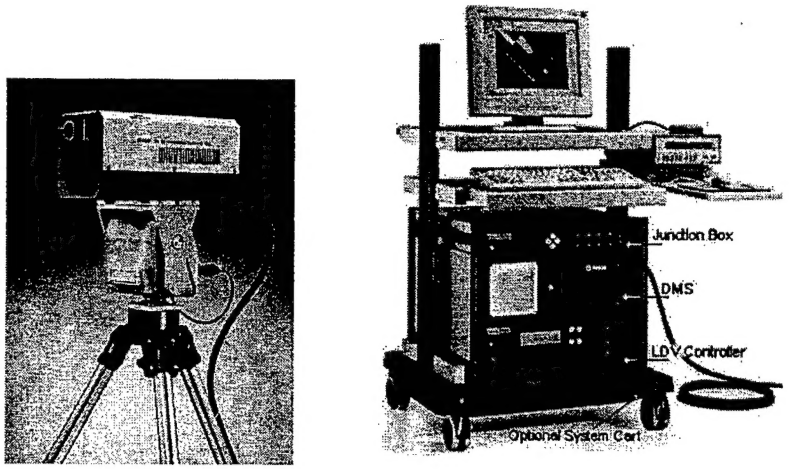

Figure 1 Polytec Scanning Vibrometer

Some of the important features of the vibrometer are:

- The Measurements Can Be Automated
  - Built-in Function Generator drives Excitation Speaker
  - Automatically Repeats Excitation and Scans IBR for Modal Measurements (several hundred transfer functions may be required per IBR).
  - More Precise Positioning of Measurements
- Data Validation Ensures High Quality Measurements
  - Automatically Retakes Data if Signal is Not Optimal
- 12,800 FFT Lines

- High Resolution Measurements Needed Because of High Modal Density (e.g.may have 50 modes between 1300 –1350 Hz)

It was important to be able to automate the measurements because we could set up the test and let the experiment run overnight. Alternatively, they would have taken weeks, if not months, to run the same experiment if we had used our previous equipment.

Another advantage of the Polytec vibrometer is its high frequency resolution, i.e. 12,800 FFT lines. Bladed disks often have frequencies that are very close together and a high frequency resolution capability is required to determine their frequency response. An example of a representative frequency response plot for an IBR is shown in Figure 2. Note that about ten modes are located within a ten Hertz frequency band. Consequently, the very fine frequency resolution capability of the Polytec vibrometer was needed to make these measurements.

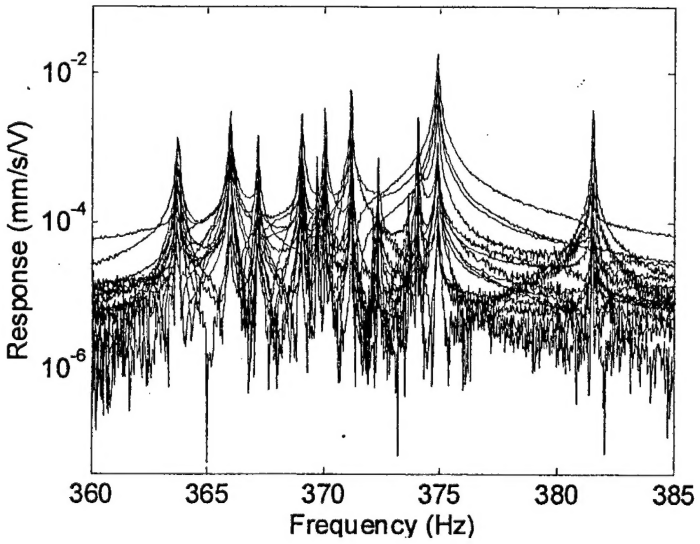

Figure 2 Frequency Response of an IBR

A list of the equipment purchased with DURIP funds is given in Attachment 1.

2.2 Additional Laboratory Components

In order to establish the System Identification Laboratory we have developed and purchased additional equipment from other funding sources. The experiments are performed on a vibration table with base isolation, Figure 3 (a). We have a signal generation system and amplification system that can either excite the blades acoustically or magnetically, see Figure 3 (b) and Figure 4. The excitation signals can be phased from blade to blade so as form a traveling wave excitation that simulates excitations found in the engine, i.e. in the lab the excitation source rotates relative to the IBR whereas in

the engine the IBR rotates relative to the excitation source. In addition, the excitations can simulate transients and pulse excitations. As a result, we can:

- Run automated modal tests
- Identify the mistuning in the system model the system and predict the response to a traveling wave (engine order) excitation
- Verify the accuracy of the predictions with a traveling wave experiment.

This capability is used extensively in the paper by Rossi et al. given in the attachment.

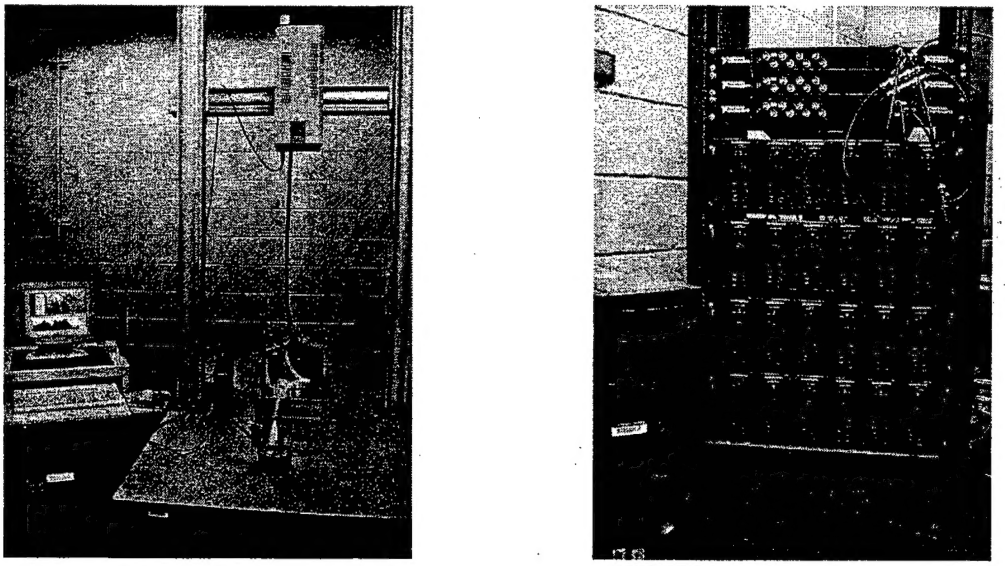

(a) Vibration Isolation Table & Vibrometer System (b) Excitation Control System

Figure 3 Mistuning System Identification Laboratory Equipment

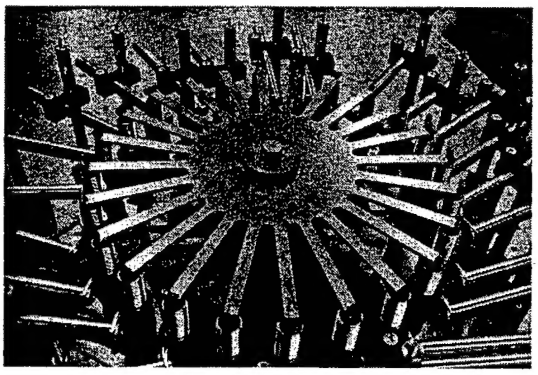

Figure 4 Academic IBR with Magnetic Exciters

3. RESULTING RESEARCH

We have used the Mistuning System Identification Laboratory extensively in our research at Carnegie Mellon University. It has contributed to the research discussed in the following papers.

1. Feiner, D.M. and Griffin, J.H., 2004, "Mistuning Identification of Bladed Disks Using a Fundamental Mistuning Model – Part I: Theory and Part II: Application", *ASME Journal of Turbomachinery,* Vol. 126, pp. 150 – 158 and 159-165.
2. D.M. Feiner, J.H. Griffin, K.W. Jones, J.A. Kenyon, O. Mehmed and A.P. Kurkov, 2003, "System Identification of Mistuned Bladed Disks from Traveling Wave Response Measurements," Proceedings of the 2003 ASME Design Engineering Technical Conference, Chicago, IL, ASME Paper DETC 2003/VIB-48448.
3. Ayers J.P., Feiner D.M, and Griffin, J.H., 2004, "A Reduced Order Model For Transient Analysis Of Bladed Disk Forced Response," 9th National Turbine Engine High Cycle Fatigue (HCF) Conference, Pinehurst ,NC.
4. Rossi, M.R., Feiner, D.M., and Griffin, J.H., 2004, "Experimental Study Of The Fundamental Mistuning Model For Probabilistic Analysis," 9th National Turbine Engine High Cycle Fatigue (HCF) Conference, Pinehurst ,NC.

Copies of these papers are provided in Attachment 2.

ATTACHMENT 1

EQUIIPMENT PURCHASED USING DURIP FUNDS

PACKING SLIP

Polytec PI

SHIP TO:
CARNEGIE MELLON UNIVERSITY
MECHANICAL ENGINEERING DEPT.
REF: PO# 127603
HAMERSCHLAG HALL C124
PITTSBURGH, PA 15213

BILL TO:
CARNEGIE MELLON UNIVERSITY
ATTN : ACCOUNTS PAYABLE
5000 FORBES AVENUE
PITTSBURGH, PA 15213-3890

ORDER INFORMATION:
23 Midstate Drive
Suite 212
Auburn, MA 01501
PH: (508) 832-3456
FX: (508) 832-0506

REMIT PAYMENT TO:
1342 BELL AVE.
SUITE 3-A
TUSTIN, CA 92780
PH: (714) 850-1835
FX: (714) 850-1831

7/1/02

Invoice No:
Shipping Date: 7/1/02
Order Number: 10591
Cust. PO# Date: 5/31/02
Customer PO: 127603
Ship Via: UPS GROUND
Invoice Terms: NET 30 DAYS
Customer No: CA0218
Sales Rep: DEO

QUANTITY ORDERED	QUANTITY SHIPPED	QUANTITY B/O	MODEL NUMBER	DESCRIPTION	UNIT PRICE	TOTAL
1	1	0	PSV-300-H	VIBRASCAN LASER VIBROMETE		
1	1	0	PSV-300-H-B	PSV-300 HARDWARE ID-31960		
1	1	0	PSV-300-H-S	PSV-300 SOFTWARE ID-31981		
1	1	0	PSV-Z-082	VIS.BASIC ENGINE ID-32548		
1	1	0	PSV-Z-061	UFF SOFTWARE ID-31057		
1	1	0	PSV-Z-062	PROF.GRID LAYOUT ID-31616		
1	1	0	PSV-SOFTDESK	DESKTOP VERSION ID-32609		
1	1	0	PSV-Z-066	HIGH RES. SCAN ID-31058		
1	1	0	PSV-Z-070-H	ZOOM FFT SOFTWRE ID-32142		
1	1	0	PSV-Z-081	HIGH RES. FFT ID-32122		
1	1	0	PSV-108	HD TRIPOD W/MOTR.PAN/TILT		
1	1	0	OFV-056-CF99	CLOSE-UP MODULE ID-32205		
1	1	0	PSV-Z-035	CART FOR PSV-300 ID-30639		
1	1	0	PSV-Z-018	VERT. TEST STAND ID-32336		
1	1	0	PSV-TTT-1	1 DAY TRAINING/INSTALLATI		
1	1	0	PSV-300-SM12	12 MTH.SFT.MAINT.ID-31991		
1	1	0	PSV-EW-300-H	1-YR EXT.HARDWARE WARRANT		
1	1	0	OMB-PSV-4	SET OF FOUR CASES		
1	1	0	PSV-Z-061-D	DSKTOP VER.W/UFF ID-32606		
1	1	0	OFV-CL-80	80MM CLOSEUP LNS ID-31551		
1	1	0	OFV-CL-150	SM. PART LENS ID-32226		
1	1	0	OMB-LUZ	RING LIGHT ILLUMINATOR		

Software

PSV-300 HARDWARE CONSIST OF:
OFV-3001-SH6 VIBROMETER CONTROLLER SN:5021175
OFV-056 SCANNING HEAD SN:6020966
OFV-056-CF99 CLOSE-UP UNIT SN:60120380008
PSV-PC-H COMPUTER CONSOLE SN:5021121
PSV-Z-040-H JUNCTION BOX SN:50207500004
PSV-Z-051 REMOTE FOCUS HANDSET SN:50151800045
OFV-303S SENSOR HEAD SN:6020922

PACKING SLIP

Polytec PI

SHIP TO:
CARNEGIE MELLON UNIVERSITY
MECHANICAL ENGINEERING DEPT.
REF: PO# 127603
HAMERSCHLAG HALL C124
PITTSBURGH, PA 15213

BILL TO:
CARNEGIE MELLON UNIVERSITY
ATTN : ACCOUNTS PAYABLE
5000 FORBES AVENUE
PITTSBURGH, PA 15213-3890

ORDER INFORMATION:
23 Midstate Drive
Suite 212
Auburn, MA 01501
PH: (508) 832-3456
FX: (508) 832-0506

REMIT PAYMENT TO:
1342 BELL AVE.
SUITE 3-A
TUSTIN, CA 92780
PH: (714) 850-1835
FX: (714) 850-1831

Invoice No:	7/1/02
Shipping Date:	
Order Number:	10591
Cust. PO# Date:	5/31/02
Customer PO:	127603
Ship Via:	UPS GROUND
Invoice Terms:	NET 30 DAYS
Customer No:	CA0218
Sales Rep:	DEO

QUANTITY ORDERED	QUANTITY SHIPPED	QUANTITY B/O	MODEL NUMBER	DESCRIPTION	UNIT PRICE	TOTAL

OMB-LUZ FIBER-OPTIC RING LIGH SN:126534
PSV-Z-035 PSV MOBILE CABINET SN;N/A
VIEWSONIC VG150 COMPUTER MINITOR SN:GQ14851965
CHERRY D91275 COMPUTER KEYBOARD SN:G026432
MICROSOFT INTELLIMOUSE COMPUTER MOUSE SN:5354164
PSV-300-H PSV-300 HARDLOCK SN: RUS-00000219
PSV-DESKTOP DESKTOP HARDLOCK SN:RUS-0000021A
PT570-24P MOTORIZED PAN/TILT HEAD SN:01036-14-0012
PSV-108 HEAVY DUTY TRIPOD SN:132X/MB28
PSV-Z-017 PAN /TILT HEAD INTERFACE PLATE SN:N/A
PSV-Z-020-A TRIPOD ADAPTER PLATE SN:N/A
PSV-Z-018 VERTICAL TEST STAND SN:60209480002
PSV-Z-018(CONT'D) CONTROL UNIT SN:3255312
OMB-PSV-4 SET OF 4 PSV CASES SN:N/A

Freight

Comment:
GARY HAYDEN 412-268-6248 / 362-1724

COMMENT ON COSTS

There were two complications that initially affected the cost of the vibrometer.

1. We received several different invoices from the manufacturer of the Polytec vibrometer. Initially, they included charges for shipping that were not consistent with their original quote and that caused the cost to exceed the funds provided by the DURIP grant. Eventually, we worked out the problem so that the actual cost matched their quote.
2. CMU normally charges overhead on maintenance contracts and the purchase of the Polytec vibrometer included $8,285 for a maintenance contract. The overhead charge was $4,143. The cost of the CMU overhead was not included in the DURIP proposal and this would have cause a cost over run. However, it was pointed out to the CMU finance person that the cost of the maintenance contract was included in the original proposal and that CMU had signed off on the budget without an overhead charge. As a result, CMU agreed to cost sharing the indirect (overhead) costs.

A copy of the "Project Detail Report" for January 2004 is provided on the next page and documents that the total cost was equal to the grant amount of $213,630.

Jan 04

CARNEGIE MELLON

Report Date: 05-FEB-04 01:13 AM
Report Page: 2

PROJECT DETAIL REPORT - PROJECT NUMBER: 8605

Project Number: 8605
Project Name: MECH ENG-GRIFFIN-AF EQUIPMENT
Project Org : MECHANICAL ENGINEERING
Project Manager : DUBRAWSKI, JOANNE
Project Type: SPONSORED
Budget Type: AC

Funding Source : AIR FORCE OFFICE OF SCIENTIFIC RESEARCH
Project Start Date: 01-MAY-02
Project End Date:
Current Month : Jan04-04
Begin Month:
End Month:
Project Funding Amount : $213,630.00

Project Number: 8605
Project Name: MECH ENG-GRIFFIN-AF EQUIPMENT
Project Org : MECHANICAL ENGINEERING
Project Manager : FRANCIS, JANET G
Project Type: SPONSORED
Budget Type: AC

Funding Source : AIR FORCE OFFICE OF SCIENTIFIC RESEARCH
Project Start Date: 01-MAY-02
Project End Date:
Current Month : Jan04-04
Begin Month:
End Month:
Project Funding Amount : $213,630.00

	INCEPTION TO Jan04-04					TOTAL PROJECT			
	(A) Month Actuals Jan04-04	(B) Total Actuals	(C) Total Open Encumbrance	(D)=(B)+(C) Total Act Plus Encumbrance	(E) Total Approved Cost Budget	(F)=(E)-(D) Total Budget Remaining	(G) Total Approved Cost Budget	(H) Total Detail Forecast	(I) Total Actual Plus Detail	(J)=(G)-(I) Total Forecast Variance
EXPENDITURES										
OTHER DIRECT COSTS										
OPERATING EXPENSES										
EQUIPMENT MAINT CONTRACTS	0	8,285	0	8,285	0	(8,285)				
TOTAL OPERATING EXPENSES	0	8,285	0	8,285	0	(8,285)				
CAPITAL EXPENDITURES										
CAPITAL EQUIPMENT	0	179,295	0	179,295	213,630	34,335				
CAPITAL SOFTWARE	0	26,050	0	26,050	0	(26,050)				
TOTAL CAPITAL EXPENDITURES	0	205,345	0	205,345	213,630	8,285				
TOTAL OTHER DIRECT COSTS	0	213,630	0	213,630	213,630	0				
TOTAL DIRECT COSTS	0	213,630	0	213,630	213,630	0				
INDIRECT COSTS										
FACILITIES & ADMINISTRATION	0	4,143	0	4,143	0	(4,143)				
F&A EXCEPTIONS	0	(4,143)	0	(4,143)	0	4,143				
TOTAL INDIRECT COSTS	0	0	0	0	0	0				
TOTAL EXPENDITURES	0	213,630	0	213,630	213,630	0				

Note : Favorable Variance - no parenthesis

ATTACHMENT 2

Relevant Publications

Mistuning Identification of Bladed Disks Using a Fundamental Mistuning Model—Part I: Theory

D. M. Feiner

J. H. Griffin

Department of Mechanical Engineering,
Carnegie Mellon University,
5000 Forbes Avenue,
Pittsburgh, PA 15213

This paper is the first in a two-part study of identifying mistuning in bladed disks. It develops a new method of mistuning identification based on measurements of the vibratory response of the system as a whole. As a system-based method, this approach is particularly suited to integrally bladed rotors, whose blades cannot be removed for individual measurements. The method is based on a recently developed reduced order model of mistuning called the fundamental mistuning model (FMM) and is applicable to isolated families of modes. Two versions of FMM system identification are presented: a basic version that requires some prior knowledge of the system's properties, and a somewhat more complex version that determines the mistuning completely from experimental data. [DOI: 10.1115/1.1643913]

1 Introduction

Bladed disks used in turbine engines are nominally designed to be cyclically symmetric. If this were the case, then all blades would respond with the same amplitude when excited by a traveling wave. However, in practice, the resonant amplitudes of the blades are very sensitive to small changes in their properties. Therefore, the small variations that result from the manufacturing process and wear cause some blades to have a significantly higher response and may cause them to fail from high cycle fatigue. This phenomenon is referred to as the mistuning problem, and has been studied extensively. Srinivasan provides a thorough review of this topic in [1].

To address the mistuning problem, researchers have developed reduced-order models (ROMs) of the bladed disk. These ROMs have the structural fidelity of a finite element model of the full rotor, while incurring computational costs that are comparable to that of a mass-spring model, [2–5]. In numerical simulations, most published ROMs have correlated extremely well with numerical benchmarks. However, some models have at times had difficulty correlating with experimental data, [6]. These results suggest that the source of the error may lie in our inability to determine the correct input parameters to the ROMs.

The standard method of measuring mistuning in rotors with attachable blades is to mount each blade in a broach block and measure its natural frequency. The difference of each blade's natural frequency from the mean value is then taken as a measure of the mistuning. However, the mistuning measured through this method may be significantly different from the mistuning present once the blades are mounted on the disk. This variation in mistuning can arise because each blade's frequency is dependent on the contact conditions at the attachment. Not only may the blade-broach contact differ from the blade-disk contact, but the contact conditions can also vary from slot-to-slot around the wheel. Therefore, in order to accurately measure mistuning, we must develop methods that can make measurements of the blade-disk assembly as a whole.

Such holistic measurement techniques are particularly important for integrally bladed rotors, since their blades cannot be removed for individual measurement. In this paper, we present a new method of identifying mistuning in bladed disks that is based on the vibration characteristics of the whole system. The key concept is that system modes are highly sensitive to small variations in mistuning. Consequently, the modes themselves provide a sensitive and accurate basis for identifying mistuning in the system.

Our method of system identification is based on a recently developed reduced order model called the fundamental mistuning model (FMM), [5], that accurately represents the vibratory response of an isolated family of modes. FMM is a highly reduced-order model that can completely describe a mistuned rotor using only its tuned system frequencies and the frequency mistuning of each blade/disk sector. As a result, when the FMM based identification method (FMM ID) is applicable, it is very easy to use and requires very little analytical information about the system, e.g., no finite element mass or stiffness matrices. We have developed two forms of FMM ID: a basic version of FMM ID that requires some information about the system properties, and a somewhat more advanced version that is completely experimentally based. The basic FMM ID requires the frequencies of the tuned system[1] as input. Then, given measurements of a limited number of mistuned modes and frequencies,[2] FMM ID solves for the mistuned frequency of each sector. The advanced form of FMM ID uses measurements of some mistuned modes and frequencies to determine all of the parameters in FMM, i.e., the frequencies that the system would have if it were tuned as well as the mistuned frequency of each sector. Thus, the tuned system frequencies determined from the second method can also be used to validate finite element models of the nominal system.

Judge and Pierre have developed an approach for determining mistuning in IBRs, [7], that also uses mistuned modes and frequencies to infer the rotor's mistuning. However, it is based on a more complicated reduced-order model that results in a more complex methodology, and requires significantly more analytically generated input data to implement. However, it is not inherently limited to an isolated family of modes as is FMM ID. Mignolet and Rivas-Guerra have also studied mistuning identification, [8,9]. Their focus, however, was on discerning the difference between mass and stiffness mistuning in an isolated blade.

This paper is Part I of a two part investigation and develops the

Contributed by the International Gas Turbine Institute and presented at the International Gas Turbine and Aeroengine Congress and Exhibition, Atlanta, GA, June 16—19, 2003. Manuscript received by the IGTI Dec. 2002; final revision Mar. 2003. Paper No. 2003-GT-38952. Review Chair: H. R. Simmons.

[1]The frequencies of the tuned system are typically calculated using a finite element analysis of a single blade/disk sector with cyclic symmetric boundary conditions applied to the disk.

[2]The modes required in FMM ID are the circumferential modes that correspond to the tip displacement of each blade around the wheel.

theory of the FMM ID methods, then confirms their applicability with numerical test cases. The second paper, Part II, examines the application of the methods to actual hardware.

This paper is organized as follows. Section 2 presents the basic FMM ID theory, and provides numerical test cases of the method. In Section 3, we present the completely experimental version of FMM ID that also identifies the tuned system frequencies. Section 4 discusses an extrapolation method that allows mistuning measured at rest to be used to predict the response of a rotor at speed. Lastly, the key attributes of the method are summarized in Conclusions.

2 Basic FMM ID

This section presents the basic FMM ID method. The basic method uses tuned system frequencies along with measurements of the mistuned rotor's system modes and frequencies to infer mistuning.

2.1 Theory. The FMM ID method is derived from the fundamental mistuning model (FMM). The first part of this section describes the FMM method. Then we invert the equations to obtain a formulation that can be used for system identification.

2.1.1 FMM Method. FMM is a highly simplified reduced-order model that can accurately predict the vibratory response of realistic bladed disks in an isolated family of modes, [5]. FMM requires only two sets of input parameters to calculate the modes and natural frequencies of the mistuned system: the tuned system frequencies of one isolated family of modes, and the frequency deviation of each blade-disk sector. In Appendix A, we derived a more general form of the FMM modal equation than was given in [5] that is applicable to systems with more flexible disks. The more general modal equation is

$$(\mathbf{\Omega}^{\circ 2}+2\mathbf{\Omega}^{\circ}\bar{\mathbf{\Omega}}\mathbf{\Omega}^{\circ})\vec{\beta}_j=\omega_j^2\vec{\beta}_j. \tag{1}$$

The eigenvector of this equation, $\vec{\beta}_j$, contains weighting factors that describe the jth mistuned mode as a sum of tuned modes, i.e.,

$$\vec{\phi}_j=\sum_{m=0}^{N-1}\beta_{jm}\vec{\phi}_m^{\circ} \tag{2}$$

where $\vec{\phi}_m^{\circ}$ is the mth tuned mode of the family of interest. The corresponding eigenvalue, ω_j^2, is the jth mode's natural frequency squared.

The matrix of the eigenvalue problem contains two terms, $\mathbf{\Omega}^{\circ}$ and $\bar{\mathbf{\Omega}}$. $\mathbf{\Omega}^{\circ}$ is a diagonal matrix of the tuned system frequencies, ordered by ascending inter-blade phase angle of their corresponding mode. The notation $\mathbf{\Omega}^{\circ 2}$ is shorthand for $\mathbf{\Omega}^{\circ T}\mathbf{\Omega}^{\circ}$, which results in a diagonal matrix of the tuned system frequencies squared. The matrix $\bar{\mathbf{\Omega}}$ contains the discrete Fourier transforms (DFT) of the sector frequency deviations. $\bar{\mathbf{\Omega}}$ has the form

$$\bar{\mathbf{\Omega}}=\begin{bmatrix}\bar{\omega}_0 & \bar{\omega}_1 & \cdots & \bar{\omega}_{N-1}\\ \bar{\omega}_{N-1} & \bar{\omega}_0 & \cdots & \bar{\omega}_{N-2}\\ \vdots & \vdots & & \vdots\\ \bar{\omega}_1 & \bar{\omega}_2 & \cdots & \bar{\omega}_0\end{bmatrix} \tag{3}$$

where $\bar{\omega}_p$ is the pth DFT of the sector frequency deviations. Note that $\bar{\mathbf{\Omega}}$ is a circulant matrix, in which each column is equal to the previous column rotated down a row. Therefore, for an N bladed disk, it has only N distinct values.

One of the key changes in the generalized FMM is that it uses a new quantity called a "sector frequency deviation" as a measure of the mistuning for each blade-disk sector. In the original FMM formulation, mistuning was measured by blade frequency deviations. The advantage of the new mistuning measure is that it not only accounts for mistuning in the blade, but also captures mistuning in the disk as well as variations in the way the blades are attached to the disk. The definition of a sector frequency deviation is provided in Appendix A.

FMM treats the rotor's mistuning as a known quantity that it uses to determine the system's mistuned modes and frequencies. However, if we were to treat the mistuned modes and frequencies as known, we could solve the inverse problem to determine the rotor's mistuning. This is the basis of FMM ID.

2.1.2 Inversion of FMM Equation. This section manipulates the FMM equation of motion to solve for the mistuning in the rotor. Consider Eq. (1). All quantities are treated as known except $\bar{\mathbf{\Omega}}$, which describes the system's mistuning. Subtracting the $\mathbf{\Omega}^{\circ 2}$ term from both sides of (1) and regrouping terms yields

$$2\mathbf{\Omega}^{\circ}\bar{\mathbf{\Omega}}[\mathbf{\Omega}^{\circ}\vec{\beta}_j]=(\omega_j^2\mathbf{I}-\mathbf{\Omega}^{\circ 2})\vec{\beta}_j. \tag{4}$$

The bracketed quantity on the left-hand side of (4) contains a known vector, which will be denoted as $\vec{\gamma}_j$,

$$\vec{\gamma}_j=\mathbf{\Omega}^{\circ}\vec{\beta}_j. \tag{5}$$

Thus, $\vec{\gamma}_j$ simply contains the modal weighting factors, $\vec{\beta}_j$, scaled on an element-by-element basis by their corresponding natural frequencies. Substituting $\vec{\gamma}_j$ into (4) yields

$$2\mathbf{\Omega}^{\circ}[\bar{\mathbf{\Omega}}\vec{\gamma}_j]=(\omega_j^2\mathbf{I}-\mathbf{\Omega}^{\circ 2})\vec{\beta}_j. \tag{6}$$

Consider the bracketed term of this expression. After some algebra, it can be shown that this product may be rewritten in the form

$$\bar{\mathbf{\Omega}}\vec{\gamma}_j=\mathbf{\Gamma}_j\vec{\bar{\omega}} \tag{7}$$

where the vector $\vec{\bar{\omega}}$ equals $[\bar{\omega}_0,\bar{\omega}_1\ldots\bar{\omega}_{N-1}]^T$. The matrix $\mathbf{\Gamma}_j$ is composed from the elements in $\vec{\gamma}_j$ and has the form

$$\mathbf{\Gamma}_j=\begin{bmatrix}\bar{\gamma}_{j0} & \bar{\gamma}_{j1} & \cdots & \bar{\gamma}_{j(N-1)}\\ \bar{\gamma}_{j1} & \bar{\gamma}_{j2} & \cdots & \bar{\gamma}_{j0}\\ \vdots & \vdots & & \vdots\\ \bar{\gamma}_{j(N-1)} & \bar{\gamma}_{j0} & \cdots & \bar{\gamma}_{j(N-2)}\end{bmatrix} \tag{8}$$

where γ_{jn} denotes the nth element of the vector $\vec{\gamma}_j$; the $\vec{\gamma}_j$ elements are numbered from 0 to N-1.

Substituting (7) into (6) produces an expression in which the matrix of mistuning parameters, $\bar{\mathbf{\Omega}}$, has been replaced by a vector of mistuning parameters, $\vec{\bar{\omega}}$

$$2\mathbf{\Omega}^{\circ}\mathbf{\Gamma}_j\vec{\bar{\omega}}=(\omega_j^2\mathbf{I}-\mathbf{\Omega}^{\circ 2})\vec{\beta}_j. \tag{9}$$

Observe that pre-multiplying (9) by $(2\mathbf{\Omega}^{\circ}\mathbf{\Gamma}_j)^{-1}$ would solve this expression for the DFT of the rotor's mistuning. Furthermore, the vector $\vec{\bar{\omega}}$ can then be related to the physical sector mistuning through an inverse discrete Fourier transform. However, (9) only contains data from one measured mode and frequency. Therefore, error in the mode's measurement may result in significant error in the predicted mistuning.

To minimize the effects of measurement error, we will incorporate multiple mode measurements into our solution for the mistuning. We construct (9) for each of the M measured modes, and combine them into the single matrix expression,

$$\begin{bmatrix}2\mathbf{\Omega}^{\circ}\mathbf{\Gamma}_1\\ 2\mathbf{\Omega}^{\circ}\mathbf{\Gamma}_2\\ \vdots\\ 2\mathbf{\Omega}^{\circ}\mathbf{\Gamma}_m\end{bmatrix}\vec{\bar{\omega}}=\begin{bmatrix}(\omega_1^2\mathbf{I}-\mathbf{\Omega}^{\circ 2})\vec{\beta}_1\\ (\omega_1^2\mathbf{I}-\mathbf{\Omega}^{\circ 2})\vec{\beta}_2\\ \vdots\\ (\omega_1^2\mathbf{I}-\mathbf{\Omega}^{\circ 2})\vec{\beta}_m\end{bmatrix}. \tag{10}$$

For brevity, we rewrite (10) as

$$\tilde{\mathbf{L}}\vec{\bar{\omega}}=\vec{\tilde{r}} \tag{11}$$

where $\tilde{\mathbf{L}}$ is the matrix on the left-hand side of the expression, and $\tilde{\vec{r}}$ is the vector on the right-hand side. The "~" is used to indicate that these quantities are composed by vertically stacking a set of submatrices or vectors.

Note that expression (11) is an over determined set of equations. Therefore, we can no longer solve for $\vec{\omega}$ by direct inverse. However, we can obtain a least squares fit to the mistuning, i.e.,

$$\vec{\omega} = Lsq\{\tilde{\mathbf{L}}, \tilde{\vec{r}}\}. \tag{12}$$

Equation (12) produces the vector $\vec{\omega}$ that best fits all the measured data. Therefore, the error in each measurement is compensated for by the balance of the data. The vector $\vec{\omega}$ can then be related to the physical sector mistuning through the inverse transform,

$$\Delta\omega_{\psi}^{(s)} = \sum_{p=0}^{N-1} e^{-isp2\pi/N}\bar{\omega}_p \tag{13}$$

where $\Delta\omega_{\psi}^{(s)}$ is the sector frequency deviation of the sth sector. The following section describes how Eqs. (12) and (13) can be applied to determine a rotor's mistuning.

2.1.3 Experimental Application. In order to solve Eqs. (12) and (13) for the sector mistuning, we must first construct $\tilde{\mathbf{L}}$ and $\tilde{\vec{r}}$ from the tuned system frequencies and the mistuned modes and frequencies. The tuned system frequencies can be calculated through finite element analysis of a tuned, cyclic symmetric, single blade/disk sector model. However, the mistuned modes and frequencies must be obtained experimentally.

The modes used by FMM ID are circumferential modes, corresponding to the tip displacement of each blade on the rotor. Since FMM ID is designed for isolated families of modes, it is sufficient to measure the displacement of only one point per blade. In practice, modes and frequencies are obtained by first measuring a complete set of frequency response functions (FRFs). Then, the modes and frequencies are extracted from the FRFs using modal curve fitting software.

The mistuned frequencies obtained from the measurements appear explicitly in the FMM ID equations as ω_j. However, the mistuned modes enter into the equations indirectly through the modal weighting factors $\vec{\beta}_j$. As described by Feiner and Griffin [5], each vector $\vec{\beta}_j$ is obtained by taking the inverse discrete Fourier transform of the corresponding single point-per-blade mode, i.e.,

$$\beta_{jn} = \sum_{m=0}^{N-1} \phi_{jm} e^{-imn2\pi/N}. \tag{14}$$

These quantities may then be used with the tuned system frequencies to construct $\tilde{\mathbf{L}}$ and $\tilde{\vec{r}}$ as outlined in earlier portions of this section. Finally, (12) and (13) may be solved for the sector mistuning.

This process is demonstrated through the two examples in the following section.

2.2 Numerical Examples. This section presents two numerical examples of the basic FMM ID method. In the first example, we consider an integrally bladed compressor whose blades are geometrically mistuned. The sector frequency deviations identified by FMM ID are verified by comparing them with values directly determined by finite element analyses. The second test case highlights FMM ID's ability to detect mistuning caused by variations at the blade-disk interface.

2.2.1 Geometric Blade Mistuning. Consider the finite element model of the twenty blade compressor shown in **Fig. 1.** Although the airfoils on this model are simply flat plates, the rotor design reflects the key dynamic behaviors of a modern, integrally bladed compressor. We mistuned the rotor through a combination of geometric and material property changes. Approximately one-third of the blades were mistuned through length variations, one-third through thickness variations, and one-third through elastic modulus variations. The magnitudes of the variations were chosen so that each form of mistuning would contribute equally to a 1.5% standard deviation in the sector frequencies.

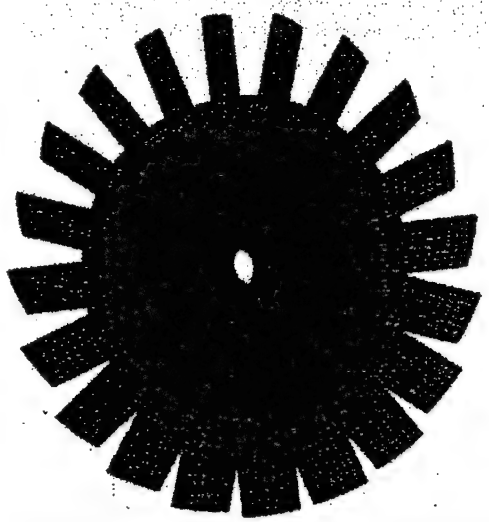

Fig. 1 Finite element model used to represent compressor

We first performed a finite element analysis of the tuned rotor, and generated its nodal diameter map, **Fig. 2.** Observe that the lowest frequency family of first bending modes is isolated, and is therefore a good candidate for FMM ID. The sector mistuning of this rotor was then determined through two different methods: finite element analyses of the mistuned sectors using the commercially available ANSYS finite element code, and FMM ID.

The finite element calculations serve as a benchmark to assess the accuracy of the FMM ID method. In the benchmark, a finite element model was made for each mistuned blade. In the model the blade is attached to a single disk sector. The frequency change in the mistuned blade/disk sector was then calculated with various cyclic symmetric boundary conditions applied to the disk. It was found that the phase angle of the cyclic symmetric constraint had little effect on the frequency change caused by blade mistuning. The values quoted in this paper are for a disk phase constraint of 90 deg, i.e., for the five nodal diameter mode.

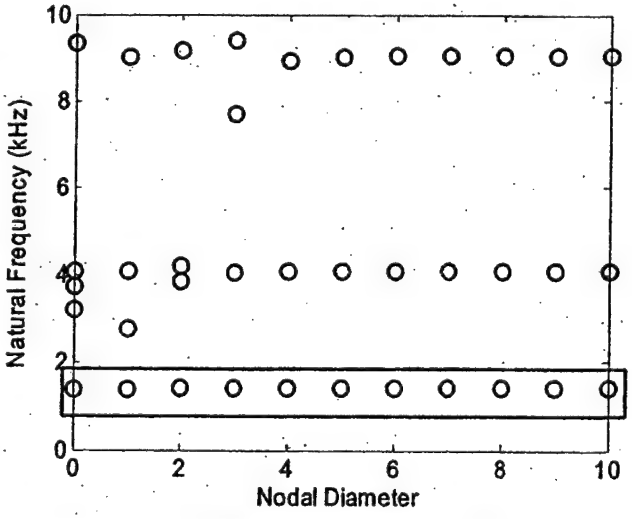

Fig. 2 Natural frequencies of the compressor with no mistuning

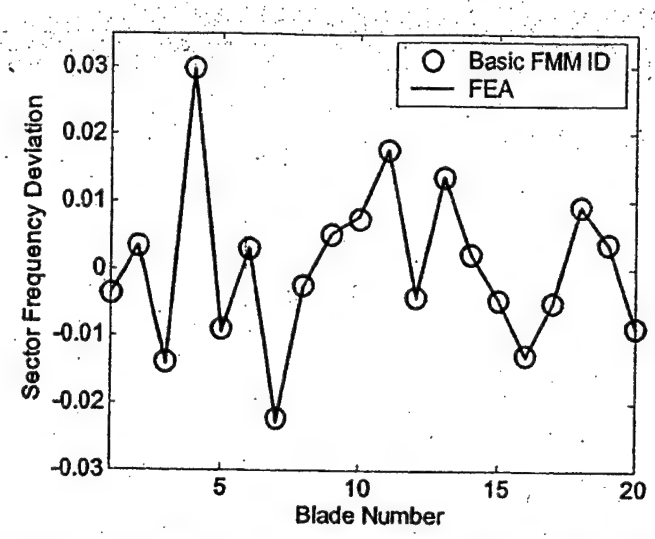

Fig. 3 Comparison of mistuning from FMM ID with FEM benchmark

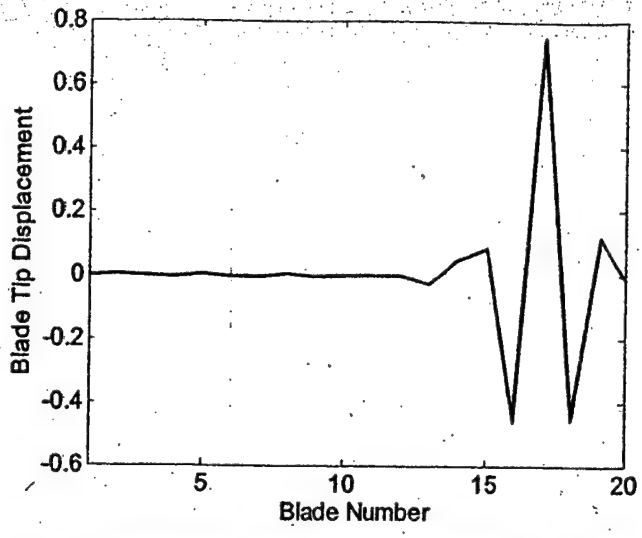

Fig. 5 Representative mistuned mode caused by stagger angle mistuning

A finite element model of the full, mistuned bladed disk was also constructed and used to compute its mistuned modes and natural frequencies. The modes and frequencies were used as input data for FMM ID. In an actual experiment, the mistuned modes and frequencies would be obtained through a modal fit of the rotor's frequency response functions. Typically, the measurements will not detect modes that have a node point at the excitation source. To reflect this phenomenon in our numerical test case, we eliminated all mistuned modes that had a small response at blade one. This left 16 modes and natural frequencies to apply to FMM ID.

The mistuned modes and frequencies were combined with the tuned system frequencies of the fundamental mode family to construct the basic FMM ID equations, (10). These equations were solved using a least-squares fit. The solution was then converted to the physical sector frequency deviations through the inverse transform given in (13).

Figure 3 shows the comparison between the sector mistuning calculated directly by finite element simulations of each mistuned blade/sector and the mistuning identified by FMM ID. The two results are in good agreement.

2.2.2 Stagger Angle Mistuning. One of the key differences between FMM ID and other mistuning identification methods is its measure of mistuning. FMM ID uses a frequency quantity that characterizes the mistuning of an entire blade-disk sector. Other methods in the literature consider mistuning to be confined to the blades, [7]. The advantage of the sector frequency approach used by FMM is that it not only identifies the mistuning in the blades, but it also captures the mistuning in the disk and the blade-disk interface. To highlight this capability, the following example considers a rotor in which the blades are identical except they are mounted on the disk with slightly different stagger angles. **Figure 4** schematically illustrates a rotor with exaggerated stagger angle variations as viewed from above.

Consider the compressor shown in **Fig. 1.** To mistune this rotor, we randomly altered the stagger angle of each blade with a maximum variation of ±4 deg. Otherwise the blades are identical. The modes of the system were then calculated using the ANSYS finite element code. **Figure 5** shows a representative mode. Observe that the mode is localized, indicating that varying the stagger angles does indeed mistune the system.

We then used the mistuned modes and frequencies calculated by ANSYS to perform an FMM ID analysis of the mistuning. The resulting sector frequency deviations are plotted as the solid line in **Fig. 6.** The squares correspond to the stagger angle variations applied to each blade. The vertical axes have been scaled so that the maximum frequency and angle variation data points (blade 14) are coincident. This was done to highlight the fact that the stagger angle variations are proportional to the sector frequency deviations detected by FMM ID. Thus, not only can FMM ID accurately detect mistuning in the blades, as illustrated in the previous example, but it can also accurately detect other forms of mistuning such as variation in the blade stagger angle.

3 A Completely Experimental Method of Identification

The basic FMM ID method presented in Section 2 provides an effective means of determining the mistuning in an IBR. This

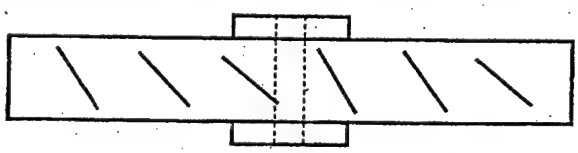

Fig. 4 Illustration of a rotor with exaggerated stagger angle mistuning

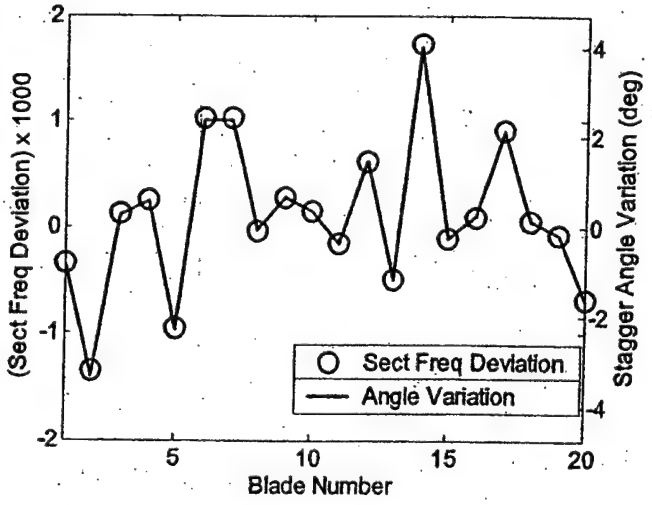

Fig. 6 Comparison of mistuning from FMM ID and the variations in the stagger angles

technique requires a set of simple vibration measurements and the natural frequencies of the tuned system. However, at times neither the tuned system frequencies nor a finite element model from which to obtain them are available to researchers interested in determining an IBR's mistuning. Furthermore, even if a finite element model is available, there is often concern as to how accurately the model represents the actual rotor. Therefore, we have developed an alternative FMM ID method that does not require any analytical data. The approach requires only a limited number of mistuned modes and frequency measurements to determine a bladed disk's mistuning. Furthermore, the method also identifies the bladed disk's tuned system frequencies. Thus, it not only serves as a method of identifying mistuning the system, but can also provide a method of corroborating the finite element model of the tuned system.

3.1 Theory. This version of FMM ID is derived from the basic FMM ID equations. Recall that an important step in the development of the basic FMM ID theory was to transform the mistuning matrix $\bar{\Omega}$ into a vector form. Once we expressed the mistuning as a vector, it could then be calculated using standard methods from linear algebra. A similar approach is used in the current development to solve for the tuned system frequencies. However, the resulting equations are nonlinear, and require a more sophisticated solution approach.

3.1.1 Development of Nonlinear Equations. Consider the basic FMM ID equation given in (9). Moving the $\Omega^{\circ 2}$ term to the left-hand side, the expression becomes

$$\Omega^{\circ 2}\vec{\beta}_j + 2\Omega^{\circ}\Gamma_j\vec{\bar{\omega}} = \omega_j^2\vec{\beta}_j. \tag{15}$$

We assume that from measurement of the mistuned modes and frequencies, $\vec{\beta}_j$ and ω_j are known. All other quantities are unknown. Note that although Γ_j is not known, the matrix contains elements from $\vec{\beta}_j$. Therefore, we do have some knowledge of the matrix.

After some algebra, one can show that the term $\Omega^{\circ 2}\vec{\beta}_j$ may be re-expressed as

$$\Omega^{\circ 2}\vec{\beta}_j = \mathbf{B}_j\vec{\lambda}^{\circ} \tag{16}$$

where $\vec{\lambda}^{\circ}$ is a vector of the tuned frequencies squared, and $\mathbf{B}_j$ is a matrix composed from the elements of $\vec{\beta}_j$. If we define η to be the maximum number of nodal diameters on the rotor, i.e., η=N/2 if N is even or (N-1)/2 if N is odd, then $\vec{\lambda}^{\circ}$ is given by

$$\vec{\lambda}^{\circ} = \begin{bmatrix} \omega_{0ND}^{\circ 2} \\ \omega_{1ND}^{\circ 2} \\ \vdots \\ \omega_{\eta ND}^{\circ 2} \end{bmatrix}. \tag{17}$$

For N even, the matrix $\mathbf{B}_j$ has the form

$$\mathbf{B}_j = \begin{bmatrix} \beta_{j0} & & & & & \\ & \beta_{j1} & & & & \\ & & \beta_{j2} & & & \\ & & & \ddots & & \\ & & & & \beta_{j\eta} & \\ & & & \iddots & & \\ & & \beta_{j2} & & & \\ & \beta_{j1} & & & & \end{bmatrix}. \tag{18}$$

A similar expression can be derived for N odd.

Substituting (16) into (15) and regrouping the left-hand side results in a matrix equation for the tuned frequencies squared and the sector mistuning,

$$[\mathbf{B}_j \;\; 2\Omega^{\circ}\Gamma_j]\begin{bmatrix} \vec{\lambda} \\ \vec{\bar{\omega}} \end{bmatrix} = \omega_j^2\vec{\beta}_j. \tag{19}$$

Equation (19) contains information from only one of the M measured modes and frequencies. However, (19) can be constructed for each measured mode, and combined into the single matrix expression

$$\begin{bmatrix} \mathbf{B}_1 & 2\Omega^{\circ}\Gamma_1 \\ \mathbf{B}_2 & 2\Omega^{\circ}\Gamma_2 \\ \vdots & \vdots \\ \mathbf{B}_M & 2\Omega^{\circ}\Gamma_M \end{bmatrix}\begin{bmatrix} \vec{\lambda} \\ \vec{\bar{\omega}} \end{bmatrix} = \begin{bmatrix} \omega_1^2\vec{\beta}_1 \\ \omega_2^2\vec{\beta}_2 \\ \vdots \\ \omega_M^2\vec{\beta}_M \end{bmatrix}. \tag{20}$$

Thus we have formed a single expression that incorporates all of the measured data. For brevity, (20) is rewritten as

$$[\tilde{\mathbf{B}} \;\; 2\widetilde{(\Omega^{\circ}\Gamma)}]\begin{bmatrix} \vec{\lambda} \\ \vec{\bar{\omega}} \end{bmatrix} = \vec{\tilde{r}}' \tag{21}$$

where $\tilde{\mathbf{B}}$ is the stacked matrix of $\mathbf{B}_j$, the term $\widetilde{(\Omega^{\circ}\Gamma)}$ is the stacked matrix of $\Omega^{\circ}\Gamma_j$, and $\vec{\tilde{r}}'$ is the right-hand side of (20).

To complete our formulation, we must introduce an additional constraint equation. It is required because the Eqs. (21) are underdetermined. To understand the cause of this indeterminacy, consider a rotor in which each sector is mistuned the same amount. Due to the symmetry of the mistuning, the rotor's mode shapes will still look tuned, but its frequencies will be shifted. If one has no prior knowledge of the tuned system frequencies, there is no way to determine that the rotor has in fact been mistuned. The same difficulty arises in solving (21) since there is no way to distinguish between a mean shift in the mistuning and a corresponding shift in the tuned system frequencies. To eliminate this ambiguity, we will define mistuning so that it has a mean value of zero.

Mathematically, a zero mean in the mistuning translates to prescribing the first element of $\vec{\bar{\omega}}$ to be zero. With the addition of this constraint, (21) takes the form

$$\begin{bmatrix} \tilde{\mathbf{B}} & 2\widetilde{(\Omega^{\circ}\Gamma)} \\ 0 & \vec{c} \end{bmatrix}\begin{bmatrix} \vec{\lambda}^{\circ} \\ \vec{\bar{\omega}} \end{bmatrix} = \begin{bmatrix} \vec{\tilde{r}} \\ 0 \end{bmatrix} \tag{22}$$

where $\vec{c}$ is a row vector whose first element is 1 and whose remaining elements are zero.

3.1.2 Iterative Solution Method. Consider Eq. (22). If the term $\widetilde{(\Omega^{\circ}\Gamma)}$ were known, then we could obtain a least-squares solution for the tuned eigenvalues $\vec{\lambda}^{\circ}$ and the DFT of the sector mistuning $\vec{\bar{\omega}}$. However, since $\widetilde{(\Omega^{\circ}\Gamma)}$ is based in part on the unknown quantities $\vec{\lambda}^{\circ}$, the equations are nonlinear. Therefore, we must use an alternative solution method. This section describes how these equations may be solved using an iterative approach.

In iterative form, the least squares solution to (22) can be written as

$$\begin{bmatrix} \vec{\lambda}^{\circ} \\ \vec{\bar{\omega}} \end{bmatrix}_{(k)} = Lsq\left\{\begin{bmatrix} \tilde{\mathbf{B}} & 2\widetilde{(\Omega^{\circ}\Gamma)}_{(k-1)} \\ 0 & \vec{c} \end{bmatrix}, \begin{bmatrix} \vec{\tilde{r}} \\ 0 \end{bmatrix}\right\} \tag{23}$$

where the subscripts indicate the iteration number. For each iteration, we then construct a new matrix $\widetilde{(\Omega^{\circ}\Gamma)}$ based on the previous iteration's solution for $\vec{\lambda}^{\circ}$. This process is repeated until we obtain a converged solution. With a good initial guess, this method typically converges within a few iterations. Appendix B describes an effective approach for obtaining a good initial guess.

3.2 Numerical Test Case. This section presents a numerical example of the FMM ID method that identifies the tuned system frequencies as well as the mistuning. This example uses the geometrically mistuned compressor model presented in Section 2.

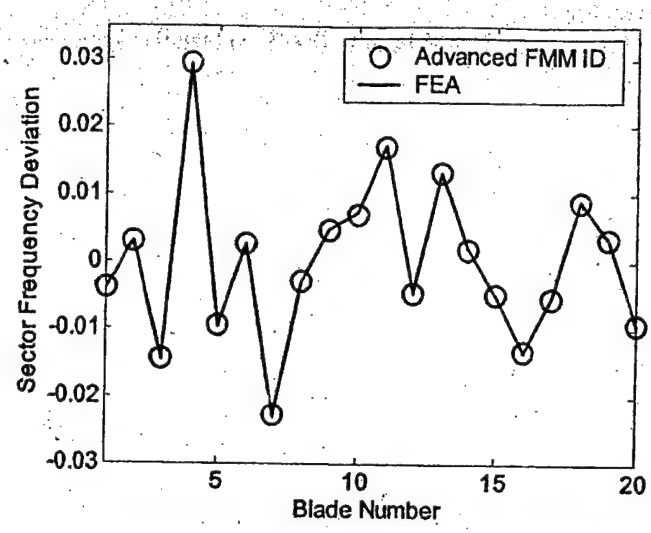

Fig. 7 Comparison of mistuning from FMM ID with FEM benchmark

The tuned system frequencies and sector mistuning identified by FMM ID are then compared with finite element results.

We calculated the modes and natural frequencies of the mistuned bladed disk using a finite element model of the mistuned system. We then converted the physical modes to vectors of modal weighting factors, $\vec{\beta}_j$, through (14). The weighting factors were used to form the elements of Eq. (48) in Appendix B which was solved to obtain an initial estimate of the tuned system frequencies. This was used as an initial guess to iteratively solve Eq. (23). The solution vector contains two parts: a vector of the tuned system frequencies squared, and a vector of the DFT of the sector frequency deviations. The sector mistuning was converted to the physical domain using the inverse transform (13).

The resulting sector frequency deviations are compared with the benchmark finite element values in **Fig. 7** using the same procedure as in Section 2.2. A comparison of the tuned frequencies identified by FMM ID and those computed directly with the finite element model is shown in **Fig. 8.** In each case the agreement is good.

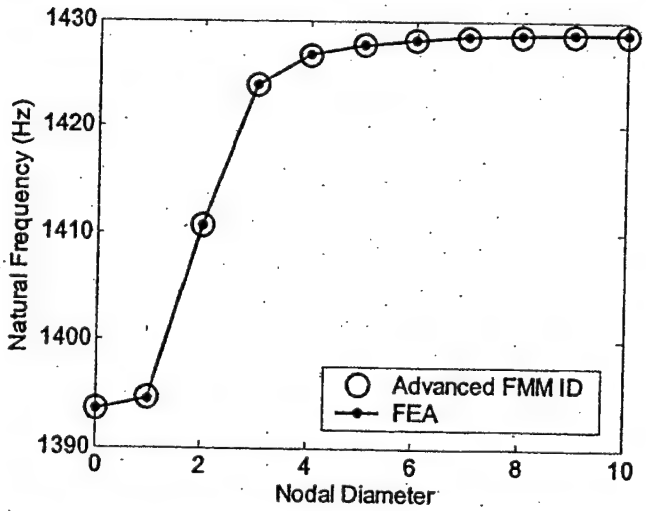

Fig. 8 Comparison of the tuned system frequencies from FMM ID and FEM

4 Response Prediction at Speed

The FMM ID methods presented in Sections 2 and 3 determine the mistuning in bladed disks while they are stationary. However, once the rotor is spinning, centrifugal forces can alter the effective mistuning in the rotor. Section 4.1 presents a method for approximately calculating the effect of rotational speed on mistuning. Then, in Section 4.2, we present a numerical example that applies this technique and then uses FMM to predict its forced response at speed. The accuracy of the method is assessed by comparing the results with a numerical benchmark.

4.1 Mistuning Extrapolation. Centrifugal effects cause the sector frequency deviations to change when the disk is rotating. This section gives a simple method for approximating the effect of rotational speed on mistuning. Details of the derivation are provided by Feiner [10]. Here we summarize the result.

To investigate centrifugal stiffening in [10] the blade is modeled as a pendulum, constrained to a rigid disk by a torsion spring. While the disk is at rest, the blade's frequency is perturbed (mistuned). Then, the model is used to determine the corresponding change in the blade's frequency when the disk is rotating. To first order one finds that

$$\Delta\omega(S)^{(s)} \approx \Delta\omega(0)^{(s)} \left[\frac{\omega^{*}_{\alpha ND}(0)^2}{\omega^{*}_{\alpha ND}(S)^2} \right] \tag{24}$$

where S is the rotation speed of the disk, $\Delta\omega(S)^{(s)}$ is the sector mistuning ratio of the sth sector and $\omega^{*}_{\alpha ND}(S)$ is the frequency of a representative tuned system mode. For example, in the case reported in 4.2, $\omega^{*}_{\alpha ND}(S)$ is the frequency of the system mode with a 90 deg interblade phase angle. A key result from (24) is that mistuning is larger at rest than at speed, and that this reduction in mistuning can be estimated by calculating how the tuned system frequencies change with speed. It has been confirmed that (24) works reasonably well for realistic geometric mistuning in real compressor blades, [10]. This will be also be demonstrated by the next example.

4.2 Numerical Test Case. This section uses a numerical test case that shows how FMM ID, Eq. (24), and the FMM forced response code can be combined to predict the response of a bladed disk under rotating conditions. Consider the geometrically mistuned rotor studied in Section 2.2.1, and illustrated in **Fig. 1.** This compressor has a 6th engine order crossing with the first bending modes at a rotational speed of 20,000 rpm. However, to create a more severe test case, we will proceed as if the crossing occurred at 40,000 rpm.

In order to use FMM to predict the rotor's forced response at this speed, we must provide the FMM prediction code, [5], with the bladed disk's tuned system frequencies and the sector frequency deviations that are present at 40,000 rpm. In Section 2.2.1 we determined these two sets of parameters at rest using ANSYS and Basic FMM ID, respectively. However, since both of these properties change with rotation speed, they must first be adjusted to reflect their values at 40,000 rpm.

To adjust the tuned system frequencies, we recalculated them in ANSYS using the centrifugal load option to simulate rotational effects. The centrifugal stiffening caused the tuned system frequencies to increase by about 30%. Then we used the change in the five nodal diameter, tuned system frequency and (24) to analytically extrapolate the sector frequency deviations to 40,000 rpm. In this case, the centrifugal loading reduces the mistuning ratios by about 40%.

Finally, the adjusted parameters were used with the FMM forced response code to calculate the rotor's response to a 6E excitation using the method described in [5]. As a benchmark, the forced response was also calculated directly in ANSYS using a full 360 deg mistuned finite element model. Tracking plots of the FMM and ANSYS results are shown in Fig. 9. For clarity, we

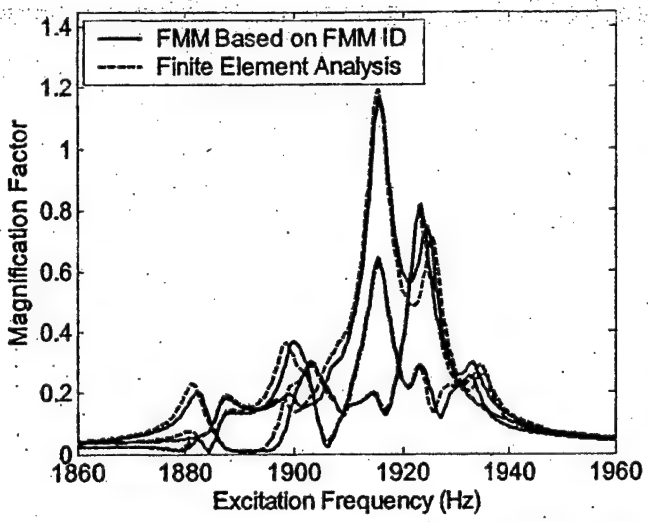

Fig. 9 Frequency response of blades to a six engine order excitation

have shown the response of only three blades: the high responding blade, the median responding blade, and the low responding blade. Observe that each blade's peak amplitude and the shape of its overall response as predicted by FMM agree well with the benchmark results. Thus, by combining FMM ID, the mistuning extrapolation equation, and FMM, we were able to identify the mistuning of a rotor at rest, and use it to accurately predict the system's forced response under rotating conditions.

5 Conclusions

A new method of identifying mistuning in bladed disks is developed. This approach is called FMM ID because it is based on the fundamental mistuning model (FMM). FMM and the methods presented in this paper are applicable to isolated families of modes. Often the frequencies of the first bending and first torsion families of modes satisfy this requirement. Identifying mistuning in these modes is important not only for predicting forced response, but also for predicting flutter. Since mistuning tends to stabilize flutter, the issue is how to relate a particular flutter test to the fleet as a whole. We are pursuing the application of FMM ID to the flutter problem in a joint research effort with Honeywell research engineers.

FMM ID uses measurements of the system mode shapes and natural frequencies to infer the rotor's mistuning. The key concept behind FMM ID is that the high sensitivity of system modes to small variations in mistuning, causes measurements of those modes themselves to be an accurate basis for mistuning identification. Since FMM ID does not require individual blade measurements, it is particularly suited to integrally bladed rotors. We have developed two forms of FMM ID: Basic FMM ID and a version that also identifies the frequencies of the tuned system.

Basic FMM ID uses tuned system frequencies from finite element analysis and measurements of the mistuned system modes and frequencies to determine a rotor's mistuning. The mistuned mode shape and frequencies can be measured with standard modal analysis techniques.

Since Basic FMM ID is derived from FMM, it requires very little analytical information. Specifically, it needs only the tuned system frequencies of the mode family of interest. Thus, for an N bladed disk, we only need approximately $N/2$ pieces of analytical data. These frequencies can be obtained from finite element analysis of a single-sector model using cyclic symmetric boundary conditions. The alternate form of FMM ID requires no analytical data. It relies solely on experimental measurements of the mistuned modes and frequencies. Thus, the second form of FMM ID can be used to identify mistuning even if a finite element model of the bladed disk is not available. Furthermore, this approach not only identifies the mistuning in a rotor, but it also infers its tuned system frequencies. Identifying the tuned system frequencies may be particularly useful for assessing the validity of a finite element model of the nominal system.

A number of numerical test cases are analyzed to demonstrate the applicability of the methods. One of these involve introducing mistuning by varying the stagger angle of each blade in what was otherwise a perfectly tuned system. FMM ID accurately detects the pattern of the stagger angle mistuning. This example is important because it illustrates the fact that mistuning in the bladed disk can be caused by sources that cannot be measured simply in terms of blade frequencies.

FMM ID can be used to identify the mistuning in a bladed disk when it is tested in the laboratory. A method has been demonstrated for approximating how centrifugal loading will change the mistuning when it is rotating in the engine. Other factors may also be present in the engine that can affect the mistuned response. These may include: temperature effects, gas bending stresses, how the disk is constrained in the engine, and how the teeth in the attachment change their contact if the blades are conventionally attached to the disk. Except for the constraints on the disk, these additional effects may be relatively unimportant in integrally bladed compressor stages. The disk constraints can be taken into account by performing the system ID on the IBR after the full rotor is assembled. Consequently, it seems feasible that the methodology presented in this paper can be used to predict the vibratory response of actual compressor stages. U.S. Air Force engineers have agreed to try this approach in forthcoming tests in the Compressor Research Facility (CRF) at Wright Patterson Air Force Base in Dayton, Ohio. If the approach proves successful, then the plan is to use the methodology to select which blades will be instrumented, interpret test data, and relate the vibratory response measured in the CRF to the vibration that will occur in the fleet as a whole.

Acknowledgments

The authors would like to acknowledge that this research was supported in part by the U.S. Air Force, contract number F33615-01-C-2186, under the direction of Dr. Charles Cross and by the GUIde Consortium.

The authors would also like to thank Prof. David J. Ewins of Imperial College, London, for stimulating discussions that helped lead to some of the concepts presented in this paper. Specifically, the idea of stagger angle mistuning used in this paper grew out of an observation by Professor Ewins that he had seen significant levels of mistuning in systems that had had the individual blades carefully tuned. It also lead us to broaden our concept of mistuning from simple blade mistuning used in [5] to the more general concept of sector mistuning as discussed in Appendix A.

Appendix A

A More General Form of FMM. This appendix presents the derivation of a more general form of the modal equation for the fundamental mistuning model (FMM) that is applicable to rotors with more flexible disks. The generalized FMM formulation differs from the original in two ways. First, it no longer approximates the tuned system frequencies by their average value. This allows for a much larger variation among the tuned frequencies. Second, rather than using the blade-alone mode as an approximation of the various nodal diameter sector modes, we now use a representative mode of a single blade-disk sector. Consequently, the approach now includes the disk portion of the mode shape, and thus allows for more strain energy in the disk.

The changes in the formulation also modify our measure of mistuning. In the original FMM form, we measured mistuning as a percent deviation in the blade-alone frequency. However, mistuning is now measured as a percent deviation the frequency of

each blade-disk sector. The advantage is that the sector frequency deviations not only capture mistuning in the blade, but can also capture mistuning in the disk as well as variations in the ways the blades are attached to the disk.

Section 1 of this appendix describes how the SNM approach, 11, is used to reduce the order of the mistuned free-response equations and formulates the problem in terms of reduced-order sector matrices. Section 2 relates the sector matrices to mistuned sector frequencies. Section 3 simplifies the resulting mathematical expressions.

1 Reduction of Order. Consider a mistuned, bladed disk in the absence of an excitation. The order of its equation of motion is reduced through a subset of nominal modes approach. The resulting reduced-order equation can be written as, 11:

$$[(\mathbf{\Omega}^{\circ 2}+\Delta\hat{\mathbf{K}})-\omega_j^2(\mathbf{I}+\Delta\hat{\mathbf{M}})]\vec{\beta}_j=0 \tag{25}$$

$\mathbf{\Omega}^{\circ 2}$ is a diagonal matrix of the tuned system eigenvalues,[3] and $\mathbf{I}$ is the identity matrix. $\Delta\hat{\mathbf{K}}$ and $\Delta\hat{\mathbf{M}}$ are the variations in the modal stiffness and modal mass matrices caused by stiffness and mass mistuning. The vector $\vec{\beta}_j$ contains weighting factors that describe the jth mistuned mode as a limited sum of tuned modes, i.e.,

$$\vec{\phi}_j=\mathbf{\Phi}^{\circ}\vec{\beta}_j \tag{26}$$

where $\mathbf{\Phi}^{\circ}$ is a matrix whose columns are a limited number of the tuned system modes.

Note that to first order, $(\mathbf{I}+\Delta\hat{\mathbf{M}})^{-1}\approx(\mathbf{I}-\Delta\hat{\mathbf{M}})$. Thus, by pre-multiplying (25) by $(\mathbf{I}+\Delta\hat{\mathbf{M}})^{-1}$ and keeping only first-order terms, the expression becomes

$$(\mathbf{\Omega}^{\circ 2}+\hat{\mathbf{A}})\vec{\beta}_j=\omega_j^2\vec{\beta}_j \tag{27}$$

where

$$\hat{\mathbf{A}}=\Delta\hat{\mathbf{K}}-\Delta\hat{\mathbf{M}}\mathbf{\Omega}^{\circ 2}. \tag{28}$$

Next, we will relate the matrix $\hat{\mathbf{A}}$ to the frequency deviations of the mistuned sectors.

2 Relating Mistuning to Sector Frequency Deviations. Relating $\hat{\mathbf{A}}$ to frequency deviations is a three-step process. First, the mistuning matrix is expressed in terms of the system mode shapes of an individual sector. Then, the system sector modes are related to the corresponding mode of a single, isolated sector. Finally, the resulting sector-mode terms in $\hat{\mathbf{A}}$ are expressed in terms of the frequency deviations of the sectors.

2.1 Relating mistuning to system sector modes. Consider the mistuning matrix, $\hat{\mathbf{A}}$, in (28). This matrix can be expressed as a sum of the contributions from each mistuned sector.

$$\hat{\mathbf{A}}=\sum_{s=0}^{N-1}\hat{\mathbf{A}}^{(s)} \tag{29}$$

where the superscript denotes that the mistuning corresponds to the sth sector. The expression for a single element of $\hat{\mathbf{A}}^{(s)}$ is

$$\hat{\mathbf{A}}_{mn}^{(s)}=\vec{\phi}_m^{\circ(s)H}(\Delta\mathbf{K}^{(s)}-\omega_n^{\circ 2}\Delta\mathbf{M}^{(s)})\vec{\phi}_n^{\circ(s)} \tag{30}$$

where $\Delta\mathbf{K}^{(s)}$ and $\Delta\mathbf{M}^{(s)}$ are the physical stiffness and mass perturbations of the sth sector. The modes $\vec{\phi}_m^{\circ(s)}$ and $\vec{\phi}_n^{\circ(s)}$ are the portions of the mth and nth columns of $\mathbf{\Phi}^{\circ}$ which describe the sth sector's motion. The term $\omega_n^{\circ 2}$ is the nth diagonal element of $\mathbf{\Omega}^{\circ 2}$.

Equation (30) relates the mistuning to the system sector modes. In the next section, these modes are related to the mode of a single isolated blade-disk sector.

[3]An eigenvalue is equal to the square of the natural frequency of a mode.

2.2 Relating system sector modes to an average sector mode The tuned modes in (30) are expressed in complex traveling wave form. Thus, the motion of the sth sector can be related to the motion of the 0th sector by a phase shift. This allows us to restate (30) as

$$\hat{\mathbf{A}}_{mn}^{(s)}=e^{is(n-m)2\pi/N}\vec{\phi}_m^{\circ(0)H}(\Delta\mathbf{K}^{(s)}-\omega_n^{\circ 2}\Delta\mathbf{M}^{(s)})\vec{\phi}_n^{\circ(0)}. \tag{31}$$

Because the tuned modes used in the SNM formulation are an isolated family of modes, the sector modes of all nodal diameters look nearly identical. Therefore, we can approximate the various sector modes by an average sector mode. Applying the average sector mode approximation for the system sector modes in (31), $\hat{\mathbf{A}}_{mn}^{(s)}$ can be written as

$$\hat{\mathbf{A}}_{mn}^{(s)}=\left(\frac{\omega_m^{\circ}\omega_n^{\circ}}{\omega_{\psi}^{\circ 2}}\right)e^{is(n-m)2\pi/N}[\vec{\psi}^{\circ(0)H}(\Delta\mathbf{K}^{(s)}-\omega_n^{\circ 2}\Delta\mathbf{M}^{(s)})\vec{\psi}^{\circ(0)}] \tag{32}$$

where $\vec{\psi}^{\circ(0)}$ is the average tuned system sector mode, and ω_{ψ}° is its natural frequency. In practice, $\vec{\psi}^{\circ(0)}$ can be taken to be the median modal diameter mode. The factor $(\omega_m^{\circ}\omega_n^{\circ})/(\omega_{\psi}^{\circ 2})$ scales the average sector mode terms so that they have the approximately the same strain energy as the sector modes they replace.

2.3 Introduction of sector frequency deviation. This version of FMM uses the deviation in a sector frequency quantity to measure mistuning. To understand this concept, consider an imaginary "test" rotor. In the test rotor every sector is mistuned in the same fashion, so as to match the mistuning in our sector of interest. Since our test rotor's mistuning is cyclically symmetric, its mode shapes are virtually identical to those of the tuned system. However, there will be a shift in the tuned system frequencies. For small levels of mistuning, the frequency shift is nearly the same in all of the tuned system modes and can be approximated by the fractional change in the frequency of the median nodal diameter mode.[4] Thus, the fractional shift in the median nodal diameter's frequency is taken as our measure of mistuning and is defined as the sector frequency deviation.

The bracketed terms of (32) are related to these frequency deviations in the following manner. Consider a bladed disk that is mistuned in a cyclic symmetric fashion, i.e., each sector undergoes the same mistuning. Its free-response equation of motion is given by the expression

$$[(\mathbf{K}^{\circ}+\Delta\mathbf{K})-\omega_n^2(\mathbf{M}^{\circ}+\Delta\mathbf{M})]\vec{\phi}_n=0. \tag{33}$$

Take the mode $\vec{\phi}_n$ to be the mistuned version of the tuned median nodal diameter mode, $\vec{\psi}^{\circ}$. $\vec{\psi}^{\circ}$ is the full system mode counterpart of the average sector mode $\vec{\psi}^{\circ(0)}$. Since mistuning is symmetric, the tuned and mistuned versions of the mode are nearly identical. Substituting $\vec{\psi}^{\circ}$ for $\vec{\phi}_n$ and pre-multiplying by $\vec{\psi}^{\circ H}$ yields

$$(\omega_{\psi}^{\circ 2}+\vec{\psi}^{\circ H}\Delta\mathbf{K}\vec{\psi}^{\circ})-\omega_n^2(1+\vec{\psi}^{\circ H}\Delta\mathbf{M}\vec{\psi}^{\circ})=0. \tag{34}$$

These terms may be rearranged to isolate the frequency terms

$$\vec{\psi}^{\circ H}(\Delta\mathbf{K}-\omega_n^2\Delta\mathbf{M})\vec{\psi}^{\circ}=\omega_j^2-\omega_{\psi}^{\circ 2}. \tag{35}$$

Since the mistuning is symmetric, each sector contributes equally to (35). Thus, the contribution from the 0th sector is

$$\vec{\psi}^{\circ(0)H}(\Delta\mathbf{K}-\omega_n^2\Delta\mathbf{M})\vec{\psi}^{\circ(0)}=\frac{1}{N}(\omega_j^2-\omega_{\psi}^{\circ 2}). \tag{36}$$

By factoring the frequency terms on the right-hand side of (36), it can be shown that

[4]This is the case for an isolated family of modes in which the strain energy is primarily in the blades. If there is a significant amount of strain energy in the disk then the frequency of the modes change significantly as a function of nodal diameter and the modes are not isolated, i.e., they cover such a broad frequency range that they interact with other families of modes.

$$\vec{\psi}^{\circ(0)H}(\Delta\mathbf{K}-\omega_n^2\Delta\mathbf{M})\vec{\psi}^{\circ(0)}\approx\frac{2\omega_\psi^{\circ 2}\Delta\omega_\psi}{N} \tag{37}$$

where $\Delta\omega_\psi$ is the fractional change in $\vec{\psi}$'s natural frequency due to mistuning, given by $\Delta\omega_\psi=(\omega_\psi-\omega_\psi^\circ)/\omega_\psi^\circ$. Note that by definition $\Delta\omega_\psi$ is a sector frequency deviation. Equation (37) can be substituted for the bracketed terms of (32), resulting in an expression that relates the elements of the sector s mistuning matrix to that sector's frequency deviation

$$\hat{\mathbf{A}}_{mn}^{(s)}=\frac{2\omega_m^\circ\omega_n^\circ}{N}e^{is(n-m)2\pi/N}\Delta\omega_\psi^{(s)} \tag{38}$$

where the superscript on $\Delta\omega_\psi$ is introduced to indicate that the frequency deviation corresponds to the sth sector. These sector contributions may be summed to obtain the elements of the mistuning matrix

$$\hat{\mathbf{A}}_{mn}=2\omega_m^\circ\omega_n^\circ\left[\frac{1}{N}\sum_{s=0}^{N-1}e^{is(n-m)2\pi/N}\Delta\omega_\psi^{(s)}\right]. \tag{39}$$

3 The Simplified Form of the Fundamental Mistuning Model Modal Equation. The bracketed term in (39) is the discrete Fourier transform (DFT) of the sector frequency deviations. If we use the dummy variable p to replace the quantity $(n-m)$ in (39), then the pth DFT of the sector frequency deviations is given by

$$\bar{\omega}_p=\left[\frac{1}{N}\sum_{s=0}^{N-1}e^{isp2\pi/N}\Delta\omega_\psi^{(s)}\right] \tag{40}$$

where $\bar{\omega}_p$ denotes the pth DFT. By substituting (40) into (39), $\hat{\mathbf{A}}$ may be expressed in the simplified matrix form

$$\hat{\mathbf{A}}=2\mathbf{\Omega}^\circ\bar{\mathbf{\Omega}}\mathbf{\Omega}^\circ \tag{41}$$

where

$$\bar{\mathbf{\Omega}}=\begin{bmatrix}\bar{\omega}_0 & \bar{\omega}_1 & \cdots & \bar{\omega}_{N-1}\\ \bar{\omega}_{N-1} & \bar{\omega}_0 & \cdots & \bar{\omega}_{N-2}\\ \vdots & \vdots & & \vdots\\ \bar{\omega}_1 & \bar{\omega}_2 & \cdots & \bar{\omega}_0\end{bmatrix}. \tag{42}$$

$\bar{\mathbf{\Omega}}$ is a matrix which contains the discrete Fourier transforms of the sector frequency deviations. Note that $\bar{\mathbf{\Omega}}$ has a circulant form, and thus contains only N distinct elements. $\mathbf{\Omega}^\circ$ is a diagonal matrix of the tuned system frequencies.

Substituting (41) into (27) produces the most basic form of the eigenvalue problem that may be solved to determine the modes and natural frequencies of the mistuned system.

$$(\mathbf{\Omega}^{\circ 2}+2\mathbf{\Omega}^\circ\bar{\mathbf{\Omega}}\mathbf{\Omega}^\circ)\vec{\beta}_j=\omega_j^2\vec{\beta}_j \tag{43}$$

Appendix B

Estimating the Tuned System Frequencies. This appendix presents an effective method of obtaining a good initial guess of the tuned system frequencies for use in the iterative solution process described in Section 3.1.2. The approach is to obtain the initial guess by solving a companion problem.

To identify a good initial guess, recall that FMM ID requires that we analyze an isolated family of modes. In general, the frequencies of isolated mode families tend to span a fairly small range. Therefore, they may be reasonably well approximated by their mean value, i.e.,

$$\vec{\lambda}_{(0)}^\circ=\omega_{\text{avg}}^{\circ 2} \tag{44}$$

However, the value of $\omega_{\text{avg}}^\circ$ is not known and therefore cannot be directly applied to (23). Consequently, we will formulate a slightly modified form of (22), which incorporates the initial guess defined by (44). Consider Eq. (22). If we take the tuned frequencies to be equal to $\omega_{\text{avg}}^\circ$, then the term $\widetilde{(\mathbf{\Omega}^\circ\mathbf{\Gamma})}$ may be expressed as

$$\widetilde{(\mathbf{\Omega}^\circ\mathbf{\Gamma})}=\omega_{\text{avg}}^\circ\tilde{\mathbf{\Gamma}} \tag{45}$$

where $\tilde{\mathbf{\Gamma}}$ is the matrix formed by vertically stacking the $M\mathbf{\Gamma}_j$ matrices.

The matrix $\mathbf{\Gamma}_j$ is also related to the tuned frequencies. As a result, the elements of each matrix $\mathbf{\Gamma}_j$ simplify to the form $\omega_{\text{avg}}^\circ\beta_{jn}$. This allows us to rewrite $\mathbf{\Gamma}_j$ as

$$\mathbf{\Gamma}_j=\omega_{\text{avg}}^\circ\mathbf{Z}_j \tag{46}$$

where $\mathbf{Z}_j$ is composed of the elements β_{jn} arranged in the same pattern as the γ_{jn} elements shown in (8). Thus, consolidating all $\omega_{\text{avg}}^\circ$ terms, (45) can be written as

$$\widetilde{(\mathbf{\Omega}^\circ\mathbf{\Gamma})}=\omega_{\text{avg}}^{\circ 2}\tilde{\mathbf{Z}} \tag{47}$$

where $\tilde{\mathbf{Z}}$ is the stacked form of the $\mathbf{Z}_j$ matrices.

Substituting (47) into (22) and regrouping terms results in the expression

$$\begin{bmatrix}\tilde{\mathbf{B}} & 2\tilde{\mathbf{Z}}\\ 0 & \vec{c}\end{bmatrix}\begin{bmatrix}\vec{\lambda}^\circ\\ \omega_{\text{avg}}^{\circ 2}\vec{\bar{\omega}}\end{bmatrix}=\begin{bmatrix}\tilde{\vec{r}}\\ 0\end{bmatrix}. \tag{48}$$

Note that the $\omega_{\text{avg}}^{\circ 2}$ term was grouped with the vector $\vec{\bar{\omega}}$. Thus, all the unknown expressions are consolidated into the single vector on the left-hand side of (48). These quantities can be solved through a least squares fit of the equations. This represents the 0th iteration of the solution process. The $\vec{\lambda}^\circ$ terms of the solution may then be used as an initial guess for the first iteration of (23).

References

[1] Srinivasan, A. V., 1997, "Flutter and Resonant Vibration Characteristics of Engine Blades," ASME J. Eng. Gas Turbines Power, **119**, pp. 742–775.

[2] Castanier, M. P., Ottarsson, G., and Pierre, C., 1997, "A Reduced Order Modeling Technique for Mistuned Bladed Disks," ASME J. Vibr. Acoust., **119**, pp. 439–447.

[3] Yang, M.-T., and Griffin, J. H., 2001, "A Reduced Order Model of Mistuning Using a Subset of Nominal Modes," ASME J. Eng. Gas Turbines Power, **123**, pp. 893–900.

[4] Petrov, E., Sanliturk, K., Ewins, D., and Elliott, R., 2000, "Quantitative Prediction of the Effects of Mistuning Arrangement on Resonant Response of a Practical Turbine Bladed Disk," 5th National Turbine Engine High Cycle Fatigue Conference, Chandler, AZ.

[5] Feiner, D. M., and Griffin, J. H., 2002, "A Fundamental Model of Mistuning for a Single Family of Modes," ASME J. Turbomach., **124**, 597–604.

[6] Seinturier, E., Lombard, J. P., Berthillier, M., and Sgarzi, O., 2002, "Turbine Mistuned Forced Response Prediction: Comparison With Experimental Results," ASME Paper 2002-GT-30424.

[7] Judge, J. A., Pierre, C., and Ceccio, S. L., 2002, "Mistuning Identification in Bladed Disks," *Proceedings of the International Conference on Structural Dynamics Modeling*, Madeira Island, Portugal.

[8] Mignolet, M. P., Rivas-Guerra, A. J., and Delor, J. P., 2001, "Identification of Mistuning Characteristics of Bladed Disks From Free Response Data—Part I," ASME J. Eng. Gas Turbines Power, **123**, pp. 395–403.

[9] Rivas-Guerra, A. J., Mignolet, M. P., and Delor, J. P., 2001, "Identification of Mistuning Characteristics of Bladed Disks From Free Response Data—Part II," ASME J. Eng. Gas Turbines Power, **123**, pp. 404–411.

[10] Feiner, D. M., 2002, "A Fundamental Model of Mistuning for Forced Response Prediction and System Identification," Ph.D. dissertation, Carnegie Mellon University, Pittsburgh, PA.

Mistuning Identification of Bladed Disks Using a Fundamental Mistuning Model—Part II: Application

D. M. Feiner

J. H. Griffin

Department of Mechanical Engineering,
Carnegie Mellon University,
5000 Forbes Avenue,
Pittsburgh, PA 15213

This paper is the second in a two-part study of identifying mistuning in bladed disks. It presents experimental validation of a new method of mistuning identification based on measurements of the vibratory response of the system as a whole. As a system-based method, this approach is particularly suited to integrally bladed rotors, whose blades cannot be removed for individual measurements. The method is based on a recently developed reduced-order model of mistuning called the fundamental mistuning model (FMM) and is applicable to isolated families of modes. Two versions of FMM system identification are applied to the experimental data: a basic version that requires some prior knowledge of the system's properties, and a somewhat more complex version that determines the mistuning completely from experimental data. [DOI: 10.1115/1.1643914]

1 Introduction

This is the second of two papers on identifying mistuning in bladed disks. The first paper [1] reviews the literature, derives a new theory of identifying mistuning, and illustrates its applicability using numerical examples. Since the method is based on measurements of the system as a whole, it is particularly suited to integrally bladed rotors (IBRs). Two versions of system identification were derived in the first paper: a basic version that requires some prior knowledge of the system's properties, and a somewhat more complex version that determines the mistuning completely from experimental data. The second method not only determines the mistuning in the IBR but also determines the natural frequencies that it would have had if all the blade and disk sectors were identical, i.e., the "tuned" system frequencies. In this second paper, we apply the new methods to a modern compressor stage, identify the mistuning and the tuned system frequencies, and show that the results correlate well with the experimental data and also with independent measurements and calculations made by engineers at Pratt & Whitney Aircraft.

The literature in mistuning is extensive, [2], and the current research is put in context in Part I, [1]. However, it should be emphasized that Judge et al. introduced the concept of using the system modes and frequencies to determine the mistuning in IBRs, [3], and also did extensive comparisons with experimental data. The key differences between their approach and that reported here are: the relative simplicity of FMM ID and the consequence that the mistuning in the system can be determined completely from experimental data; that FMM ID uses a blade/disk sector measure of mistuning; and the fact that their method is not inherently limited to an isolated family of modes as is FMM ID.

The system identification methods presented here will be applied to two IBRs of the same design. The IBRs used in this study were designed by Prof. S. Fleeter at Purdue University in cooperation with Pratt & Whitney Aircraft to reflect the aerodynamic and structural properties of a modern compressor. The work reported in this paper is part of a major research initiative on mistuning, friction damping, and forced response that is sponsored by the U.S. Air Force, the U.S. Navy, NASA, and the industrial members of the GUIde Consortium. Consequently, the vibratory response of the compressor stages discussed in this paper will be the focus of mistuning and forced response studies for some time to come.

This paper is organized as follows. Section 2 describes the two test rotors and the testing procedure. Then, in Section 3, we present the FMM ID results. The determined values of mistuning are used as input with the standard FMM prediction code, [4], to predict the rotor's vibratory response to a traveling wave excitation and the results compared with experimental data in Section 4. An interesting result from Section 3 is that the mistuning patterns in both IBRs are very similar. The implications of this result are discussed in Section 5. Finally, the key attributes of the method are summarized in Conclusions.

2 Test Rotors and Procedures

2.1 Test Rotors. To investigate how well FMM ID works with real experimental data from actual hardware, we applied the methods in Part 1, [1], to a pair of transonic compressors, **Fig. 1.** The two rotors are designated as SN-1 and SN-3.

Our industrial partner on this project, Pratt & Whitney, provided a single blade/disk sector finite element model of the tuned compressor. By solving this model with free boundary conditions at the hub and various cyclic symmetric boundary conditions on the radial boundaries of the disk, we generated a nodal diameter map of the tuned rotor, **Fig. 2.** The free boundary conditions at the hub represented the boundary conditions in our experiment: an IBR supported by a soft foam pad and is otherwise unconstrained. Note in the figure that each of the first two families of modes have isolated frequencies. These correspond to first bending and first torsion modes, respectively. Since FMM ID is applicable for isolated families of modes, both the first bending and first torsion modes are suitable candidates for our identification method.

2.2 Experimental Procedures. FMM ID requires measurements of the mistuned rotor's system modes and natural frequencies. By system mode, we mean the tip displacement of each blade as a function of angular position. These modes were obtained using a standard modal analysis approach: measure the bladed disk's transfer functions, and then curve-fit the transfer functions to obtain the modes and natural frequencies.

Our industrial partners performed standard transfer function measurements. The rotor was placed on a foam pad to approxi-

Contributed by the International Gas Turbine Institute and presented at the International Gas Turbine and Aeroengine Congress and Exhibition, Atlanta, GA, June 16–19, 2003. Manuscript received by the IGTI December 2002; final revision March 2003. Paper No. 2003-GT-38953. Review Chair: H. R. Simmons.

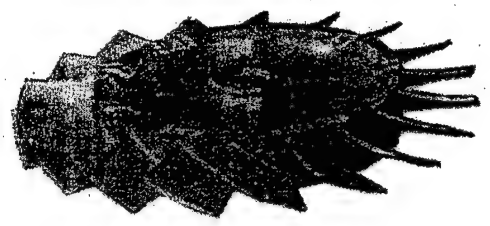

Fig. 1 One of two nominally identical test compressors

mate a free boundary condition. Then, they excited one of the blades over the frequency range of interest, measured the response of each blade with a laser vibrometer, and determined the transfer functions using a spectrum analyzer. A typical transfer function is shown in **Fig. 3.** Note that due to the high modal density, it was necessary to measure the response with a very high frequency resolution. This process was repeated for both compressors over two frequency bands in order to capture the response of both the first bending and first torsion modes.

We then used the commercially available MODENT modal analysis package to curve-fit the transfer functions. This resulted in measurements of the mistuned first bending and torsion modes of each rotor, along with their natural frequencies. Because the blade that was excited was at a low response point in some modes,

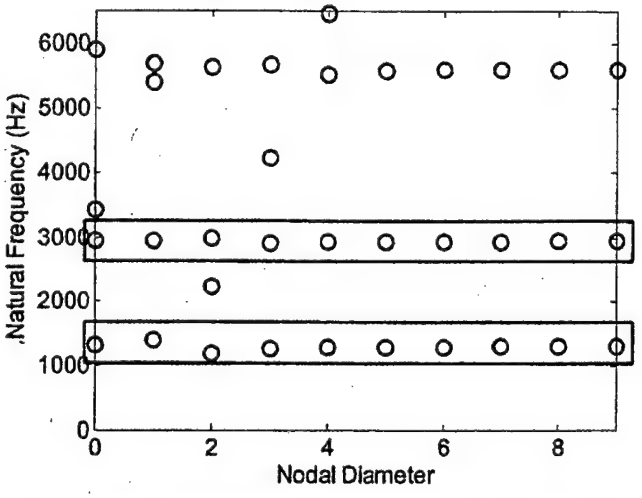

Fig. 2 Natural frequencies of compressor with no mistuning

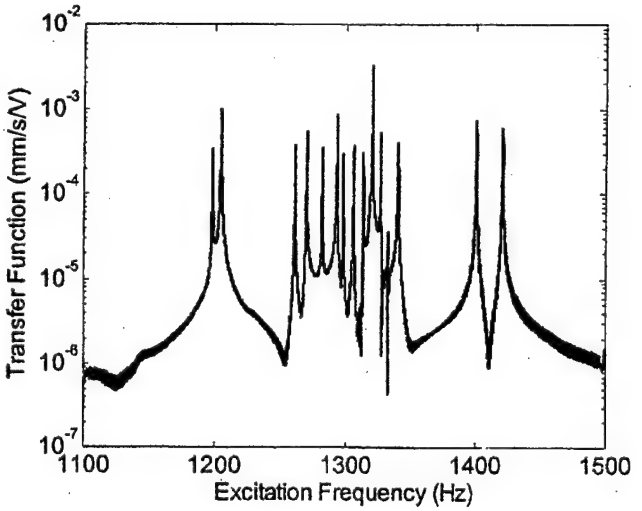

Fig. 3 Representative transfer function from compressor SN-1

we were not able to measure two or three of the modes in each family. In the following section, we use these measured mistuned modes and natural frequencies to demonstrate the applicability of FMM ID to actual hardware.

3 FMM ID Results

The measured modes and frequencies were used to test both forms of the FMM ID method: Basic FMM ID and the completely experimental Advanced FMM ID. The method was applied to each rotor, for both the first bending and torsion families of modes. The tuned frequencies required by basic FMM ID were the same as those depicted in **Fig. 2.**

In order to assess the accuracy of FMM ID, the results were compared to benchmark data. In Section 3.1, we discuss a method for obtaining a benchmark measure of mistuning. Then, in Sections 3.2 and 3.3 we present the results of FMM ID for the first bending and first torsion modes, respectively.

3.1 Benchmark Measure of Mistuning. In order to assess the accuracy of the FMM ID method, the results must be compared to benchmark data. However, since the test rotors are integrally bladed, their mistuning could not be measured directly. Therefore, an indirect approach was used to obtain the benchmark mistuning. Our industrial partners carefully measured the geometry of each blade on the two rotors. From the geometries, they constructed finite element models for each blade and calculated the frequencies that it would have if it were clamped at its root. Since each blade had a slightly different geometry it also had slightly different frequencies. Thus, the variations in the blade frequencies caused by geometric variations were determined. This data was provided to CMU and we put it in a form that could be compared with the values identified by FMM ID. First, we calculated the frequency variations as a fraction of the mean so that we knew the deviation in the blade frequencies. These in turn had to be related to the sector frequency deviations determined by FMM ID. For modes with most of their strain energy in the blade, sector frequency deviations can be obtained from blade frequency mistuning by simple scaling, i.e.,

$$\Delta\omega_{\psi} = a(\Delta\omega_{b}) \tag{1}$$

where a is the fraction of strain energy in the blade for the average nodal diameter mode.

Section 3.2 presents the results for the family of bending modes, and Section 3.3 presents the results from the torsion modes.

3.2 FMM ID Results for Bending Modes

3.2.1 SN-1 Results. The measured mistuned modes and natural frequencies for the compressor SN-1 were used as input to both versions of FMM ID, as described in [1]. In the case of basic FMM ID, the tuned system frequencies of the first bending family from Fig. 2 were also used as input.

Figure 4 shows the sector frequency deviations identified by each FMM ID method along with the benchmark results. In both cases, the agreement is good. This implies that the mistuning is predominantly caused by geometric variations and that the variations are, in fact, accurately captured by Pratt & Whitney's process.

In order to make these comparisons easier, we plotted all mistuning in **Fig. 4** as the variation from a zero mean. However, it should be noted that this rotor had a mean frequency 1.3% higher than that of the tuned finite element model. This DC shift was detected by Basic FMM ID as a constant amount of mistuning added to each blade's frequency. However, since the Advanced FMM ID formulation does not incorporate the tuned finite ele

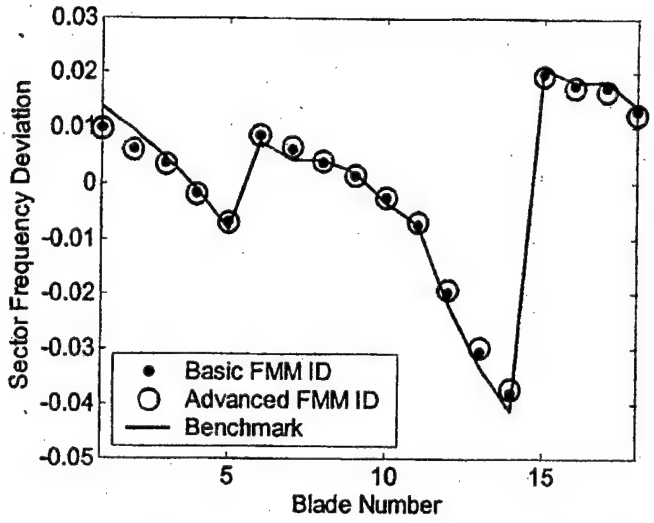

Fig. 4 Comparison of mistuning from FMM ID with benchmark results for SN-1

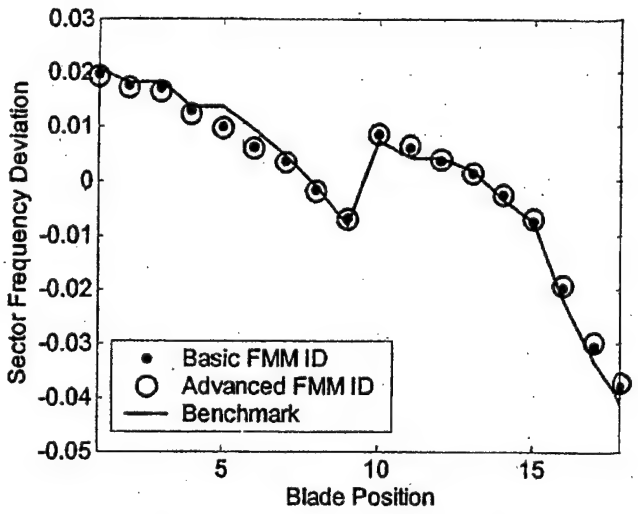

Fig. 6 Comparison of mistuning from FMM ID with benchmark results for SN-1

ment frequencies, it has no way to distinguish between a mean shift in the mistuning and a corresponding shift in the tuned system frequencies. Therefore, in Advanced FMM ID we define mistuning to have a zero mean, and then infer a corresponding set of tuned frequencies.

The tuned frequencies identified by Advanced FMM ID are compared with the finite element values in **Fig. 5.** Notice that the FMM ID frequencies are approximately 17 Hz higher than the finite element values. This corresponds to a 1.3% shift in the mean of the tuned system frequencies that compensates for fact that the blade mistuning now has a zero mean. To facilitate the comparison of the finite element and FMM ID results, we have subtracted off the mean shift, and then plotted the results as circles on **Fig. 5.** Once this adjustment is made, it can be seen that the distribution of the tuned frequencies determined by FMM ID agree quite well with the values calculated from the finite element model. Clearly, the finite element model captures the same variations in the tuned system frequencies as identified by Advanced FMM ID. However, advanced FMM ID identifies the fact that SN-1 had slightly higher average frequencies than the FEM model—a fact that could be important in establishing frequency margins for the stage.

Consider the sector frequency deviations of SN-1 shown in **Fig. 4.** Notice that the mistuning varies from blade-to-blade in a regular pattern. To highlight this pattern, we will reassign the blade numbering so that blade position 1 corresponds to the high frequency blade, **Fig. 6.** Notice that when plotted in the new numbering scheme, the mistuning pattern has a predominantly decreasing trend, with a jump at position 9. This trend suggests that the mistuning might have been caused by tool wear during the machining process and that an adjustment in the process was made after half of the 18 blades were manufactured. This hypothesis will be reexamined after reviewing the results for SN-3.

3.2.2 SN-3 Results. The Basic and Advanced FMM ID methods were then applied in a similar manner to rotor SN-3's family of first bending modes. The identified mistuning and tuned system frequencies are shown in **Figs. 7** and **8.** For comparison purposes, we have again plotted the mistuning with a zero mean, and subtracted a corresponding mean shift from the predicted tuned system frequencies. The agreement is also good for rotor SN-3.

In **Fig. 7,** we numbered the blades so that blade 1 corresponds to the high frequency sector. Since we used a similar numbering scheme in SN-1, we can more easily compare the mistuning in

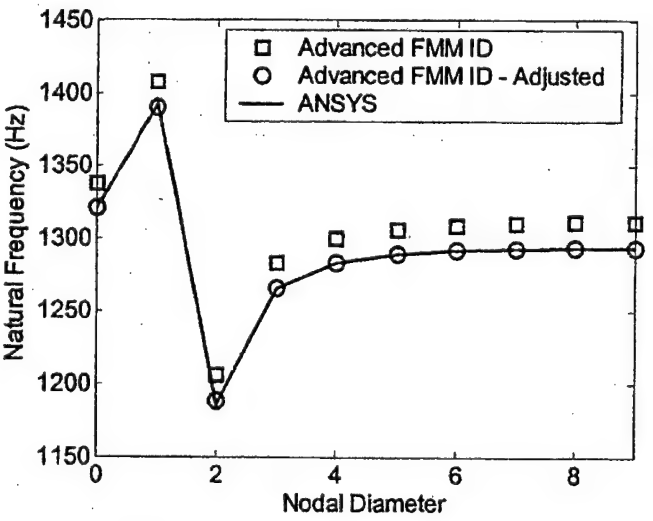

Fig. 5 Comparison of tuned system frequencies from FMM ID and FEM for SN-1

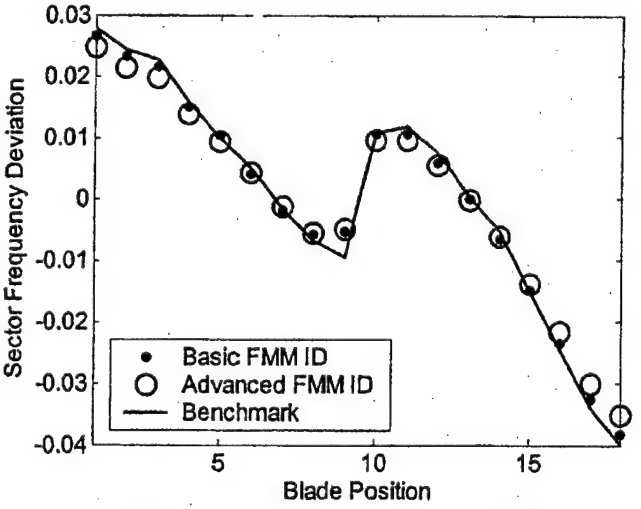

Fig. 7 Comparison of mistuning from FMM ID with benchmark results for SN-3

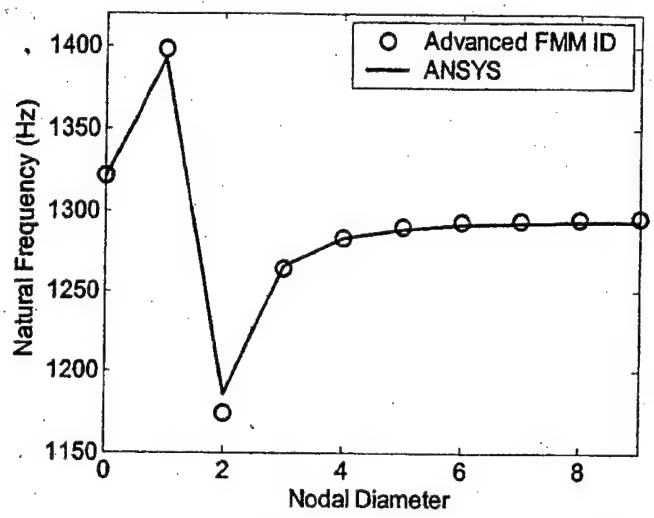

Fig. 8 Comparison of tuned system frequencies from FMM ID and FEM for SN-3

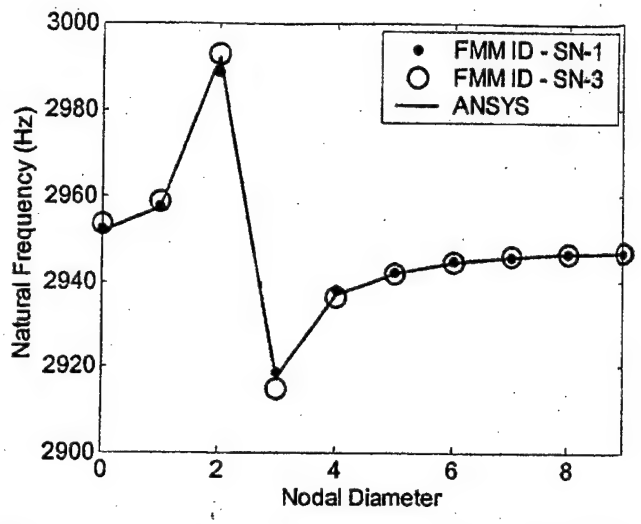

Fig. 10 Comparison of tuned system frequencies from FMM ID and FEM for torsion modes

both rotors. It is interesting to note that the mistuning pattern in **Fig. 7** for SN-3 is quite similar to that of **Fig. 6** for SN-1. This result proves that in IBRs mistuning is not always a random phenomenon. The implication of this fact on the predictability of the vibratory response is discussed in Section 5.

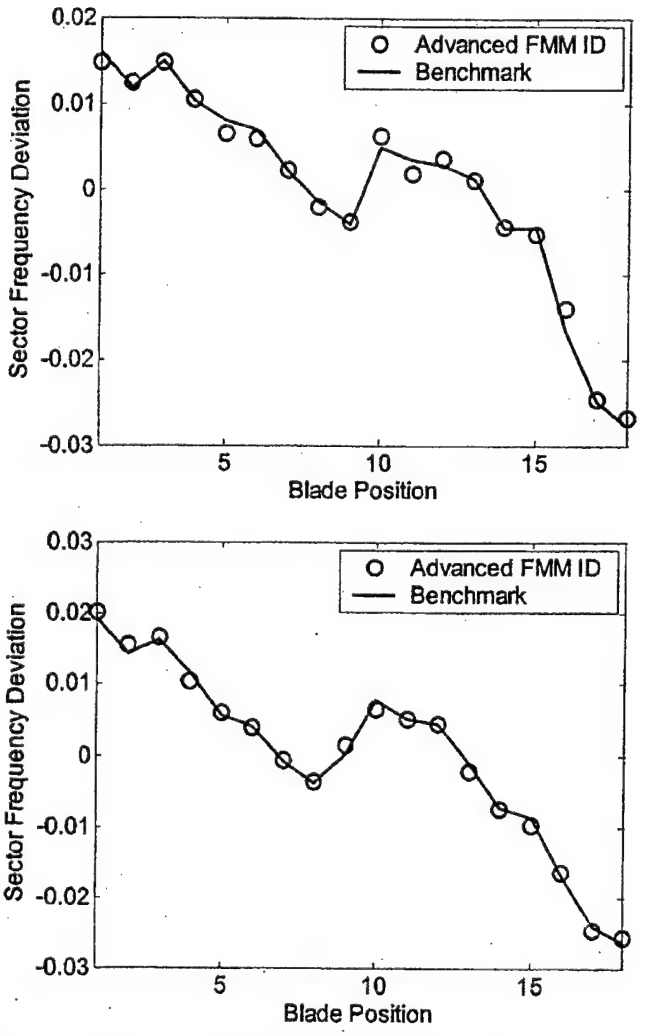

Fig. 9 Comparison of mistuning from FMM ID with benchmark results for torsion modes, (*a*) SN-1, (*b*) SN-3

3.3 FMM ID Results for Torsion Modes. In this section we will examine FMM ID's ability to identify mistuning in the first torsion modes. Only the results for Advanced FMM ID are presented in order to conserve space.

Advanced FMM ID was applied to each test rotor's family of torsion modes. **Figure 9** compares the mistuning identified by FMM ID with the values inferred by our industrial partners from their geometric measurements. The agreement between the two methods for SN-1 is quite good, while the agreement for SN-3 is remarkable. In **Fig. 9,** the blades are numbered in the same order as in plots 6 and 7. Thus, the mistuning patterns in the torsion modes are very similar to those observed for the bending modes, e.g., the blades with the highest and lowest frequencies are the same for both sets of modes. This suggests that the mistuning in these systems may well be caused by relatively uniform thickness variations in the blades since this would affect the frequencies of both types of modes in a very similar manner.

In addition to identifying the mistuning in these rotors, Advanced FMM ID simultaneously inferred the tuned system frequencies of the system's torsion modes, as shown in Fig. 10. Again, the agreement is good. Thus, FMM ID worked well on both the torsion and bending modes of the test compressors.

4 Forced Response Prediction

In the previous section, we found that both forms of FMM ID inferred mistuning that agreed very well with benchmark data. In this section, the identified mistuning will be used to predict the forced response of the compressors to a traveling wave excitation. The results will be compared with measurements done by our industrial partners.

Pratt & Whitney has developed an experimental capability for simulating traveling wave excitation in stationary rotors. Their technique was applied to SN-1 in order to measure its first bending family's response to a 3E excitation. We then predicted the response of SN-1 with the methods developed here and in [1,4].

The issue is: do the 28 parameters (18 mistuned frequencies and 10 tuned system frequencies) identified by FMM ID from one set of transfer functions determine the system properties sufficiently well that we can accurately predict the traveling wave response? To make the prediction, we use the mistuning and tuned system frequencies from Advanced FMM ID as input to the FMM reduced-order model. FMM calculates the system's mistuned modes and natural frequencies. Then, we use modal summation to

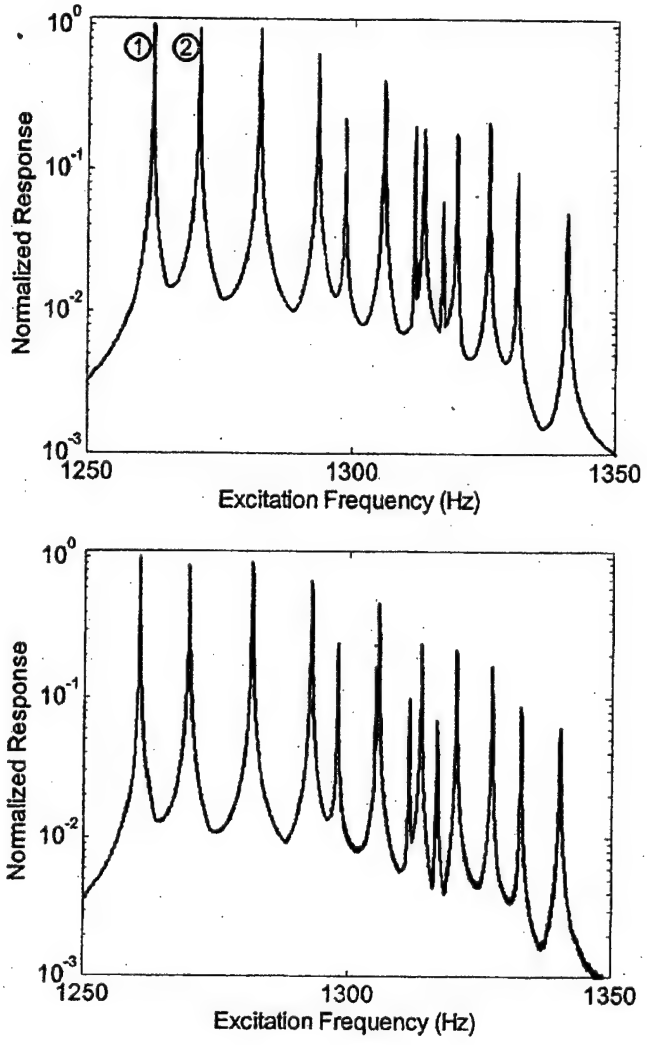

Fig. 11 Comparison of FMM based forced response with experimental data, (*a*) FMM, (*b*) experiment

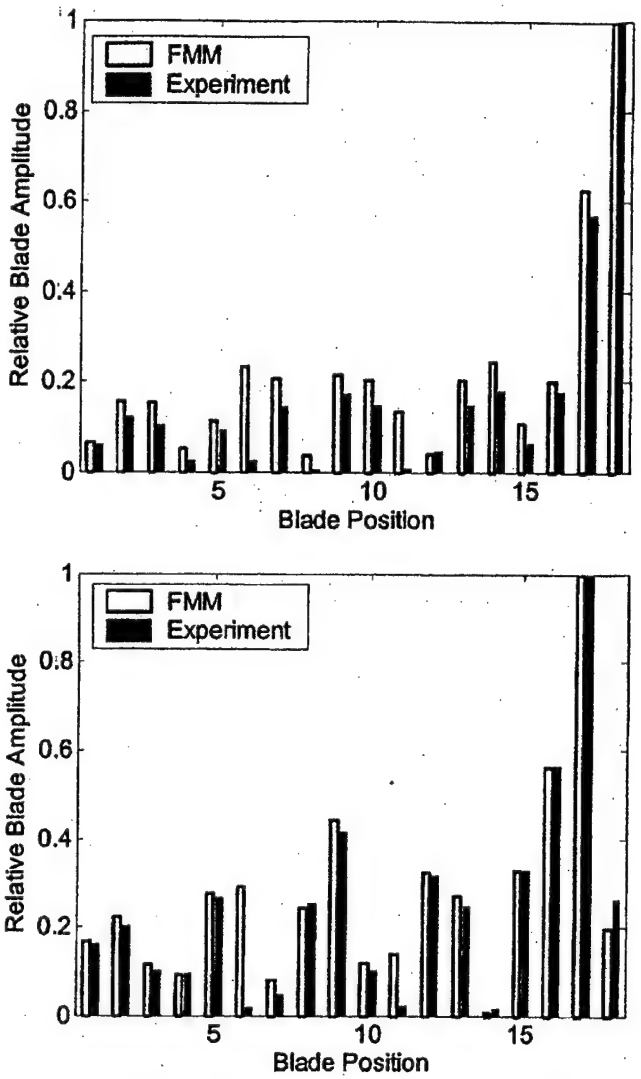

Fig. 12 Relative blade amplitudes at forced response resonance, (*a*) Resonance 1, (*b*) Resonance 2

calculate the response to a 3E excitation. The modal damping used in the summation was calculated from the half-power bandwidth of the transfer function peaks.

Figure 11 shows the comparison of the benchmark forced response results with that predicted by FMM. For clarity, only the envelope of the blade response is shown. Also, the plots have been normalized so that the maximum response is equal to one. In general, the two curves agree reasonably well. In order to observe how well the response of individual blades was predicted we have also compared the relative responses of the blades at two resonant peaks, the peaks labeled ① and ② in **Fig. 11.** The relative amplitude of each blade as determined by both methods is plotted for both resonant peaks in **Fig. 12.** The agreement is also reasonably good. Thus, the FMM based method not only captured the overall shape of the response, but also determined the relative amplitudes of the blades at the various resonances.

5 Cause and Implications of Repeated Mistuning Pattern

In the literature, the mistuning in bladed disks is generally considered to be a random phenomenon. However, in Section 3 we saw that both test rotors have very similar mistuning patterns that are far from random. If such repeated mistuning matters are found to be common among IBRs, it will have broad implications on the predictability of these systems. In Section 5.1 we discuss the cause of the repeated mistuning. Then in Section 5.2, we examine its implications on forced response predictability for a larger sample.

5.1 Possible Cause of Repeated Mistuning. The similarity between the mistuning patterns identified in SN-1 and SN-3 is highly suggestive that the mistuning was caused by a consistent manufacturing effect. In addition, we observed that the mistuning in the torsion modes follows the same trends as in the bending modes. Thus, the dominant form of mistuning is most likely caused by relatively uniform blade-to-blade thickness variations. One plausible explanation for the observed patterns is tool wear. Suppose that the blades were machined in descending order from blade 18 to blade 1. Then, due to tool wear, each subsequent blade will be slightly larger than the previous one. This effect would cause the sector frequencies to monotonically increase around the wheel. With the exception of the frequency jump observed at blade 9, this behavior matches the observed mistuning. Since there are 18 blades, the discontinuity at blade 9 could well be the result of a tool adjustment made halfway through the machining process.

5.2 Implications of Repeated Mistuning. The repeating mistuning patterns caused by such machining effects can significantly increase our ability to accurately predict the response of the fleet through probabilistic methods. For example, consider an en-

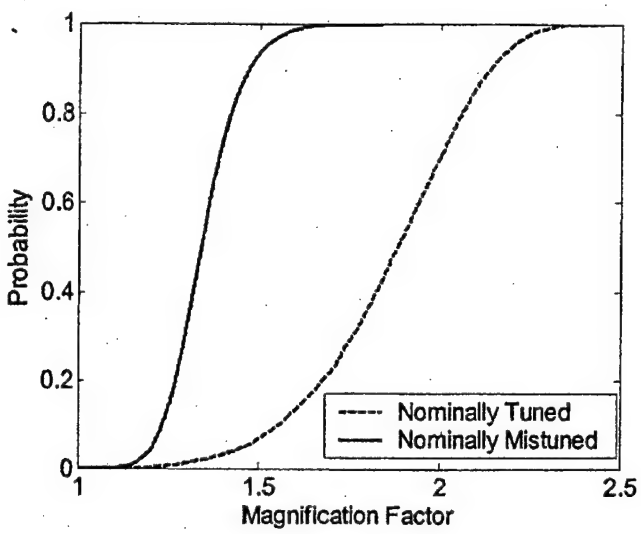

Fig. 13 CDF of peak blade amplitude for a nominally tuned and nominally mistuned compressor

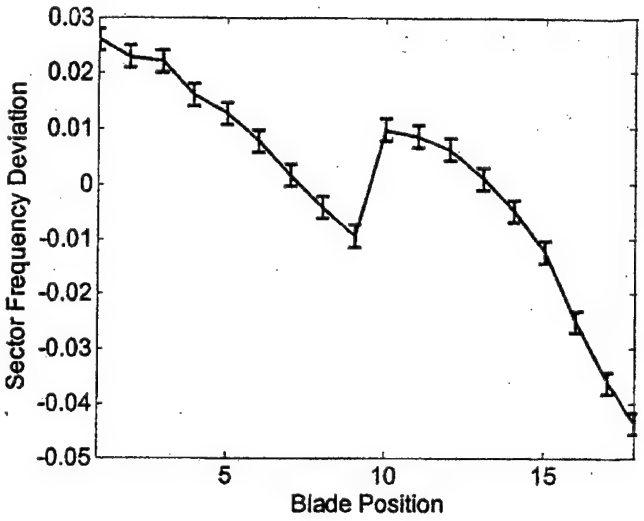

Fig. 14 Mean and standard deviation of each sector's mistuning for a nominally mistuned compressor

tire fleet of the transonic compressors studied in this paper. If we were to incorrectly assume that the mistuning in these rotors was completely random, then we would estimate that the sector frequency deviation of each sector has a mean of zero and a standard deviation of about 2%. Assuming these variations, we used FMM to perform 10,000 Monte Carlo simulations to represent how a fleet of engines would respond to a 3E excitation. We used the data to compute the cumulative distribution function (CDF) of the maximum blade amplitude on each compressor. The CDF of a fleet of engines with random mistuning have a standard deviation of 2% is shown as the dashed line in **Fig. 13.** Notice that the maximum amplitude varies widely across the fleet, ranging in magnification from 1.1 to 2.5.

However, these rotors are in fact nominally mistuned with a small random variation about the nominal pattern. Since the random variation is much smaller than that considered above, the fleet's response is actually far more predictable. To illustrate this point, we approximated the nominal mistuning pattern as the mean of the patterns measured for the two test rotors. Based on this pattern, we found that the sector frequency deviations differed from the nominal values with a standard deviation of only 0.2%, as shown in **Fig. 14.** Making use of the fact that the rotors are nominally mistuned, we repeated the Monte Carlo simulations. We then computed the CDF of the maximum amplitude on each rotor. The results are plotted as the solid line on **Fig. 13.** Notice that by accounting for nominal mistuning, the range of maximum amplitudes is significantly reduced. Thus, if we can measure and make use of nominal mistuning when it occurs then the fleet's behavior will be far more predictable.

6 Conclusions

A new method of identifying mistuning in bladed disks is demonstrated using actual hardware. The method is called FMM ID because it is based on the fundamental mistuning model (FMM), [4]. To test the FMM ID approach, we used it to identify the mistuning in a pair of modern transonic compressors and compared the results with values that were determined by Pratt & Whitney using a completely independent method.

FMM ID uses measurements of the system mode shapes and natural frequencies to infer the rotor's mistuning. The key concept behind FMM ID is that the high sensitivity of system modes to small variations in mistuning causes measurements of those modes themselves to be an accurate basis for mistuning identification. Since FMM ID does not require individual blade measurements, it is particularly suited to integrally bladed rotors. The method is only applicable to isolated families of modes. We have developed two forms of FMM ID: Basic FMM ID, and an advanced version that also identifies the frequencies of the tuned system.

We applied both forms of FMM ID to the two test rotors. To provide benchmark values of mistuning, our industrial partners in this research, Pratt & Whitney, also identified the mistuning in the rotors by measuring the geometry of each blade and then determining its natural frequencies through a finite element analysis. The results from both methods of identifying mistuning agreed very well. In addition to identifying mistuning, the advanced form of FMM ID can also infer the tuned system frequencies of the rotor. Except for a slight shift in their mean value, the identified tuned frequencies agreed well with finite element values. In practice, the ability of FMM ID to identify the tuned frequencies of the system could provide a useful method of confirming that the manufacturing process resulted in an IBR that is consistent with the original design.

We observed that the mistuning patterns in the two test rotors were very similar. This suggests that the mistuning was caused by a repeating feature of the manufacturing process, perhaps tool wear. The cause of the repeating mistuning pattern will be the subject of further investigation. If the mistuning in the two IBRs that we have tested are, in fact, representative of the manufacturing process, then a larger sample of rotors would exhibit similar behavior, i.e., they would have significant levels of nominal mistuning with small levels of random mistuning superimposed. In this case, the forced response of a fleet of these compressors would be far more predictable than might have been previously foreseen. If the manufacturing process can be understood and controlled, then we may be able to use optimization techniques such as those proposed in [5,6] to manufacture IBRs that have low, robust response.

The FMM ID method provides a simple approach for accurately identifying mistuning in integrally bladed rotors for isolated families of modes. In fact, because of its simplicity one version of the method requires only experimental data to determine the key parameters that characterize its response. Once determined, the mistuning can be used with the FMM reduced-order model, [4], to predict how much the mistuning will increase the stage's forced response to a traveling wave, engine order excitation. This technology is useful since it will allow test engineers to determine how the vibratory response of a specific IBR that is tested in a spin pit, rig test or engine relates to the vibratory response of the population as a whole. Ultimately, this technology should allow us

to reduce the number of tests required to characterize the vibratory response of components and still have more durable engines.

Acknowledgments

The authors would like to acknowledge that this research was supported in part by the U.S. Air Force, contract number F33615-01-C-2186, under the direction of Dr. Charles Cross and by the GUIde Consortium.

The authors also would like to thank Mr. Robert J. Morris of Pratt & Whitney Aircraft for providing the experimental and analytical data on the two test compressors. We would also like to acknowledge that the IBRs were provided by Prof. S. Fleeter from Purdue University.

References

[1] Feiner, D. M., and Griffin, J. H., 2004, "Mistuning Identification of Bladed Disks Using a Fundamental Mistuning Model—Part I: Theory," ASME J. Eng. Gas Turbines Power, **126**, pp. 150–158.

[2] Srinivasan, A. V., 1997, "Flutter and Resonant Vibration Characteristics of Engine Blades," ASME J. Eng. Gas Turbines Power, **119**, pp. 742–775.

[3] Judge, J. A., Pierre, C., and Ceccio, S. L., 2002, "Mistuning Identification in Bladed Disks," *Proceedings of the International Conference on Structural Dynamics Modeling*, Madeira Island, Portugal.

[4] Feiner, D. M., and Griffin, J. H., 2002, "A Fundamental Model of Mistuning for a Single Family of Modes," ASME J. Turbomach., **124**, pp. 597–605.

[5] Jones, K. W., and Cross, C. J., 2002, "Reducing Mistuned Bladed Disk Forced Response Below Tuned Resonant Amplitudes," *Proceedings of the 7th National Turbine Engine High Cycle Fatigue Conference*, Palm Beach Gardens, FL.

[6] Petrov, E., and Ewins, D., 2002, "Search for the Best Blade Arrangement in a Mistuned Bladed Disc Assembly," *Proceedings of the 7th National Turbine Engine High Cycle Fatigue Conference*, Palm Beach Gardens, FL.

Proceedings of DETC'03
ASME 2003 Design Engineering Technical Conferences and
Computers and Information in Engineering Conference
Chicago, Illinois USA, September 2-6, 2003

DETC2003/VIB-48448

SYSTEM IDENTIFICATION OF MISTUNED BLADED DISKS FROMTRAVELING WAVE RESPONSE MEASUREMENTS

D.M. Feiner and J.H. Griffin
Department of Mechanical Engineering
Carnegie Mellon University

K.W. Jones and J.A. Kenyon
Air Force Research Laboratory
Propulsion Directorate

O. Mehmed and A.P. Kurkov
NASA Glenn Research Center
Structures and Acoustics Division

ABSTRACT

A new approach to modal analysis is presented that allows the modes and natural frequencies of a mistuned bladed disk to be determined from its response to a traveling wave excitation. The resulting modes and natural frequencies are then used as input to a system identification method to determine the bladed disk's mistuning while it is rotating. This capability is useful since it provides a basis for determining blade frequencies under engine operational conditions and could help monitor the health of the engine.

INTRODUCTION

Bladed disks used in turbine engines are nominally designed to be cyclically symmetric. If this were the case, then all blades would respond with the same amplitude when excited by a traveling wave. However, in practice, the resonant amplitudes of the blades are very sensitive to small changes in their properties. These variations are referred to as mistuning, and may result from the manufacturing process or wear. Mistuning causes some blades to have a significantly higher vibratory response and may cause them to fail from high cycle fatigue. Thus, mistuning is a primary source of uncertainty in a bladed disk system's response. Srinivasan provides a review of this topic in [1].

Two types of tools have recently been developed to help predict the response of mistuned systems [2-5]: reduced order models (ROMs) and system identification methods. The ROMs are very efficient methods for accurately predicting the forced response of a bladed disk. They provide structural fidelity comparable to a finite element analysis of a full mistuned bladed disk with the numerical efficiency similar to that of a simple mass spring model. Thus, they can be used as the basis of Monte Carlo probabilistic analyses and optimization programs. In addition, they reduce the number of parameters that characterize mistuning to a manageable level and become the basis of system identification methods.

System identification methods can determine the mistuning of a specific bladed disk. Two methods have been reported in the literature for determining mistuning from the vibratory response of the coupled bladed disk system. The methods are based on different ROMs of the mistuned system. The first is derived from the reduced order model REDUCE [3] and the second from FMM [5]. For the purpose of system identification, the equations in the ROMs are reformulated so that they can be used to solve the inverse problem, i.e. given the mistuned modes and natural frequencies of the system determine the amount of mistuning in each blade/disk sector.

The first method to use system modes to determine mistuning was based on REDUCE. Since REDUCE was derived using component mode synthesis, it requires a significant amount of preliminary finite element analysis before it can be used for system identification [6]. The second method was based on the Fundamental Mistuning Model (FMM) and is called FMM ID [7, 8]. The advantage of this method is that it is much simpler and, as a result, the mistuning in the system can be identified without any preliminary modeling of the system, i.e. the method is completely experimental. Its disadvantage is that it only works if the family of modes under consideration has frequencies that are relatively isolated. In both methods of system identification, the mistuned modes and natural

frequencies of the bladed disk are used as input data to determine the mistuning in the system.

These recent system identification methods overcome a significant limitation of the traditional approach for determining a bladed disk's mistuning. Traditionally, mistuning in rotors with attachable blades is measured by mounting each blade in a broach block and measuring its natural frequency. The difference of each blade's frequency from the mean value is then taken as a measure of its mistuning. However, this method cannot be applied to integrally bladed rotors (IBRs) whose blades cannot be removed for individual testing. In contrast, the recent system identification techniques rely on measurements of the bladed disk system as a whole, and are thus well suited to IBRs.

These modern methods are also potentially valuable tools for determining the mistuning in conventional bladed disks. Even when applied to bladed disks with conventionally attached blades, the traditional broach block method of mistuning identification is limited. In particular, it does not take into account the fact that the mistuning measured in the broach block may be significantly different from the mistuning that occurs when the blades are mounted on the disk. This variation can arise because each blade's frequency is dependent on the contact conditions at the attachment. In the engine, the attachment is loaded by centrifugal force from the blade which provides a different contact condition than the clamping action used in broach block tests. This difference is accentuated in multi-tooth attachments since different teeth may come in contact depending on how the attachment load is applied. In addition, the contact in multi-tooth attachments may be sensitive to manufacturing variations and, consequently, vary from one location to the next on the disk. To address these issues, a method of system identification is needed that can be used to directly determine mistuning while the stage is rotating. The method will need to identify mistuning from the response of the entire system since the blades are inherently coupled under rotating conditions. This paper presents such a method.

The method presented in this paper provides an approach for extracting the mistuned modes and natural frequencies of the bladed disk under rotating conditions from its response to naturally occurring, engine order excitations. The method is not a new modal analysis method but rather a coordinate transformation that makes traveling wave response data compatible with the existing, proven modal analysis algorithms. Once the modes and natural frequencies are known they can be used as input to either method of system identification. This paper will use FMM ID to demonstrate the process.

This paper is organized as follows. Section 2 presents the theoretical basis of the mode extraction approach for use with traveling wave excitations. Then in Section 3, we present two experimental test cases that illustrate the method. In each case, the extracted modes are used with FMM ID to determine the rotor's mistuning, which is then compared with benchmark values. Finally, the results are summarized in Conclusions.

2. THEORY

Both of the mistuning identification methods cited require the mistuned modes and natural frequencies of the bladed disk as input. Under stationary conditions, they can be determined by measuring the transfer functions of the system and using standard modal analysis procedures. One way of measuring the transfer functions is to excite a single point with a known excitation and measure the frequency response of all of the other points that define the system. However, when the bladed disk is subjected to an engine order excitation all of the blades are simultaneously excited and it is not clear how the resulting vibratory response can be related to the transfer functions typically used for modal identification. It is shown here that if the blade frequency response data is transformed in a particular manner then the traveling wave excitation constitutes a point excitation in the transform space and that standard modal analysis techniques can then be used to extract the transformed modes. Once the transformed modes are determined the physical modes of the system can be calculated from an inverse transformation.

Section 2.1 describes the traditional Single-Input-Single-Output (SISO) modal analysis method and identifies its limitations with respect to multi-point excitation data such as the response to a traveling wave. In section 2.2 a general coordinate transformation is presented that can be used to express multi-point excitation response data in a form that is compatible with traditional SISO modal analysis techniques. Then in section 2.3 we describe how the coordinate transformation may be simplified for the case of traveling wave response data.

2.1 Traditional Modal Analysis

Standard modal analysis techniques are based on measurements of a structure's frequency response functions (FRFs). These frequency response functions are then assembled as a frequency dependant matrix, $\mathbf{H}(\omega)$, in which the element $H_{i,j}(\omega)$ corresponds to the response of point i to the excitation of point j [9]. Modal analysis methods require that one row or column of this frequency response matrix be measured. In the cases considered in this paper, the mistuned modes correspond to a single isolated family of modes. For example, the lower frequency modes such as first bending and first torsion families often have frequencies that are relatively isolated. When this is the case the "modes" of interest are defined in terms of how the blade displacements vary from one blade to the next around the wheel and can be characterized by the response of one point per blade. Thus, the standard modal analysis experiment may be performed in one of two ways when measuring the mistuned modes of a bladed disk. First, the structure's frequency response may be measured at one point on

each blade, while it is excited at only one blade. This would result in the measurement of a single column of $\mathbf{H}(\omega)$. Alternatively, a row of $\mathbf{H}(\omega)$ may be obtained by measuring the structure's response at only one blade and exciting the system at each blade in turn. Notice that in either of these acceptable test configurations, the structure is excited at only one point at a time. However, in a traveling wave excitation, all blades are excited simultaneously. Thus, the response of systems subjected to such multi-point excitations cannot be directly analyzed by standard SISO modal analysis methods.

2.2 General Multi-Point Excitation Analysis

Since a traveling wave excitation is not directly compatible with standard SISO modal analysis methods, a different approach that allows for multi-point excitations is needed. A significant amount of research has been performed on the topic of multiple-input data analysis. However, the work has tended to focus on the case of random excitations, in which each excitation point drives the structure with a different set of randomly selected frequencies [10-12]. In contrast, a traveling wave excites each measurement point with the same frequency at any given time. The method presented here is applicable to any multi-input system, in which the frequency profile is consistent from one excitation point to the next; however, the amplitude and phase of the excitation sources are free to vary spatially. Suitable excitation forms include traveling waves, acoustic pressure fields, and even shakers when appropriately driven.

In typical applications, the i,j element of the frequency response matrix $\mathbf{H}(\omega)$ corresponds to the response of point i to the excitation of point j. However, in order to analyze frequency response data from a multi-point excitation, we must view $\mathbf{H}_{i,j}(\omega)$ in a more general fashion. In a more general sense, the i,j element describes the response of the i^{th} coordinate to an excitation at the j^{th} coordinate. Although these coordinates are typically taken to be the displacement at an individual measurement point, this need not be the case.

The structure's excitation and response can instead be transformed into a different coordinate system. For example, an N degree-of-freedom coordinate system can be defined by a set of N orthogonal basis vectors which span the space. In this representation, each basis vector is a coordinate. The key to performing modal analysis on multi-point excitation data is to select a coordinate system in which the excitation is described by just one basis vector. Thus, within this newly defined modal analysis coordinate system, the structure is subjected to only a single coordinate excitation. Therefore, when our response measurements are expressed in this same domain, they represent a single column of the FRF matrix, and can be analyzed by standard SISO modal analysis techniques. The following section describes how this approach may be applied to traveling wave excitations.

2.3 Traveling Wave Modal Analysis

Consider an N-bladed disk subjected to a traveling wave excitation. It is assumed that the amplitude and phase of each blade's response is measured as a function of excitation frequency. In practice, these measurements could be made under rotating conditions with a Non-intrusive Stress Measurement System (NSMS), whereas a laser vibrometer could be used in a stationary bench test. For simplicity, we will only consider one measurement point per blade.

It is assumed that the blades are excited harmonicly by the force $\mathbf{f}(\omega)e^{i\omega t}$, where the vector $\mathbf{f}$ describes the spatial distribution of the excitation force. Similarly, the response of each measurement point is given by $\mathbf{h}(\omega)e^{i\omega t}$. The components of $\mathbf{f}$ and $\mathbf{h}$ are complex since they contain phase as well as magnitude information. It is this excitation and response data from which we wish to extract modes shapes and natural frequencies. However, in order for this data to be compatible with standard SISO modal analysis methods, it must first be transformed to an appropriate modal analysis coordinate system.

As indicated in Section 2.2, an appropriate coordinate system that would allow this to occur is one in which the spatial distribution of the force, $\mathbf{f}$, is itself a basis vector. The spatial distribution of a traveling wave excitation has the form:[1]

$$\mathbf{f}_E = F_\circ \begin{bmatrix} e^{0} \\ e^{-i(\frac{2\pi}{N})E} \\ \vdots \\ e^{-i(N-1)(\frac{2\pi}{N})E} \end{bmatrix} \tag{1}$$

where E is the engine order of the excitation. Therefore, a coordinate system whose basis vectors are the N possible values of $\mathbf{f}$, corresponding to all N distinct engine order excitations, 0 through N-1 may be used as a basis. The basis vectors are complete and orthogonal.

The vectors $\mathbf{f}$ and $\mathbf{h}$ are transformed into this modal analysis coordinate system by expressing them as a sum of the basis vectors. Denoting our basis vectors as the set $\{\mathbf{b}_0, \mathbf{b}_1, \ldots, \mathbf{b}_{N-1}\}$, this summation takes the form,

$$\mathbf{f} = \sum_{m=0}^{N-1} \bar{f}_m \mathbf{b}_m \tag{2a}$$

$$\mathbf{h}(\omega) = \sum_{m=0}^{N-1} \bar{h}(\omega)_m \mathbf{b}_m \tag{2b}$$

[1]Note, that in order to simplify the concepts, we have included only the phase difference that occurs from one blade to the next. In the case of higher frequency applications it would be necessary to also include the spatial variation of the force over the airfoil if more than one family of modes interact.

where the coefficients $\bar{f}_m$ and $\bar{h}(\omega)_m$ describe the value of the m^{th} coordinate in the modal analysis domain. To identify the values of these coefficients, we could use orthogonality; this is a general approach that is applicable for any orthogonal coordinate system. However, for the case of traveling wave excitations, the coordinate transformation may be simplified.

Consider the n^{th} element of the vectors in (2). For convenience, let all vector indices run from 0 to N-1. Thus, these elements may be expressed as,

$$f_n = \sum_{m=0}^{N-1} \bar{f}_m e^{-i(\frac{2\pi}{N})mn} \tag{3a}$$

$$h(\omega)_n = \sum_{m=0}^{N-1} \bar{h}(\omega)_m e^{-i(\frac{2\pi}{N})mn} \tag{3b}$$

where the exponential term is the n^{th} component of the basis vector $\mathbf{b}_m$. Observe that (3) is the inverse discrete Fourier Transform (DFT^{-1}) of $\bar{f}$. This relation allows us to state the transformation between physical coordinates and the modal analysis domain in the simpler form,

$$\mathbf{f} = \mathrm{DFT}^{-1}\{\bar{\mathbf{f}}\} \tag{4a}$$

$$\mathbf{h} = \mathrm{DFT}^{-1}\{\bar{\mathbf{h}}\} \tag{4b}$$

and conversely,

$$\bar{\mathbf{f}} = \mathrm{DFT}\{\mathbf{f}\} \tag{5a}$$

$$\bar{\mathbf{h}} = \mathrm{DFT}\{\mathbf{h}\} \tag{5b}$$

where DFT is the discrete Fourier Transform of the vector.

By applying equation (5), the force and response vectors are transformed to the modal analysis coordinate system. Due to our selection of basis vectors, the resulting vector $\bar{\mathbf{f}}$ will contain only one nonzero term that corresponds to the engine order of the excitation, i.e. a 5E excitation will produce a nonzero term in element 5 of $\bar{\mathbf{f}}$. This indicates that within the modal analysis domain, we have excited only the E^{th} coordinate. Therefore, $\bar{\mathbf{h}}(\omega)$ represents column E of the FRF matrix.

The transformed response data, $\bar{\mathbf{h}}(\omega)$, may now be analyzed using standard SISO modal analysis algorithms. The resulting modes will also be in the modal analysis coordinate system, and must be converted back to physical coordinates though an inverse discrete Fourier Transform, (4). These identified modes and natural frequencies may in turn be used as inputs to FMM ID to determine the mistuning of a bladed disk from its response to an engine order excitation.

There are two further details of this method that should be noted. First, for the purpose of notation convenience we have numbered the indices of all matrices and vectors from 0 to N-1. However, most modal analysis packages use a numbering convention that starts at 1. Therefore, an E^{th} coordinate excitation in our notation, corresponds to an $(E+1)^{th}$ coordinate excitation in the standard convention. This must be taken into account when specifying the "excitation point" in the modal analysis software. Second, the coordinate transformation used in this method is based on a set of complex basis vectors. Since the modes are extracted in the modal analysis domain they will be highly complex, even for lightly damped systems. Thus it is necessary to use a modal analysis package that can properly handle highly complex mode shapes. Not all commercial algorithms are suitable. In our experience, we found that the MODENT Suite by ICATS [13] works quite well for this purpose.

The next section presents two experimental examples of the method and shows how it can be used for system identification.

3. EXPERIMENTAL TEST CASES

This section presents two experimental test cases of the traveling wave system identification technique. In the first example, we excited an integrally bladed fan (IBR) with a traveling wave while it was in a stationary configuration. Because the IBR was stationary, we were able to make very accurate response measurements using a laser vibrometer. Thus, this example serves as a benchmark test of the traveling wave identification theory. Then, in the second example we explore the method's effectiveness on a rotor that is excited in a spin pit under rotating conditions. The amplitude and phase of the response are measured using an NSMS system; NSMS is a non-contacting measurement method which is commonly used in the gas turbine industry for rotating tests. The purpose of this example is to assess if NSMS technology is sufficiently accurate that it can be used with our traveling wave system identification technique to determine the IBR's mistuning from its engine order response.

3.1 Stationary Benchmark

Consider the integrally bladed fan shown in Fig. 1. This fan was tested using the traveling wave excitation system at Wright Patterson Air Force Base's Turbine Engine Fatigue Facility [14]. Since the facility's test system uses an array of phased electromagnets to generate a traveling wave excitation, the bladed disk remains stationary during the test. This configuration is ideal for benchmark mistuning studies since it allows us to use laser vibrometry to obtain very accurate measurements of the rotor's response.

This example serves two purposes. First, it validates the traveling wave modal analysis method presented in this paper, and second it demonstrates that the resulting modes and natural frequencies may be used to determine the bladed disk's mistuning. The experiment was performed with the fan placed on a rubber mat to approximate a free boundary condition.

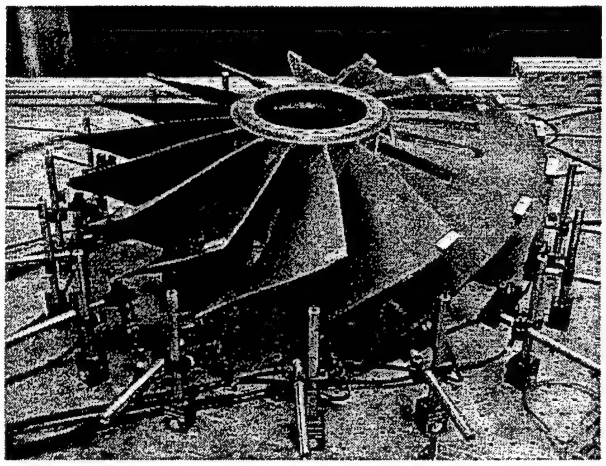

Figure 1: Fan tested for stationary benchmark

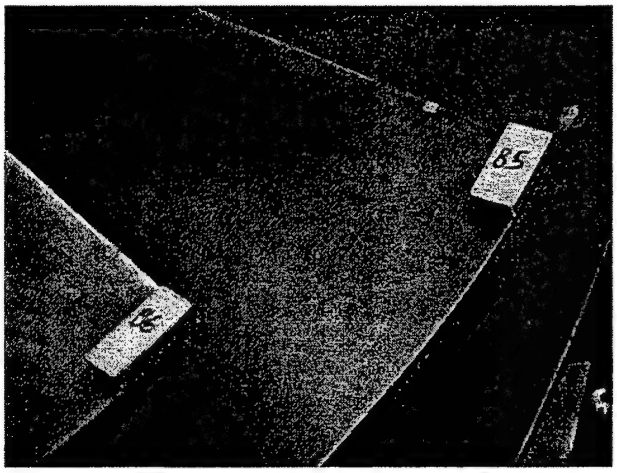

Figure 2: Masses used to mistune fan

First, we intentionally mistuned the IBR by fixing a different mass to the leading edge tip of each blade with wax, Fig. 2. The masses ranged between 0 and 7g, and were selected randomly. Then, to obtain a benchmark measure of the mistuned fan's mode shapes, we performed a standard SISO modal analysis test. Specifically, we used a single electromagnet to excite blade 1 over the frequency range of the first bending modes while we measured the response at all 16 blades with a Scanning Laser Doppler Vibrometer (SLDV). The modes were then extracted from the measured FRFs using the commercially available MODENT modal analysis package. Figure 3 shows a portion of a representative FRF of this system. Notice that the modes are very densely packed, however due to extremely light damping we were able to extract all of the modes within the desired frequency range.

Next, to validate the traveling wave modal analysis method the fan was excited using a 5th engine order traveling wave excitation. Again, the response of each blade was measured using the SLDV. The blade responses to the traveling wave excitation were transformed using equation (5) and then analyzed with MODENT to extract the transformed modes. Since MODENT numbers its coordinates starting at 1 (0E), a 5E excitation corresponds to the excitation of coordinate 6. Therefore, in the mode extraction process, we specified that the excitation was applied at the 6th coordinate. Lastly, equation (4) was used to transform the resulting modes back to physical coordinates.

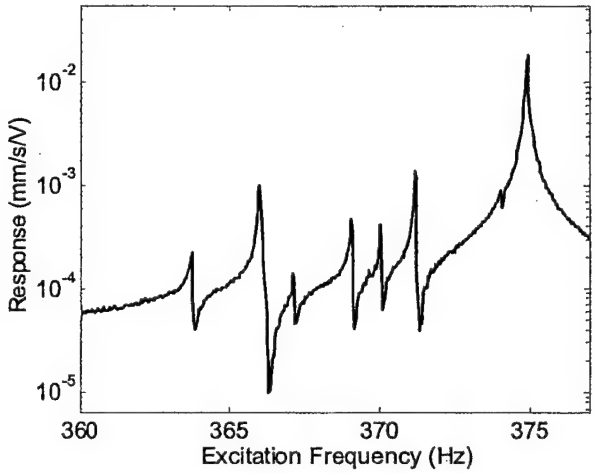

Figure 3: Representative FRF

The modes measured through the traveling wave test were then compared with those from our benchmark analysis. If this system were tuned, its modes would be sine and cosine waves. However, the presence of mistuning alters the mode shapes to various extents. Some modes appear to be nearly pure sinusoids, while others more heavily distorted. Figure 4 shows several representative sets of mode shape comparisons that range from nearly tuned-looking modes to modes that are very localized. In all cases, the modes from the two methods agree quite well. In addition, the natural frequencies were also accurately identified, Fig. 5. Thus, the traveling wave modal analysis method can accurately determine the modes and natural frequencies of a bladed disk based on its response to a traveling wave excitation.

Next, we will demonstrate that the resulting modes and natural frequencies can be used with FMM ID to identify the mistuning in the bladed disk. Since most of the mistuning in this fan was caused by the attached masses, to a large extent the mistuning is known. Therefore, we will use these mass values as a benchmark with which to assess the accuracy of the FMM ID results.

Since we wish to use the mass values as a benchmark, we must isolate the mistuning caused by the masses from the inherent mistuning in the fan. Therefore, we first performed a standard SISO modal analysis on the rotor with the masses

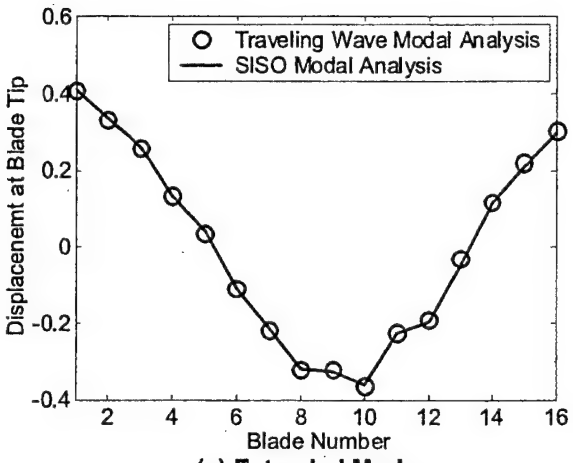

(a) Extended Mode

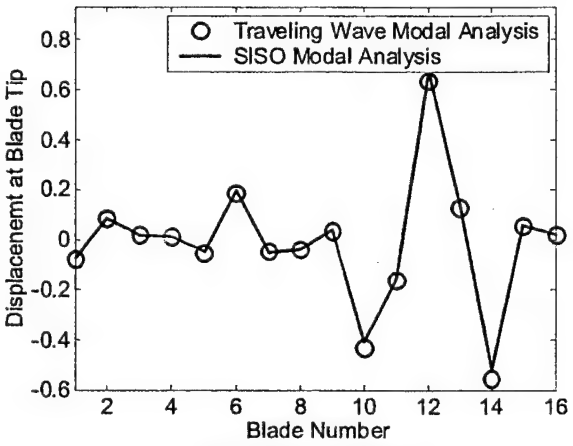

(b) Distorted Mode

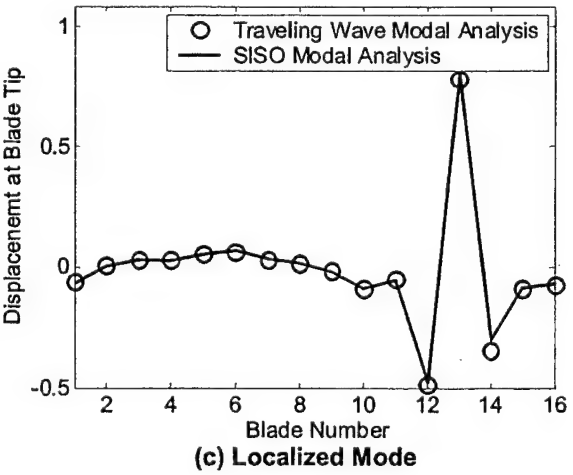

(c) Localized Mode

Figure 4: Comparison of the representative mode shape extracted from the traveling wave response data with benchmark

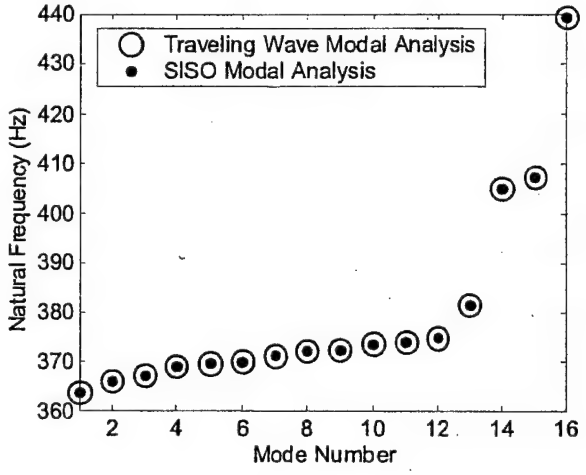

Figure 5: Comparison of the natural frequencies extracted from the traveling wave response data with benchmark

removed, and used the resulting modal data as input to FMM ID. This resulted in an assessment of the IBR's inherent mistuning, expressed as a percent change in each sector's frequency

Next, we performed an FMM ID analysis of the modes and frequencies extracted from the traveling wave response of the rotor with mass-mistuning. The resulting mistuning represents the total effect of the masses and the IBR's inherent mistuning. To isolate the mass effect, we then subtracted the rotor's nominal mistuning. Again, the resulting mistuning was expressed as a percent change in each sector's frequency.

In order to compare these mistuning values with the actual masses placed on the blade tips, we must first translate each sector frequency change into its corresponding mass. A calibration curve to relate these two quantities was generated through two independent methods. First, the calibration was determined through a series of finite element analyses in which we placed known mass elements on the tip of a blade, and used the finite element model to directly calculate their effect on the corresponding sector's frequency.[2] While this method is sufficient in this case, there are often times when a finite element model is not available. For such cases, a similar calibration curve can be generated experimentally by varying the mass on a single blade, and repeating the FMM ID analysis. This experimental method was performed as an independent check of the calibration. Both approaches gave very similar results, Fig. 6. For the range of masses used in this experiment, we found that mass and sector frequency change are linearly related. This calibration curve was then used to translate the

[2] A single blade disk sector of the tuned bladed disk with cyclic symmetric boundary conditions applied to the disk is used in this calculation. Changing the phase in the cyclic symmetric boundary condition only had a slight effect on the results. The results given in Figure 5 are representative and corresponded to a phase constraint of 90 degrees.

identified sector frequency changes into their corresponding masses.

Figure 7 shows the comparison between the mass mistuning identified through FMM ID with the values of the actual masses placed on each blade tip. The agreement is quite good. Thus, by combining the traveling wave modal analysis method with FMM ID, we can determine the mistuning in a bladed disk from its traveling wave response

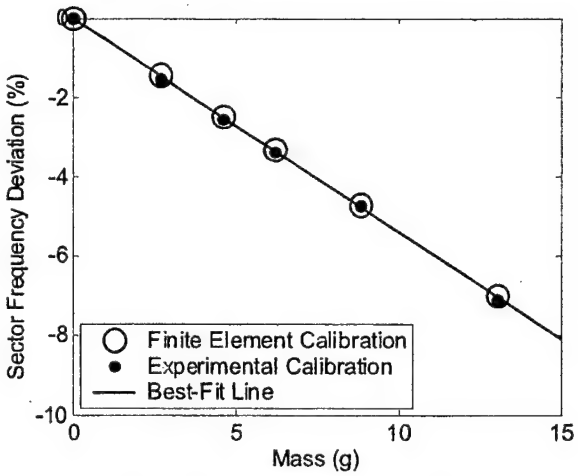

Figure 6: Calibration curve relating the effect of a unit mass on a sector's frequency deviation

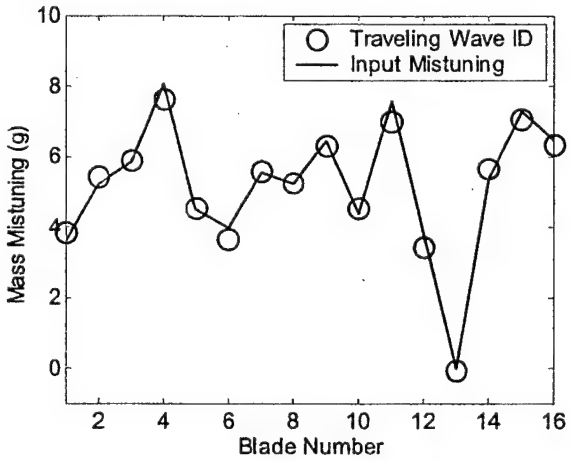

Figure 7: Comparison of the mistuning from the traveling wave system identification method with benchmark value

3.2 Rotating Test Case

In the previous example, we verified the traveling wave modal analysis method and showed that the resulting modes and natural frequencies could be used to determine the bladed disk's mistuning. This was a useful benchmark experiment since the rotor was excited while it was stationary, and thus we could make very accurate measurements using a SLDV. However, if the method is to be applicable to conventional bladed disks, we must be able to make response measurements under rotating conditions. This second test case is intended to assess if the measurement techniques commonly used in rotating tests are sufficiently accurate to be used with FMM ID to determine the mistuning in a bladed disk.

For this example, we considered the fan shown in Fig. 8. To obtain a benchmark measure of the rotor's mistuning in its first bending modes, we used an impact hammer and a laser vibrometer to perform a SISO modal analysis test. The resulting modes and natural frequencies were then used as input to FMM ID to determine the fan's mistuning.

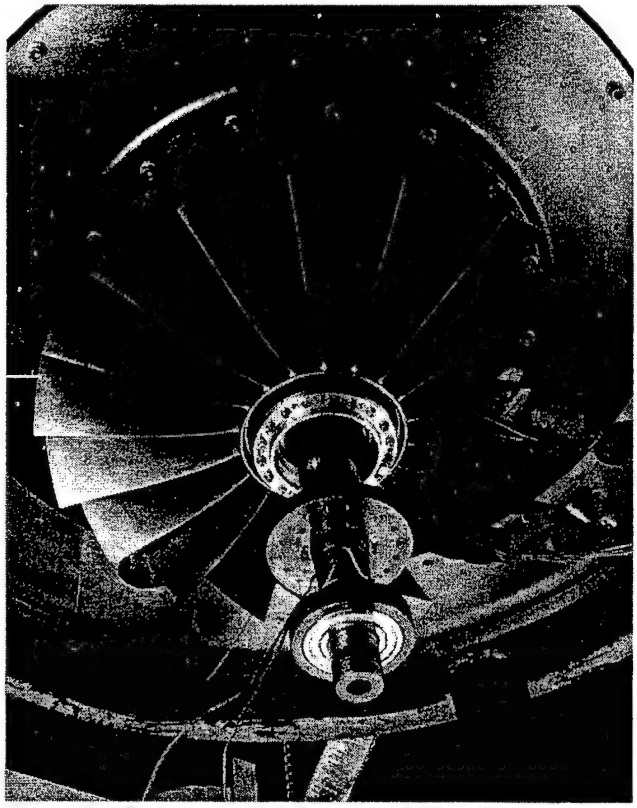

Figure 8: Fan studied in rotation tests

Next, the fan was tested in the spin pit facility at NASA Glenn Research Center. The system uses an array of permanent magnets to generate an eddy current excitation that drives the blades. The blade response is then measured with an NSMS system. For this test, the fan was driven with a 7E excitation, over a rotational speed range of 1550 to 1850 RPM. The test was performed twice, at two different acceleration rates. The NSMS signals were then processed to obtain the amplitude and phase of each blade as a function of its excitation frequency, Fig. 9. The NSMS system measures the amplitude and phase of

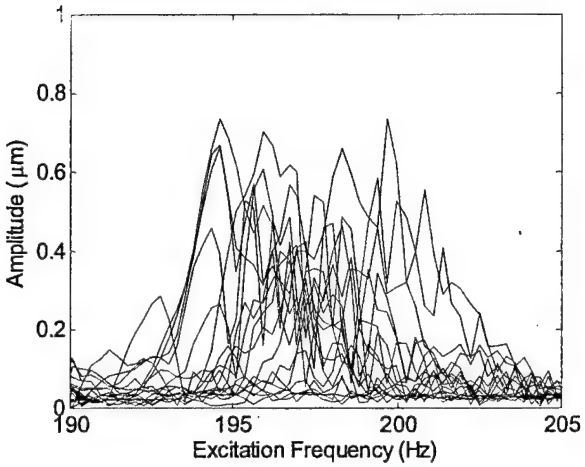

(a) Fast Acceleration

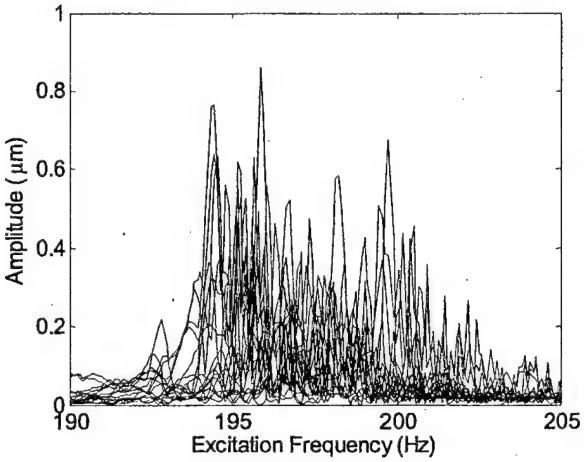

(b) Slow Acceleration

Figure 9: Tracking plot of blade amplitudes measured in spin pit

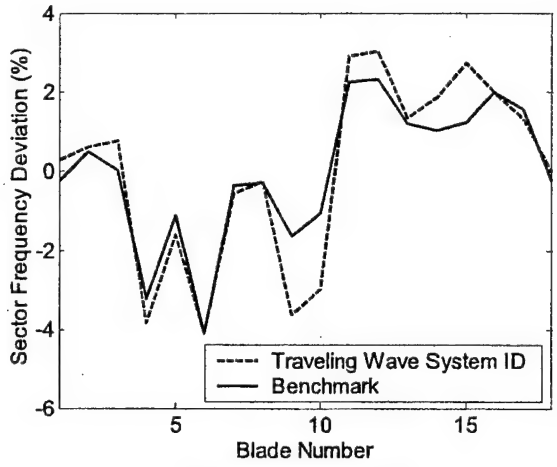

(a) Fast Acceleration

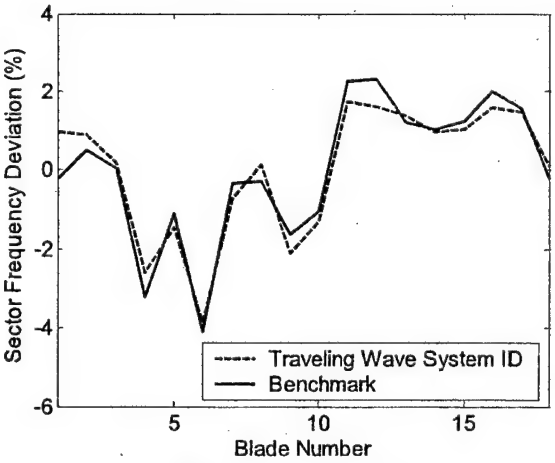

(b) Slow Acceleration

Figure 10: Comparison of the mistuning determined through the traveling wave system identification method with benchmark values

each blade once per revolution. Thus, the data taken at the slower acceleration rate has a higher frequency resolution than that obtained from the faster acceleration rate. In both cases, the data is significantly noisier than the measurements obtained in the previous example using an SLDV

Next, we applied the traveling wave system identification method to extract the mode shapes from the response data. First, we transformed the measurements to the modal analysis domain by using (5), and extracted the mode shapes and natural frequencies with MODENT. The extracted modes were then transformed back to the physical domain through equation (4). Finally, the resulting modes and frequencies were used as input to FMM ID to identify the fan's mistuning.

The mistuning identified from the two spin pit tests was then compared with the benchmark values, as shown in Fig. 10. In the case of the faster acceleration rate, we were able to identify the trends of the mistuning pattern, but were not able to accurately determine the mistuning values for all blades, Fig. 10(a). The key limitation in this analysis was our ability to extract accurate mode shapes from data with such coarse frequency resolution. However, the frequency resolution of the data measured at a slower acceleration rate was 3 times higher than the previous case. Thus, when FMM ID was applied to this higher resolution data set, the agreement between the traveling wave based ID and the benchmark values was significantly improved, as shown in Fig. 10(b). These results are very encouraging. They suggest that with

adequate frequency resolution, NSMS measurements can be used to determine the mistuning of a bladed disk under rotating conditions.

4. CONCLUSIONS

A method for extracting a bladed disk's mode shapes and natural frequencies from its response to a traveling wave excitation was presented. By using the resulting information as input to the FMM ID system identification method, we were in turn able to determine the mistuning in the bladed disk. Thus, this approach allows us to perform system identification of bladed disks from traveling wave response measurements. Furthermore, it was demonstrated that the measurement technology that is commonly used in rotating tests, NSMS, may be used for this purpose.

There are a number of advantages to performing system identification based on a bladed disk's response to a traveling wave excitation. First, it allows us to use data taken in a spin pit or stage test to determine a rotor's mistuning. In this way, the mistuning we identify will include all effects present during the test conditions, i.e. centrifugal stiffening, gas loading, mounting conditions, as well as temperature effects. In particular, it will allow us to assess the effect that centrifugal loading of the attachments has on the mistuning in conventional bladed disks. Thus, this technique extends the applicability of FMM ID from IBRs to conventional bladed disks.

In addition, the traveling wave system identification method allows us to accurately assess the mistuning of some bladed disks in a far more efficient manner. In order to determine a rotor's mistuning, FMM ID uses its mode shapes and natural frequencies as input. Although FMM ID theoretically only needs measurements of one or two modes, the method's robustness and accuracy is greatly improved when more modes are included. For certain bladed disks, a single traveling wave excitation can be used to measure more modes than would be possible from a single point excitation test. For example, consider a highly mistuned rotor that has a large number of localized modes. It is often hard to excite all of these modes with only one single point excitation test, because the excitation source will likely be at a node of many of the modes. Therefore, if we wish to detect all of the mode shapes, the test must be repeated at various excitation points. However, if we were to drive the system with a traveling wave excitation, we can generally excite all localized modes with just a single engine order excitation. This difference arises because the more localized a mode becomes in physical coordinates, the more extended it will be in the modal analysis coordinate system. Thus in highly mistuned systems, one engine order excitation can often provide more modal information than several single point excitations.

Finally, the traveling wave system identification method presented in this paper could potentially form the basis of an engine health monitoring system. If a blade develops a crack, its frequency will decrease. Thus, by analyzing blade vibration in the engine, the traveling wave system identification method could detect a cracked blade. A health monitoring system of this form would use sensors, such as NSMS, to measure the blade vibration through an accel. The measurements may be filtered to isolate an engine order response, and then analyzed using the traveling wave system identification method presented in this paper. This will result in a measure of the rotor's mistuning, which can be compared with previous measurements to identify if any blade's frequency has changed significantly, thus identifying potential cracks. The key obstacle in automating this procedure is to develop a mode extraction method that does not require user interaction. Although this may not be possible in general, it is likely that one could develop an automated modal analysis method which is tailored to a specific piece of hardware. Thus, the traveling wave system identification method has the potential to be an extremely useful tool for engine health monitoring.

The focus of this paper is on extracting the modes of a bladed disk from its response to a traveling wave excitation, however, the general approach presented may be extended to any structure subjected to a multi-point excitation in which the driving frequencies are consistent from one excitation point to the next. A particular advantage to this approach is that it allows structures to be tested in a manner that more accurately simulates their actual operating conditions. Thus, this transformation technique for multi-point excitation modal analysis is not only a useful tool for bladed disk system identification, but potentially can be used to address a much larger class of systems.

ACKNOWLEDGMENTS

The authors would like to acknowledge that this research was supported in part by the U.S. Air Force, contract number F33615-01-C-2186, under the direction of Dr. Charles Cross and by the GUIde Consortium.

The authors would also like to thank Professor David J. Ewins of Imperial College, London for suggesting a modal analysis package that can effectively identify highly complex modes. This was a key step in implementing the theory presented in this paper.

REFERENCES

[1] Srinivasan, A.V., 1997, "Flutter and Resonant Vibration Characteristics of Engine Blades," *Journal of Engineering for Gas Turbines and Power*, 119(4), pp. 742-775.

[2] Castanier, M.P., Ottarsson, G., and Pierre, C., 1997, "A Reduced Order Modeling Technique for Mistuned Bladed Disks," *Journal of Vibration and Acoustics*, 119(3), pp. 439-447.

[3] Yang, M.-T., and Griffin, J.H., 2001, "A Reduced Order Model of Mistuning Using a Subset of Nominal Modes," *Journal of Engineering for Gas Turbines and Power*, 123(4), pp. 893-900.

[4] Petrov, E. P., Sanliturk, K. Y., and Ewins, D. J., 2002, "A New Method for Dynamic Analysis of Mistuned Bladed Disks Based on the Exact Relationship Between Tuned and Mistuned Systems," *Journal of Engineering for Gas Turbines and Power*, 124, pp. 586-597.

[5] Feiner, D.M., and Griffin, J.H., 2002, "A Fundamental Model of Mistuning for a Single Family of Modes," *Journal of Turbomachinery*, 124(4), pp. 597-605.

[6] Judge, J.A., Pierre, C., and Checcio, S.L., 2002, "Mistuning Identification in Bladed Disks," Proc. International Conference on Structural Dynamics and Modeling, Madeira Island, Portugal.

[7] Feiner, D.M., and Griffin, J.H., 2003, "Mistuning Identification of Bladed Disks Using a Fundamental Mistuning Model – Part I: Theory," ASME Paper GT2003-38952, International Gas Turbine Institute Turbo Expo, Atlanta, GA.

[8] Feiner, D.M., and Griffin, J.H., 2003, "Mistuning Identification of Bladed Disks Using a Fundamental Mistuning Model – Part II: Application," ASME Paper GT2003-38953, International Gas Turbine Institute Turbo Expo, Atlanta, GA.

[9] Ewins, D.J., 2000, *Modal Testing: Theory, Practice, and Application*, Research Studies Press LTD., Baldock, UK, Chap. 1.

[10] Bendat, J.S., 1976, "Solutions for the Multiple Input/Output Problem," *Journal of Sound and Vibration*, 44(3), pp. 311-325.

[11] Leuridan, J., 1985, "The Use of Principal Inputs in Multiple-Input Multiple Output Data Analysis," *International Journal of Modal Analysis*, 1 pp. 1-8.

[12] To, W.M., and Ewins, D.J., 1991, "A Closed-Loop Model for Single/Multi-Shaker Modal Testing," *Mechanical Systems and Signal Processing*, 5(4), pp. 305-316.

[13] Imregun, M., et al, 2002, *MODENT 2002*, ICATS, London, UK, http://www.icats.co.uk.

[14] Jones, K.W., and Cross, C.J., 2003, "Traveling Wave Excitation System for Bladed Disks," *Journal of Propulsion and Power*, 19(1), pp. 135-141.

A REDUCED ORDER MODEL FOR TRANSIENT ANALYSIS OF BLADED DISK FORCED RESPONSE

J.P. Ayers, D.M. Feiner, and J.H. Griffin

Department of Mechanical Engineering

Carnegie Mellon University

ABSTRACT

Various reduced order models have been developed to predict the forced response of a bladed disk in an engine. Many of these prediction codes rely on steady state calculations. However, the high acceleration rates used in gas turbine engines can produce transient behavior in the vibratory response. Such transient effects can be significant, and may lead to poor correlation of the predicted response with experimental data. In addition, transient vibratory response may contribute significantly to fatigue damage in the engine and may not be properly modeled using steady state calculations.

A new transient reduced order model of bladed disk vibration is developed. The method is an extension of the Fundamental Mistuning Model (FMM), and relies on numerical evaluation of the differential equations of motion to capture the transient effects. The model is verified experimentally.

The transient response is found to be far more sensitive to small errors in the natural frequencies of the mistuned system than are the steady state calculations. As a result, small modeling errors that produce negligible effects in a steady state prediction have been shown to produce 20% amplitude errors in the transient solution. Thus, accurate modeling is essential for an effective transient forced response prediction.

Since the transient FMM code is far more time consuming than the steady state version, it is important to identify the acceleration regimes in which transient effects are significant, and when they may be neglected. A series of analytical and numerical analyses were performed to generate acceleration guidelines, which may be used to assess when a transient analysis is required and when the simpler steady state analysis is sufficient.

1. INTRODUCTION

Bladed disks are generally designed to be cyclically symmetric with each blade identical. However, due to imperfections in the manufacturing process as well as wear during operation, there are slight variations from blade to blade. These small differences have a large effect on the vibratory response of the disk, causing some blades to have significantly larger amplitude than would be the case in the nominal system. This is referred to as the mistuning problem, and has been studied extensively, as it contributes to high cycle fatigue and the failure of bladed disks in service. Srinivasan provides a thorough review of this topic in [1].

There have been several reduced order models developed to efficiently predict the behavior of mistuned bladed disks [2-5].

However, one thing all these models have in common are that they deal only with the steady state response of rotors. When high acceleration rates are used in engines, transient behavior is observed. An example of this type of behavior is shown in Figure 1, which is data from a spin pit test of an IBR measured at NASA Glenn. In a test such as this, the steady state response of the IBR does not reflect its actual behavior. In order to correlate data such as this with predictions, a model that accounts for transient behavior is needed. The purpose of this research was to develop and validate such a transient model.

2. THEORY

The transient simulation code is based on the Fundamental Mistuning Model (FMM), an existing steady-state reduced order model that is applicable to isolated families of modes [5]. An extension of FMM, called FMM ID, is a completely experimental method of determining the tuned system frequencies and mistuning for a rotor [6,7].

When applying this method to a forced response calculation, FMM ID is first used to determine the bladed disk's mistuning and tuned system frequencies. These identified parameters are used along with FMM to calculate the disk's mistuned modes. A modal summation is then used to calculate the forced response.

When FMM is being applied to steady state response, there is a closed form solution for the response of each mode and the modes can be summed to determine the response of the system. In the case of transient excitations the solution also can be

calculated by summing modes, but the modal response must be calculated numerically. Consider the case when the blades are excited harmonically, but the frequency of the excitation is a function of time. Then, if the modes are normalized so that they have a modal mass of one, the modal equations of motion have the form:

$$\ddot{a} + 2\zeta\omega_n\dot{a} + \omega_n{}^2 a = f_m e^{i\omega(t)\cdot t} \tag{1}$$

For purposes of discussion assume that the excitation frequency is a linear function of time , i.e. $\omega(t) = \omega_o + \frac{\alpha}{2}t$. When this expression is substituted into (1), a second order time term appears in the exponential. As there is no closed form solution to this equation, it must be solved numerically.

3. EXPERIMENTAL TEST CASES

This method was validated by comparing it with experiments on two separate disks, one with a single blade, and one with 18 blades. Photographs of each disk are shown in Figures 2 and 3.

For the single blade test case, the vibration was excited acoustically with a two second sine sweep through the blade's first bending resonance. A laser vibrometer was used to measure and record the time history of the blade's response. A plot of this time history is shown in Figure 4. Superimposed on this is a plot of the response envelope, calculated by determining the magnitude of the response at each instant. For the remainder of the plots in this paper, only this response envelope will be shown.

It may be noted from this figure that there is a beating phenomenon present in the response. This occurs due to the interaction of the mode's natural frequency and the frequency of the excitation source. The transient portion of the solution to the equation of motion always oscillates at the natural frequency, while the steady state portion of the solution oscillates at the excitation frequency. Because these frequencies are close together, a beating phenomenon is observed. When multiple modes are summed this type of beating becomes very important in establishing the overall system response. Since the beating depends on the spacing of the natural frequencies, it will be shown that the transient response is sensitive to variations in the frequencies of the mistuned modes in quite a different manner than is the steady state response.

In the first experiment, standard modal testing was used to measure the natural frequency and damping of the blade's first bending mode. This information was then used as input into the transient simulation code to simulate the response. A comparison of the measured and simulated responses is shown in Figure 5. It was not possible to directly measure the magnitude of the excitation force used in the experiments. Consequently, the value used in the simulation was chosen to minimize the error between the measured and simulated results. Clearly, there is good agreement between the experimental and analytical results for the single blade case.

In order to verify the prediction code for a more complex and realistic test involving multiple modes, we used an eighteen bladed disk. For this test, we used a magnetic excitation source applied to a single blade, and did a two second sine sweep through the disk's first bending mode resonant frequencies. Again, a laser vibrometer was used to measure the response of each blade.

This rotor's response was then simulated using the transient code. FMM ID was used to determine the mistuning and tuned frequencies in the IBR and then FMM was used to calculate the system's mistuned modes and frequencies. Each mode's response was calculated and summed to get the overall system response.

A comparison of the results from a representative blade is shown in Figure 6. Again, the results match well, showing that the transient analysis correctly predicts the response of systems with multiple modes.

4. TRANSIENT SOLUTION SENSITIVITY

A unique characteristic of transient behavior is the sensitivity of the blade response to small variations in the natural frequencies of the mistuned system. To demonstrate this effect, we changed three of the natural frequencies from the 18 blade case in our numerical solution. Specifically, the frequencies of modes seven and nine were increased by 0.25%, and mode 8 was decreased by 0.25%. The mode shapes and damping were unchanged. The steady state frequency response of a representative blade is shown in Figure 7, with the original and perturbed plots overlaid. Clearly, the change in frequencies had a negligible effect on the steady state response. In addition, the

frequency changes had a relatively small effect on the transient responses of individual modes, refer to Figure 8. However, consider the transient response of the blade shown in Figure 9. There are three lines on this plot, one from the experiment, one from the original transient calculation, and one calculated with the perturbed natural frequencies. To understand this, note from the modal responses that each mode peaks at approximately one second after the excitation begins, i.e. the midpoint on the time scale. Until that time the perturbed response follows the original simulation fairly well. However, from one second on, the perturbed response looks markedly different. This is shown in Figure 10, which expands the second half of Figure 9. The change is due to a shift in the phase of the beating of the three perturbed modes caused by the small changes in the natural frequencies. Thus, when these modes are summed, the phase changes produce a large change in the individual blade's response.

5. ACCELERATION RATES THAT CAUSE LARGE TRANSIENT EFFECTS

Transient behavior is important when the engine's acceleration rate exceeds a critical value. A dimensionless acceleration rate can be defined in terms of the natural frequency of a mode.

$$\bar{\alpha} \equiv \frac{\alpha}{\omega_n^{\,2}} \tag{2}$$

From our simulations we have found that transient effects become important if $\bar{\alpha} > \bar{\alpha}_c$ where

$$\bar{\alpha}_c = \frac{\zeta^2}{3} \tag{3}$$

and ζ is the damping ratio for the mode. This value is comparable to the critical acceleration rate used for frequency scans in modal testing [8,9]. A representative value of a fast acceleration rate used in a military engine is 6,000 rpm in 4 seconds. If you assume a natural frequency of 500 Hz. and a third engine order excitation, this works out to a dimensionless acceleration rate of around 5×10^{-5}. Assuming a damping ratio of 0.2%, the critical acceleration rate would be approximately 1.33×10^{-6}. Consequently, the actual acceleration rates that occur in military engines are significantly larger than that required to cause significant transient effects. Therefore, transient effects will be

important in the response. To illustrate this point, a numerical simulation of the 18 bladed disk was performed in which the damping was changed to 0.2% and the dimensionless acceleration rate set to 6.3×10^{-5}, in order to match representative engine conditions. The response of a representative mode is depicted in Figure 11. Clearly, transient beating effects are very prominent in the response.

6. CONCLUSIONS

The conclusions are that:

- A method of predicting the transient response of bladed disks was developed. This method uses a numerical approach to integrate the modal equation of motions. As input data, it uses the mistuned modes and natural frequencies determined by FMM ID.
- The approach was shown to be accurate for both a simple single mode system, and integrally bladed disk with eighteen blades.
- It was demonstrated that transient response is more sensitive to small errors in the system's natural frequencies than are the standard steady-state calculations. This occurs because of interactions between multiple modes beating at slightly different frequencies.
- Guidelines were developed to determine under what conditions transient calculations are required.

ACKNOWLEDGEMENTS

The authors would like to acknowledge that this research was supported in part by the U.S. Air Force, contract number F33615-01-C-2186, under the direction of Dr. Charles Cross and by the GUIde Consortium. The POLYTEC scanning vibrometer used in the experiments was purchased through a DURIP grant sponsored by an AFOSR.

REFERENCES

[1] Srinivasan, A. V., 1997, "Flutter and Resonant Vibration Characteristics of Engine Blades," *Journal of Engineering for Gas Turbines and Power*, 119(4), pp. 742-775.

[2] Castanier, M. P., Ottarsson, G., and Pierre, C., 1997, "A Reduced Order Modeling Technique for Mistuned Bladed Disks," *Journal of Vibration and Acoustics*, 119(3), pp. 439-447.

[3] Yang, M.-T., and Griffin, J. H., 2001, "A Reduced Order Model of Mistuning Using a Subset of Nominal Modes," *Journal of Engineering for Gas Turbines and Power*, 123(4), pp. 893-900.

[4] Petrov, E., Sanliturk, K., Ewins, D., and Elliott, R., 2000, "Quantitative Prediction of the Effects of Mistuning Arrangement on Resonant Response of a Practical Turbine Bladed Disk," *5th National Turbine Engine High Cycle Fatigue Conference*, Chandler, Arizona.

[5] Feiner, D.M., and Griffin, J. H., 2002, "A Fundamental Model of Mistuning for a Single Family of Modes," *Journal of Turbomachinery*, 124(4), pp. 597-605.

[6] Feiner, D.M., and Griffin, J.H., 2003a, "Mistuning Identification of Bladed Disks Using a Fundamental Mistuning Model -- Part I: Theory," ASME Journal of Turbomachinery, 126(1).

[7] Feiner, D.M., and Griffin, J.H., 2003b, "Mistuning Identification of Bladed Disks Using a Fundamental Mistuning Model -- Part II: Application," ASME Journal of Turbomachinery, 126(1).

[8] Ewins, D.J., 2000, "Modal Testing: Theory, Practice and Application," Research Studies Press.

[9] International Organisation for Standardisation (ISO), "Vibration and shock -- Experimental determination of mechanical mobility -- Part 2: Measurements using single-point translation excitation with an attached vibration exciter"

FIGURES

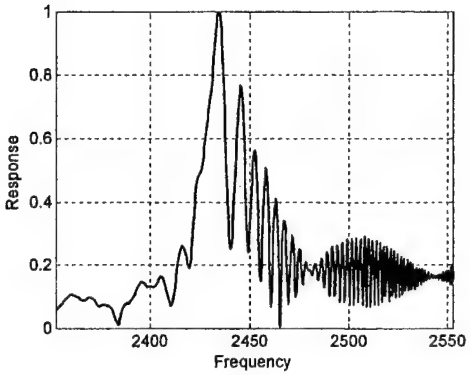

Figure 1: Transient results from NASA spin pit test.

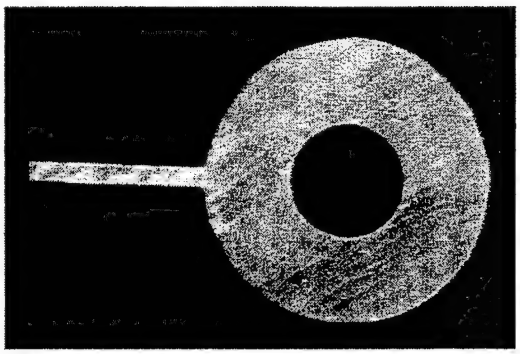

Figure 2: Single blade rotor

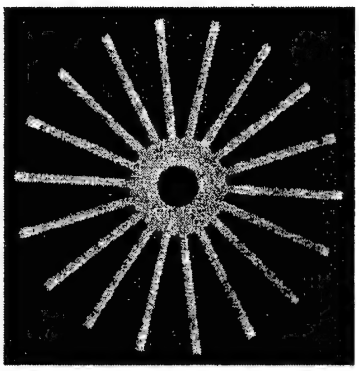

Figure 3: Eighteen blade rotor

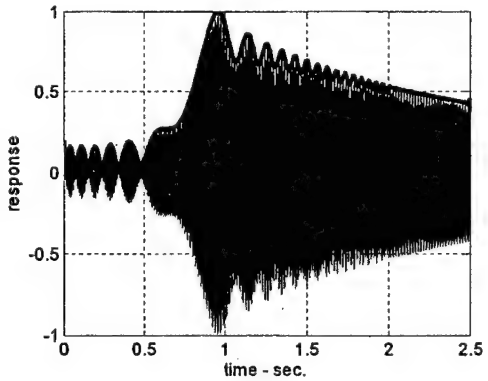

Figure 4: Time response from single blade test case, with overlaid response envelope.

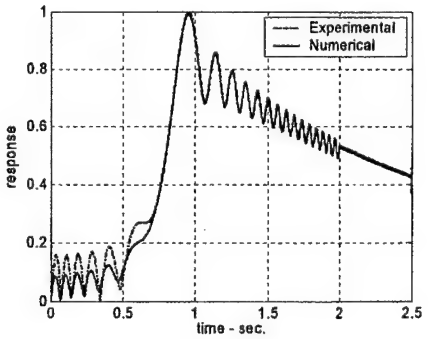

Figure 5: Comparison of measurement with simulation for single blade

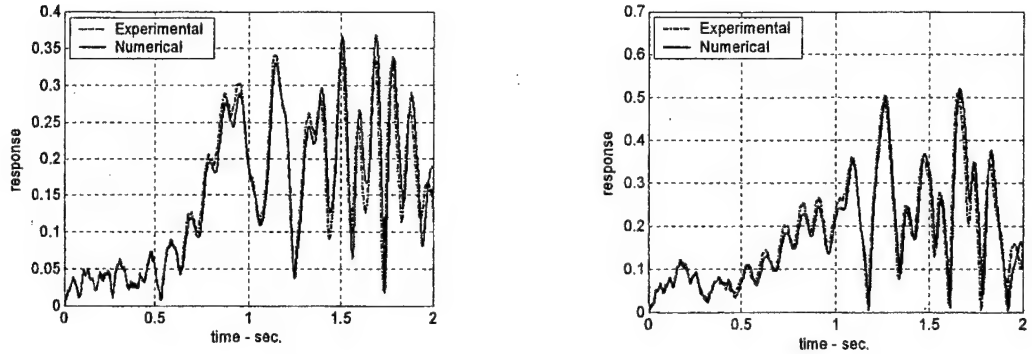

Figure 6: Comparison of measurement with simulation for two representative blades from 18 blade test case.

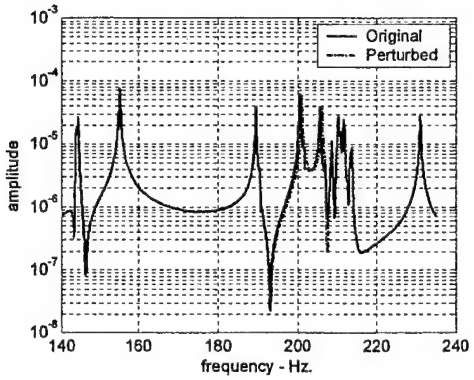

Figure 7: Comparison of actual and perturbed steady-state response for 18 blade test case.

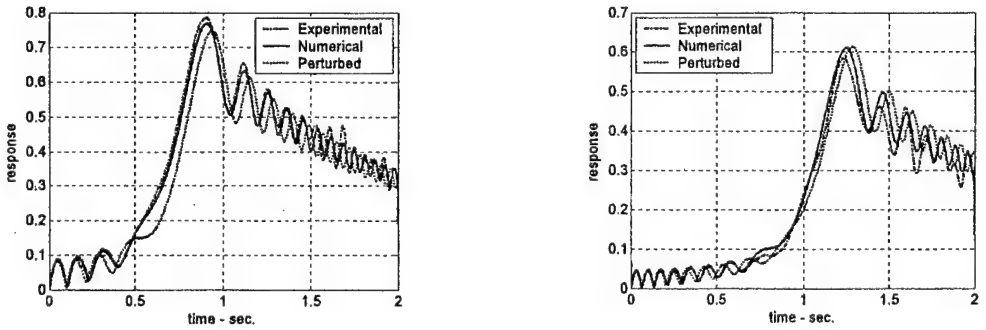

Figure 8: Comparison of measured, simulated, and perturbed response for two of the perturbed modes from 18 blade test case.

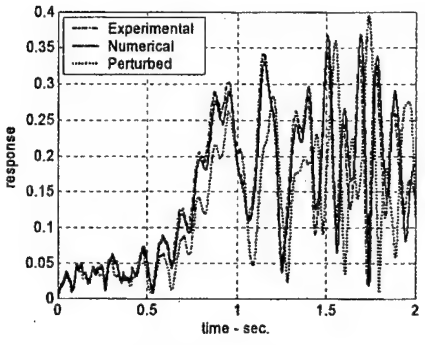

Figure 9: Comparison of measured, simulated, and perturbed response for a representative blade from 18 blade test case.

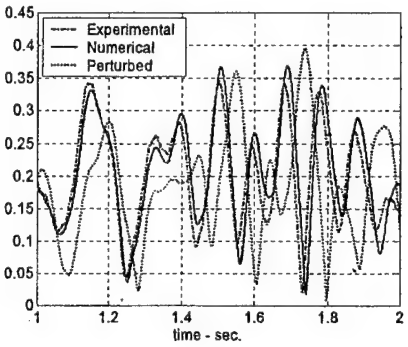

Figure 10: Zoom in on one second to two second region of figure 9.

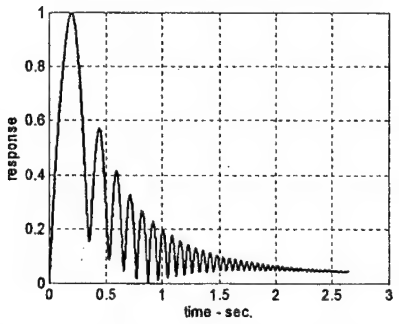

Figure 11: Transient behavior with realistic accel rate and damping level.

EXPERIMENTAL STUDY OF THE FUNDAMENTAL MISTUNING MODEL (FMM) FOR PROBABILISTIC ANALYSIS

M.R. Rossi, D.M. Feiner, and J.H. Griffin
Department of Mechanical Engineering
Carnegie Mellon University

ABSTRACT

FMM is a reduced order model for efficiently calculating the forced response of a mistuned bladed disk. FMM ID is a companion program which determines the mistuning in a particular rotor. Together, these methods provide a way to acquire data on the mistuning in a population of bladed disks, and then simulate the forced response of the fleet. This process is tested experimentally, and the simulated results are compared with laboratory measurements of a "fleet" of test rotors. The method is shown to work quite well. It is found that accuracy of the results depends on two factors: the quality of the statistical model used to characterize mistuning, and how sensitive the system is to errors in the statistical modeling.

1. INTRODUCTION

Bladed disks are generally designed to be cyclically symmetric. However, in practice manufacturing effects, non-uniform material properties, and wear cause each blade to be slightly different from the rest. These blade-to-blade variations are known as mistuning. The resonant amplitudes of turbine blades are very sensitive to these small variations in the blade properties. Therefore, mistuning can significantly amplify the vibratory response of some blades, and cause them to fail from high cycle fatigue. Srinivasan provides a thorough review of the topic [1].

One area of mistuning research has focused on the development reduced order models to efficiently predict the forced response of a mistuned bladed disk. A variety of reduced order models have been developed by researchers at Carnegie Mellon University [2-3], the University of Michigan [4], and Imperial College [5]. Although these methods have been shown to agree extremely well with finite element simulations of a full mistuned rotor, some have had difficulty predicting the response of actual hardware [6]. These results suggest that the source of the error may lie in our inability to determine the correct input parameters to the ROMs.

Therefore, researchers subsequently developed methods to accurately measure the mistuning in a bladed disk. The first advanced mistuning identification method was created by Judge and Pierre [7]. Their technique uses measurements of the bladed disk system as a whole to infer the mistuning of individual blades. More recently, Kim and Griffin developed a similar technique which is applicable to veering regions and high frequency modes [8]. However, the techniques of Judge and Kim require a finite element model of the system, and significant analysis to identify the mistuning in an IBR. A much simpler approach is the FMM ID method developed by Feiner and Griffin [9,10].

FMM ID is based on the Fundamental Mistuning Model (FMM), a simple reduced order model for mistuned bladed disks [3]. Like the methods of Judge of Kim, FMM ID also uses measurements of the whole assembly to infer blade frequencies, but it is completely experimental. FMM ID does not require a finite element model. This makes FMM ID easier to use than the other methods. Furthermore, we have found that in practice it is extremely difficult to obtain a finite element model that accurately reflects a component's true

geometry and boundary conditions. Such inaccuracies may lead to errors when using the methods of Judge and Kim. However, since FMM ID relies only on experimental data, it is not hindered by the quality of a finite element model.

FMM ID can also experimentally determine the natural frequencies that a bladed disk would have if it were tuned. The combination of tuned frequencies and mistuning provide enough information for FMM to predict the forced response of a bladed disk based solely on experimentally measured data.

Both FMM and FMM ID have been verified experimentally in deterministic calculations [10]. However, it has also been proposed that these methods may be used for probabilistic analysis. The idea is to use FMM ID to acquire data on the mistuning and tuned system frequencies in a population of bladed disks. Then, perform Monte Carlo simulations with FMM to assess the response of the fleet. In this paper, we test this process experimentally, and then compare the simulated results with measurements of a "fleet" of test rotors.

This paper is organized as follows. In Section 2, we summarize the FMM and FMM ID methods. Then, Section 3 describes the benchmark experiments. In Section 4 we discuss the probabilistic analysis, and compare our simulation results with experimental data. Finally, the key results are summarized in Conclusions.

2. FMM AND FMM ID

2.1 FMM

FMM is a simple reduced order model of mistuned bladed disk vibration. The method is a simplification of the Subset of Nominal Modes theory (SNM) developed by Yang and Griffin [2] and is designed for use in low frequency modes such as first bending and first torsion. One of the advantages of this approach is that it reduces the mistuning problem to it most basic elements. As a result, FMM requires a minimum number of input parameters, and it's extremely easy to use. This large simplification also makes FMM extremely efficient. When performing Monte Carlo simulations of forced response, FMM can simulate the response of about 200 disks per second on a 2 GHz PC.

The FMM method only requires two sets of input parameters to calculate the effect of mistuning on the mode shapes and frequencies of a bladed disk. Consider the eigenvalue problem solved by FMM to calculate mistuned modes and frequencies,

$$\left(\mathbf{\Omega}^{\circ 2} + \hat{\mathbf{A}}\right)\vec{\beta}_j = \omega_j^2 \vec{\beta}_j \tag{1}$$

Notice that the equation has only two input matrices, $\mathbf{\Omega}^{\circ 2}$ and $\hat{\mathbf{A}}$. $\mathbf{\Omega}^{\circ 2}$ is a diagonal matrix of the tuned system frequencies squared. This term describes the nominal system. The matrix $\hat{\mathbf{A}}$ characterizes the mistuning. $\hat{\mathbf{A}}$ is composed of the blade frequency deviations, which are defined as the difference in each blade's frequency from the average value. Thus, FMM shows that the effect that mistuning has on a system is completely defined by only two sets of parameters: the tuned system frequencies, and the blade frequency deviations.

This result has a large implication to probabilistic analysis because it minimizes the number of random variables which must be accounted for when calculating the response of mistuned systems. Since mistuning may be characterized by the frequencies of the blades, it is not necessary to separately model the variations in blade geometry and material properties. All we need to account for is the net effect of these variations on the blade frequencies.

Therefore, it is important to be able to accurately measure the frequencies of individual blades. Blade frequencies are often difficult to measure directly, particularly in the case of IBRs, where the blades cannot be removed for individual testing. But FMM provides a method for blade frequency identification: FMM ID.

2.2 FMM ID

Recall that the FMM eigenvalue problem, Eq. (1), is used to calculate the effect of mistuning on the mode shapes and natural frequencies of a bladed disk. The equation takes as input, information on the nominal system as well as the way it's mistuned. With this data, the expression can be solved for the mode shapes and natural frequencies of the mistuned bladed disk. However, we could alternatively solve the problem in reverse. Suppose we measured the modes and natural frequencies of a mistuned rotor. We could then formulate an inverse problem to Eq. (1) [9]. The solution to this inverse problem is the mistuning of each blade, as well as the natural frequencies the system would have if it were tuned. This is the basis of FMM ID, and it is shown schematically in Fig. 1.

In practice, the mistuned system modes and frequencies are measured through standard modal testing techniques. This involves measuring a set of transfer functions, and then extracting modes with modal curve fitting software. For the purpose of FMM ID, the modes only need to be measured at one point per blade.

FMM ID does not require any finite element data. Thus, it provides us with a way to determine all of the key mistuning parameters experimentally.

2.3 Probabilistic Application of FMM and FMM ID

By measuring multiple bladed disks of the same design, FMM ID can collect data on mistuning and tuned system frequencies, which can later be used for probabilistic analysis.

Once the data is collected, we can construct statistical models of the mistuning and tuned system frequencies. Then, we can use those statistical models with FMM to perform Monte Carlo simulations of the fleet.

The goals of this research are to apply this technique to an academic rotor, and compare our simulations with experimental data. This will allow us to explore some of the challenges of probabilistic mistuning analysis.

3. BENCHMARK EXPERIMENT

The experimental approach is to first generate benchmark data with which to compare our Monte Carlo simulation results. This requires measuring the forced response of multiple bladed disks of the same design.

Next, we can apply the probabilistic procedure discussed in the previous section to simulate the response of a fleet of similarly constructed disks.

The first step in performing the benchmark experiment was to obtain a tuned bladed disk, which we could later mistune in a controlled fashion. Figure 2 shows the academic IBR used for experiment. To tune the structure, we first used FMM ID to measure the frequency of every blade. Since the blades on this disk have a simple beam-like geometry, we were then able to use beam theory to calculate the appropriate length change for every blade to compensate for its mistuning. Finally, we trimmed the blade lengths accordingly. Figure 3 shows the frequency response function (FRF) of the rotor before and after tuning. Notice that prior to tuning, the structure's mistuning caused the repeated natural frequencies to split, producing additional peaks of the FRF. After tuning, the splitting was eliminated in most of the modes. Thus, the disk was successfully tuned.

Then, the disk was mounted in the test fixture shown in Fig. 4. The disk was mistuned by adding masses to the blade tips. The masses were selected to produce variations in the blade frequencies that were approximately normally distributed with a standard deviation equal to 2% of the nominal blade frequency. Note that a mean shift in the mistuning is mathematically equivalent to a mean shift in the tuned system frequencies. Therefore, we defined the mean mistuning to be zero, and measured the corresponding tuned system frequencies through FMM ID.

We excited the disk with an array of electro-magnets positioned under the blade tips, Fig. 4. The magnets produced an engine style excitation, while the disk remained stationary. The engine style excitation system at Carnegie Mellon is similar to the one developed by Jones and Cross at the Air Force Research Laboratories [11]. The bladed disk was excited over an appropriate frequency range to simulate the effect of an engine order crossing with the first bending modes. The vibratory response of the blades was measured at each blade tip by using a scanning laser vibrometer, Fig 5a. Laser vibrometers are ideal tools for mistuning measurements since they are very accurate, non-contacting sensors which don't alter the mistuning of the structure.

This measurement process was repeated with 10 different mistuning patterns, each drawn from the same normal distribution. This effectively gave us measurements of 10 different disks from the same population. On each test, we recorded the peak amplitude of every blade over the frequency range of interest, Fig 5b. Since each disk has 24 blades, this produced a total of 240 peak amplitude measurements, which we will later use for comparison with our simulation results. Furthermore, every "disk" was tested with four different engine order excitations: 1E, 3E, 6E, and 9E. Thus, we will be able to assess the accuracy of the probabilistic analysis method over a wide variety of excitation conditions.

4. PROBABILISTIC ANALYSIS

Next, we followed the probabilistic analysis process outlined in Section 2.3. We proceeded as if we knew nothing about the way the disks were mistuned.

4.1 Single Disk Model

We performed a modal analysis on one of the 10 test "disks." Then, the measured modes were used in FMM ID to determine the structure's mistuning and tuned system frequencies, Fig 6. This represents the crudest possible data for forming a statistical model of the bladed disk parameters. In practice, it is advisable

to identify the parameters of multiple bladed disks to form a reliable model of the random variables. However, for the purpose of this study, we would like to assess the effect of a crude statistical model on the accuracy of the subsequent Monte Carlo simulations. Therefore we formed an approximate statistical model based on this limited set of data. With only one measure of the tuned system frequencies, we have no basis on which to model variability. Therefore, the tuned frequencies were treated as fixed. The blade frequency deviations, however, were modeled as a random variable. Figure 7 shows a normal plot of the 24 blade frequency deviations from this disk. Notice that the data approximately falls on a straight line. This indicates that data is roughly normal. Therefore, the mistuning was modeled as being normally distributed with a mean and standard deviation given by the sample values of 0 and 1.52% respectively. However, it must me noted that there is substantial uncertainty in these parameters. For instance, the 95% confidence interval on the standard deviation covers a range from 1.18% to 2.13%. That's nearly a factor of 2 uncertainty in the model parameter.

Based on this rough model, we performed Monte Carlo simulations of the bladed disk population using FMM. These simulations were repeated for all four engine orders measured in the benchmark experiments. In each case, we simulated the forced response of 1000 bladed disks. The results are shown in Fig. 8. Each plot contains the CDF of all 240 peak blade amplitudes from the experiment, and a corresponding CDF constructed from the simulation results. For clarity, the plots are shown on a normal probability scale. The agreement is surprisingly good considering that the experimental CDFs only contain 240 data points, and are likely not converged in the tails. Furthermore, the statistical model used in the simulations was inaccurate. This suggests that the response is relatively insensitive to errors in the statistical model. To better understand this behavior, we performed a sensitivity analysis.

4.2 Sensitivity Analysis

A small change in the standard deviation used in our statistical models will produce a shift in the simulated CDF, Fig. 9. In general, the shift will not be uniform over the full range of the CDF, as shown in the figure. Thus, one method for measuring sensitivity is to plot the change in the CDF due to a perturbation in the standard deviation. This analysis was performed about a nominal standard deviation of 2%, and was repeated for all four engine orders, Fig. 10. Notice that the 6 and 9E cases are nearly zero across the full range of probability. Thus, this analysis suggests that this disk's response to 6E and 9E excitations is very insensitive to errors in the standard deviation. This is consistent with the CDFs of Fig. 8. In particular, consider the 9E CDF. Notice that despite a large error in the statistical model used to generate the simulated curve, it agrees extremely well with the experimental data from about 10% to 90% cumulative probability. The discrepancy seen in the tails is most likely a result of insufficient experimental data to produce a converged experimental CDF in those regions.

Next, consider the 1E case. The sensitivity plot indicates that the system's response to a 1E excitation is relatively sensitive to errors in the statistical model for most of the probability range. However, in the vicinity of 85% cumulative probability, the 1E line passes through zero on the sensitivity plot, and is therefore much less sensitive. Again, this is consistent with the CDF plot for this case, which shows good agreement between the simulation and experiment around 85%, yet larger discrepancies away from that area. This suggests that much of the error seen in the low engine order simulations is due to a poor statistical model. Therefore, the correlation should be improved if we use a higher quality model for the variation in mistuning.

4.3 Ten Disk Model

Next we formed a much better statistical model of the mistuning by using FMM ID to measure the blade frequency deviation in all 10 test disks. Again, the data was found to be normally distributed. In this case, the sample standard deviation was 1.92%, which is much closer to the true standard deviation of 2%. Since this sample standard deviation is based off of 10 times as much data as the crude model, our uncertainty in the parameter has been greatly reduced. The 95% confidence interval ranges from 1.77% to 2.12%.

The Monte Carlo simulations were then repeated with this improved statistical model. The resulting CDFs are shown in Fig. 11. As expected, we see substantial improvement in the correlation of the 1E and 3E simulations with experimental data. Furthermore, simulated CDFs from the 6E and 9E cases are virtually identical to those generated from a much cruder statistical model. This result confirms that the 6 and 9E cases are insensitive to statistical modeling errors. Again, the simulations agree well with the experimental benchmark. Therefore, the FMM based probabilistic analysis process may be used to accurately determine the statistical behavior of the fleet.

4.4 Sensitivity Dependence on Mistuning Level

We found throughout Section 4 that the accuracy of a probabilistic mistuning analysis depends on two factors: the quality of the statistical model, and sensitivity of the system's response to statistical modeling errors. As shown in Fig. 10, the system's sensitivity is a function of the engine order of excitation as well as the probability range of interest. However, it should be noted that the sensitivity regime is also governed by the level of mistuning in the system.

Consider the CDFs shown in Fig. 12. Each curve corresponds to the response of a system with a different mistuning standard deviation, σ_1 and σ_2 respectively. In the case of σ_1, the 99th percentile amplitude is about 1.5. Yet, the 99th percentile amplitude for σ_2 is slightly higher. Therefore, we can plot the 99th percentile of the response as a function of the standard deviation of the mistuning, Fig 13. Figure 13 shows the 99th percentile for all four engine orders considered in this study. Notice that in the vicinity of 2% mistuning, the 6E and 9E curves have a near-zero slope. Thus, the 99th percentile amplitude in these cases is insensitive to small changes in the mistuning level (standard deviation). This is consistent with the sensitivity plot shown in Fig. 10. However, if the mistuning was instead on the order of 0.5%, then Fig. 13 indicates that the response to a 6E or 9E excitation would be much more sensitive to changes in the standard deviation. Thus, a system's sensitivity to errors in the statistical modeling depends on the level of mistuning.

5. CONCLUSIONS

It was shown that FMM and FMM ID may be used for probabilistic analysis of mistuned bladed disks. The process involves using FMM ID to collect data on the mistuning and tuned frequencies of a population of bladed disks. This data is then used to construct statistical models of the parameters. Finally, we can use those statistical models with FMM to perform Monte Carlo simulations of the fleet response. FMM is an ideal physical model for Monte Carlo simulations because it is accurate, simple to use, and extremely efficient.

The method was verified experimentally by comparing the results of our Monte Carlo simulations against laboratory measurements of mistuned disks. The FMM approach worked very well. We found that the

accuracy of the method depends on both the quality of the statistical model, and the sensitivity of the system's response to errors in the statistical modeling. The sensitivity regime may be assessed through the sensitivity analyses discussed in Sections 4.2 and 4.4. The efficiency of FMM makes these analyses fast and easy to perform. If it is found that the system is sensitive, then the statistical models may need to be improved to ensure an accurate simulation. Such improvements can be made by using FMM ID to measure the mistuning of additional hardware. Conversely, additional testing may not be necessary on systems that are insensitive to modeling errors.

FMM and FMM ID were experimentally shown to be effective tools for probabilistic analysis of mistuned bladed disks.

ACKNOWLEDGEMENTS

The authors would like to acknowledge that this research was supported by NASA Glenn Research Center, grant number NCC3 - 1058, under the direction of Dr. Shantaram Pai. The POLYTEC scanning vibrometer used in the experiments was purchased through a DURIP grant sponsored by an AFOSR. The traveling wave excitation system was developed with support from the U.S. Air Force, contract number F33615-01-C-2186, and from the GUIde Consortium.

REFERENCES

[1] Srinivasan, A. V., 1997, "Flutter and Resonant Vibration Characteristics of Engine Blades," Journal of *Engineering for Gas Turbines and Power*, **119**, 4, pp. 742-775.

[2] Yang, M.-T., and Griffin, J. H., 2001, "A Reduced Order Model of Mistuning Using a Subset of Nominal Modes," Journal of Engineering for Gas Turbines and Power, 123(4), pp. 893-900.

[3] Feiner, D.M., and Griffin, J. H., 2002, "A Fundamental Model of Mistuning for a Single Family of Modes," Journal of Turbomachinery, 124(4), pp. 597-605.

[4] Castanier, M. P., Ottarsson, G., and Pierre, C., 1997, "A Reduced Order Modeling Technique for Mistuned Bladed Disks," Journal of Vibration and Acoustics, 119(3), pp. 439-447.

[5] Petrov, E., Sanliturk, K., Ewins, D., and Elliott, R., 2000, "Quantitative Prediction of the Effects of Mistuning Arrangement on Resonant Response of a Practical Turbine Bladed Disk," 5th National Turbine Engine High Cycle Fatigue Conference, Chandler, Arizona.

[6] Seinturier, E., Lombard, J.P., Berthillier, M., and Sgarzi, O., 2002, "Turbine Mistuned Forced Response Prediction: Comparison With Experimental Results," ASME Paper 2002-GT-30424, International Gas Turbine Institute Turbo Expo, Amsterdam, The Netherlands.

[7] Judge, J.A., Pierre, C., and Ceccio, S.L., 2002, "Mistuning Identification in Bladed Disks," *Proceedings of the International Conference on Structural Dynamics Modeling*, Madeira Island, Portugal.

[8] Kim, N.E., Griffin, J.H., 2003, "System ID in High Modal Density Regions of Bladed Disks," *8th National Turbine Engine High Cycle Fatigue Conference,* Monterey, California.

[9] Feiner, D.M., and Griffin, J.H., 2003, "Mistuning Identification of Bladed Disks Using a Fundamental Mistuning Model -- Part I: Theory," Journal of Turbomachinery, 126(1).

[10] Feiner, D.M., and Griffin, J.H., 2003, "Mistuning Identification of Bladed Disks Using a Fundamental Mistuning Model -- Part II: Application," Journal of Turbomachinery, 126(1).

[11] Jones, K.W., and Cross, C.J., 2003, "Traveling Wave Excitation System for Bladed Disks," Journal of Propulsion and Power, 19(1), pp. 135-141.

FIGURES

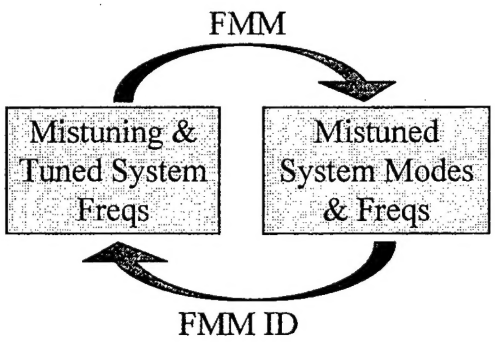

Figure 1: Schematic representation of the relation between FMM and FMM ID.

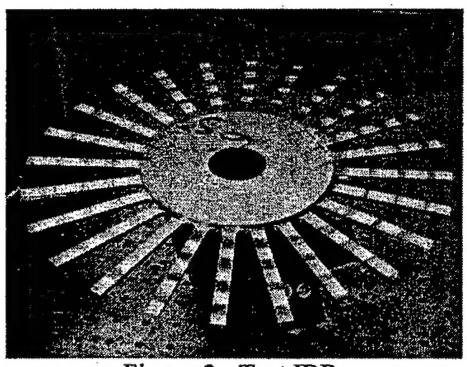

Figure 2: Test IBR.

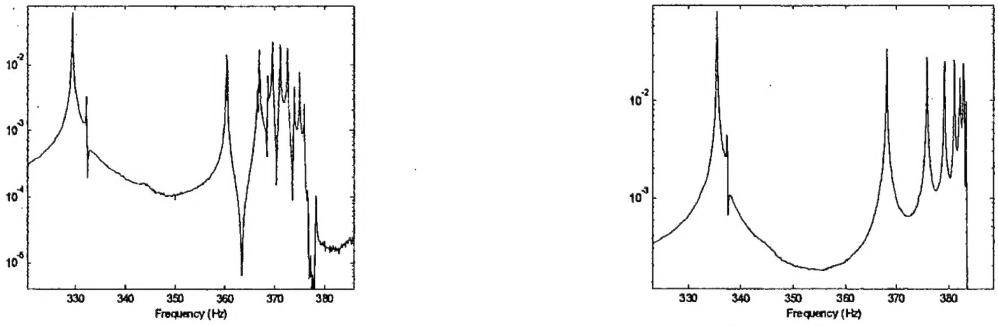

(a) Before Tuning (b) After Tuning

Figure 3: FRF's of the test IBR before and after tuning.

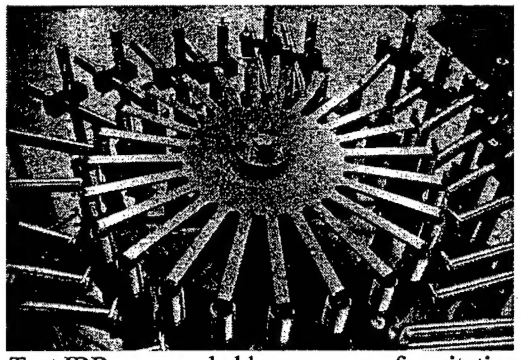

Figure 4: Test IBR surrounded by an array of excitation magnets.

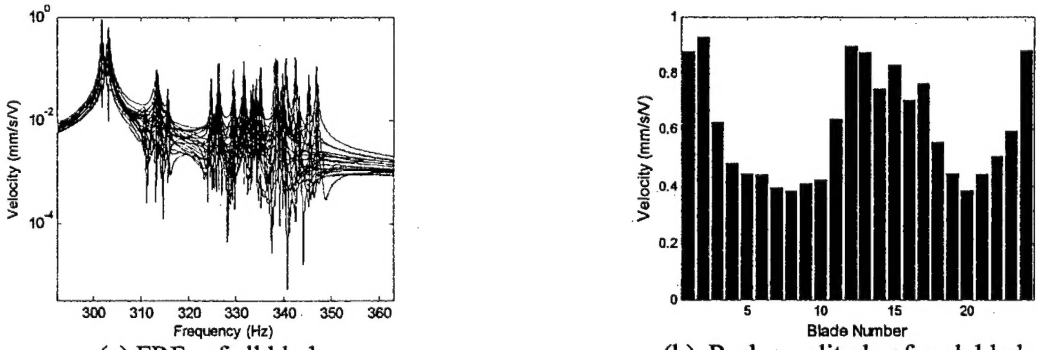

(a) FRFs of all blades (b) Peak amplitude of each blade

Figure 5: Representative measurements of one disk configuration, driven by a 1E excitation.

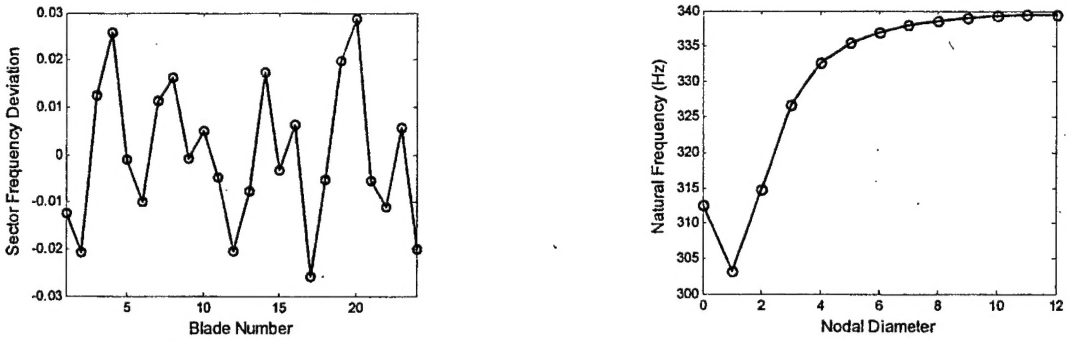

(a) Mistuning (b) Tuned system frequencies

Figure 6: Parameters of test disk as determined through FMM ID

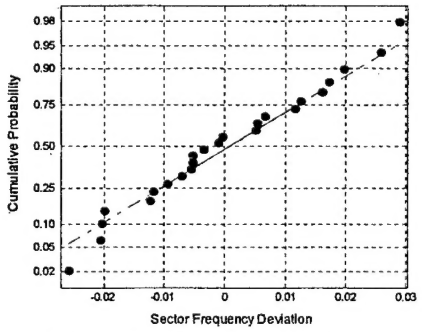

Figure 7: Normal plot of blade frequency deviations of one disk

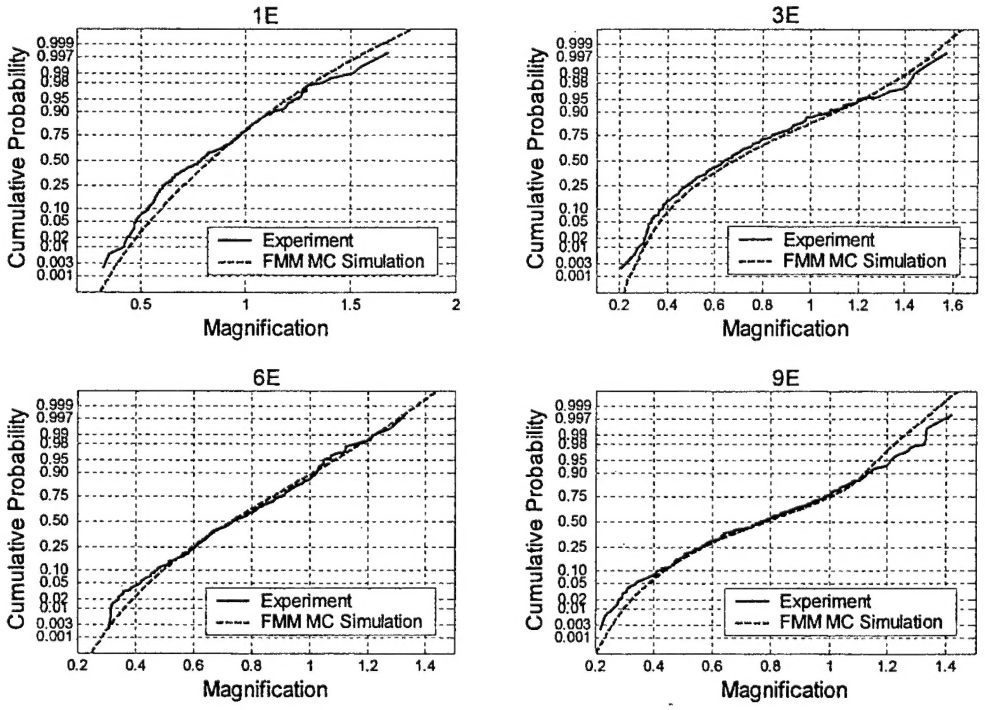

Figure 8: Comparison of the experimental and simulated CDFs of the peak blade amplitudes

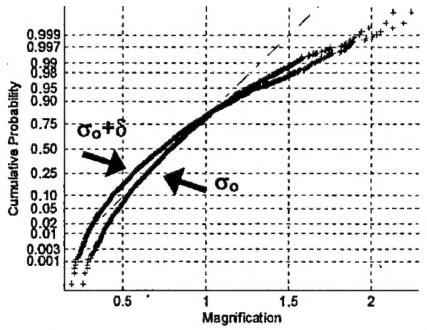

Figure 9: Change in CDF due to perturbation in standard deviation

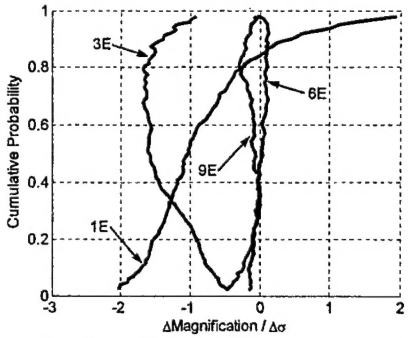

Figure 10: Sensitivity of CDF to perturbation in standard deviation, centered about σ=2%

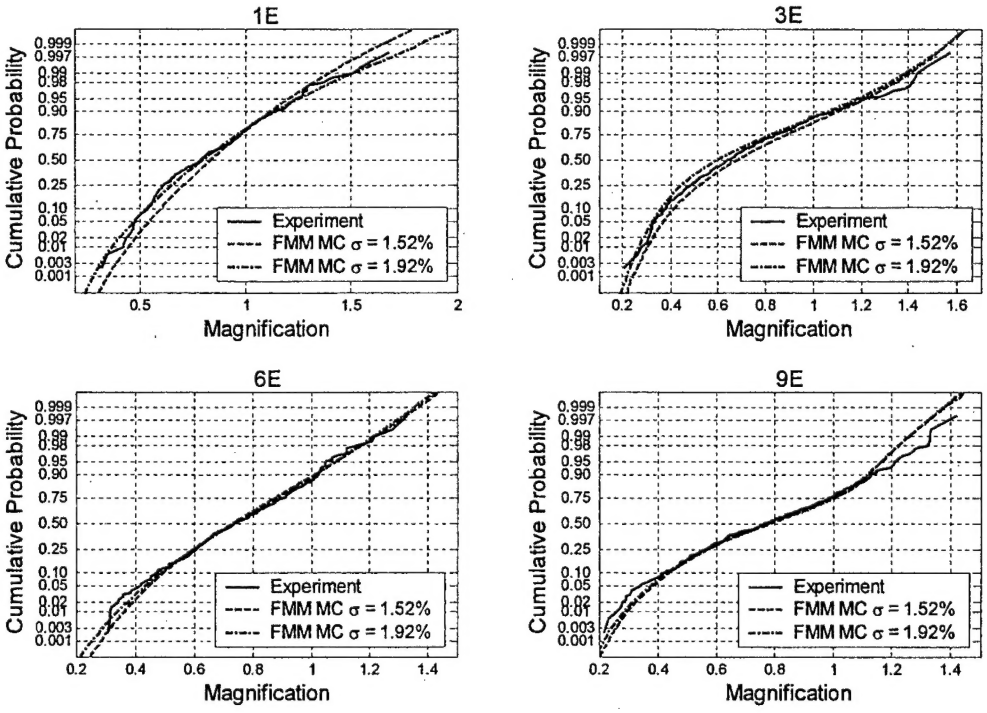

Figure 11: Comparison of the experimental and simulated CDFs of the peak blade amplitudes based on both the crude and improved statistical models.

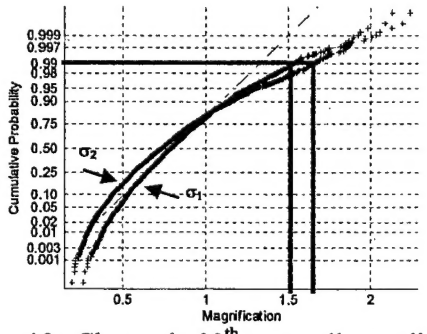

Figure 12: Change in 99th percentile amplitude due to change in mistuning standard deviation

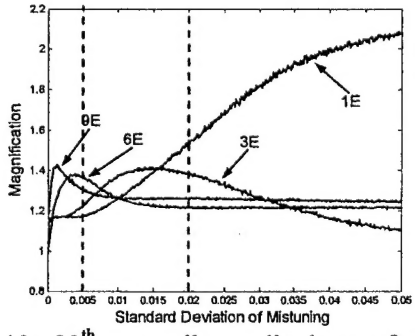

Figure 13: 99th percentile amplitude as a function of mistuning standard deviation